https://ntrs.nasa.gov/search.jsp?R=19660017577 2018-05-25T16:34:15+00:00Z

NATIONAL AERONAUTICS AND SPACE ADMINISTRATION

Technical Report No. 32-909

Dynamic Environment of the Ranger Spacecraft: I through IX (Final Report)

David B. Wiksten

W. S. Shipley, Manager
Environmental Requirements Section

JET PROPULSION LABORATORY
CALIFORNIA INSTITUTE OF TECHNOLOGY
PASADENA, CALIFORNIA

May 1, 1966

Copyright © 1966
Jet Propulsion Laboratory
California Institute of Technology

Prepared Under Contract No. NAS 7-100
National Aeronautics & Space Administration

CONTENTS

I. Introduction 1

II. Definition of Environment 3
- A. Data Acquisition 3
- B. Random Vibration Environment 11
- C. Acoustic Environment 25
- D. Shock Environment 28

III. Vibration Testing 48
- A. Historical Comments 48
- B. Test Philosophy 48
- C. Control Techniques 48
- D. Resultant Tests Compared with Specified Tests 48

IV. Comparison of Test Specifications and Flight Environments . . . 51
- A. Flight Data vs Spacecraft Test (Random Vibration) 51
- B. Acoustic Data vs PTM Acoustic Test 53
- C. Flight Data vs Spacecraft Test (Low-Frequency Sine) 55
- D. Flight Data vs Spacecraft Test (Torsional Pulse) 56
- E. Estimated Flight Environment vs Assembly Level Test 57

V. Conclusions and Recommendations 58
- A. Data Acquisition 58
- B. Environmental Prediction 59

References 60

TABLES

1. ***Ranger* dynamic instrumentation** 9
2. **Wideband high-frequency vibration levels** 24
3. **Grouping of *Ranger* flight-vibration measurements** 25
4. **Torsional pulse-test levels** 50

FIGURES

1. *Ranger* spacecraft (Block III) undergoing vibration test 2
2. Dynamic instrumentation, *Ranger I* 3
3. Dynamic instrumentation, *Ranger II, III, IV* 4
4. Dynamic instrumentation, *Ranger V* 4
5. Dynamic instrumentation, *Ranger VI, VII, VIII, IX* 5
6. Ground acoustic instrumentation 6
7. Mounting block for channels 10, 12, and 17, *Ranger VI* 7
8. Flight microphone, *Ranger VI* 8
9. Frequency response of an FM/FM telemetry channel 8
10. Frequency response, end-to-end, channel 9 8
11. Frequency response, end-to-end, channel 10 8
12. Frequency response, end-to-end, channel 11 9
13. Frequency response, end-to-end, channel 12 9
14. Frequency response, end-to-end, channel 17 10
15. Frequency response, end-to-end, channel 18 10
16. Wideband vibration time history, *Ranger IV* and *IX* 11
17. Oscillogram, *Ranger IX*, liftoff 12
18. Oscillogram, *Ranger IX*, transonic 13
19. Oscillogram, *Ranger IX*, BECO (booster engine cutoff) 14
20. Oscillogram, *Ranger IX*, booster separation 15
21. Oscillogram, *Ranger IX*, SECO (sustainer engine cutoff) 16
22. Oscillogram, *Ranger IX*, jettison horizon-sensor fairing 17
23. Oscillogram, *Ranger IX*, shroud separation 18
24. Oscillogram, *Ranger IX*, *Atlas–Agena* separation 19
25. Oscillogram, *Ranger IX*, 1st *Agena* ignition 20
26. Oscillogram, *Ranger IX*, 1st *Agena* cutoff 21
27. Oscillogram, *Ranger IX*, 2nd *Agena* ignition 22
28. Oscillogram, *Ranger IX*, 2nd *Agena* cutoff 23
29. Acceleration spectral density, *Ranger I*, axial, liftoff 24
30. Acceleration spectral density, *Ranger I, II, III, IV*, radial, liftoff 24
31. Acceleration spectral density, *Ranger VI, VIII*, radial, liftoff 25
32. Acceleration spectral density, *Ranger VII, IX*, axial, liftoff 25

FIGURES (Cont'd)

33. Acceleration spectral density, *Ranger I*, axial, transonic 26

34. Acceleration spectral density, *Ranger I, II, III, IV*, radial, transonic 26

35. Acceleration spectral density, *Ranger VI, VIII*, radial, transonic 26

36. Acceleration spectral density, *Ranger VII, IX*, axial, transonic 27

37. Acceleration spectral density, *Ranger VIII, IX*, spacecraft lateral, liftoff 27

38. Acceleration spectral density, *Ranger VIII, IX*, spacecraft lateral, transonic 27

39. Sound pressure spectrum level, *Ranger VI, VIII*, liftoff 27

40. Sound pressure spectrum level, *Ranger VI, VII*, transonic 28

41. Sound pressure level, ⅓ octave bands, *Ranger VI, VII*, liftoff 28

42. Sound pressure level, ⅓ octave bands, *Ranger VI, VII*, transonic 28

43. Sound pressure spectrum level, umbilical tower microphones, *Ranger VI, VII, VIII* 29

44. Sound pressure spectrum level, umbilical boom microphone, *Ranger IX* 29

45. Shock spectra, liftoff transient, radial, channel 10 30

46. Shock spectra, liftoff transient, tangential, channel 12 31

47. Shock spectra, liftoff transient, radial, channel 17, 18 32

48. Shock spectra, BECO, tangential, channel 12, Block I and II 33

49. Shock spectra, BECO, tangential, channel 12, Block III 34

50. Shock spectra, BECO, spacecraft lateral, channel 18 35

51. Shock spectra, BECO, radial, channel 10 36

52. Shock spectra, booster separation, tangential, channel 12 38

53. Shock spectra, SECO, tangential, channel 11, 12 40

54. Shock spectra, jettison horizon-sensor fairing, channel 17, 18 42

55. Shock spectra, shroud separation, channel 17 44

56. Shock spectra, *Atlas–Agena* separation, radial, channel 10 45

57. Shock spectra, *Atlas–Agena* separation, tangential, channel 12 46

58. Specification vs vibration test, low-frequency sine 49

59. Specification vs vibration test, high-frequency sine 49

60. Specification vs vibration test, *Ranger VII, VIII*, and *IX* FA (flight approval) random vibration 49

FIGURES (Cont'd)

61. Specification vs vibration test, torsional sine 50

62. Torsional test pulse 50

63. Flight data vs vibration specification, lateral, *Ranger I, II, III, IV* 52

64. Flight data vs vibration specification, axial, *Ranger I, II, III, IV* 52

65. Mean, 95 percentile, maximum envelope, lateral, *Ranger I, II, III, IV* 53

66. Flight data vs vibration specification, lateral, *Ranger VI, VII, VIII, IX* 53

67. Flight data vs vibration specification, axial, *Ranger VI, VII, VIII, IX* 54

68. Mean, 95 percentile, maximum envelope, lateral, *Ranger VI, VII, VIII, IX* 54

69. Average spacecraft foot environments, Block I and II vs Block III 54

70. Liftoff acoustics vs PTM (proof test model) acoustic specification 55

71. Flight transients (low frequency) vs sine vibration specification 56

72. Flight BECO transient (Block I and II) torsional pulse specification . . . 56

73. Flight BECO transient (Block III) vs torsional pulse specification 56

74. Estimated flight environment, bus assemblies 57

75. Estimated flight environment, TV assemblies 57

76. Spectra ratios, acoustic test vs vibration test 58

ABSTRACT

The dynamic environment of the *Ranger* spacecraft (*I* through *IX*) during the launch portion of flight is defined in this Report. Flight data from each of nine spacecraft launches have been reviewed and are included. The environments receiving emphasis herein include liftoff acoustics, liftoff and transonic vibration, and the transient vibrations of the various pyrotechnic and staging events in the launch sequence. The systems for data acquisition and analysis are briefly described. In addition, postflight comparison of flight data and ground test specification levels is made, and the dynamic test program is briefly discussed.

I. INTRODUCTION

This Report summarizes the dynamic environments of shock, vibration, and acoustics of the *Ranger* spacecraft as measured during the launch portion of the flight tests. A total of nine *Ranger* spacecraft, denoted as *Ranger I* through *Ranger IX*, was launched over a period from 1961 to 1965. In addition to the measured environment, some discussion of ground testing and comparison of ground test with flight data is included.

The *Ranger* spacecraft (Block III) is shown in Fig. 1 undergoing vibration testing. The spacecraft weighs approximately 850 lb and measures approximately 60 in. in diameter (D) at the base (solar panels folded) by 120 in. in length. The boost vehicle consisted of an *Atlas-Agena* combination. The spacecraft is attached at six mounting points or feet to an adapter which is connected to the forward end of the *Agena*.

Due to limited availability of telemetry channels, the flight dynamic environment has been measured with a minimum of instrumentation. Instrumentation varied slightly from flight to flight. The maximum instrumentation on any one flight consisted of six transducers utilizing six *Agena* telemetry channels for continuous time coverage throughout the launch portion of the flight. Only two of these six measurements were high frequency (10 — 2kc), the others being low frequency (0 — 400kc). Complete instrumentation system description is included in Section II. The limited quantity of flight data severely restricted complete environmental definition and required the extraction of as much information as possible from the existing data.

Section II of this Report contains data from all *Ranger* flights. The data from *Ranger I* through *VI* flights, which are presented here, are the results of a recent data-reduction task. These data which were previously reduced were redone, utilizing improved data-reduction techniques resulting in comparable presentation format for all flights. *Ranger VII* through *IX* data presented

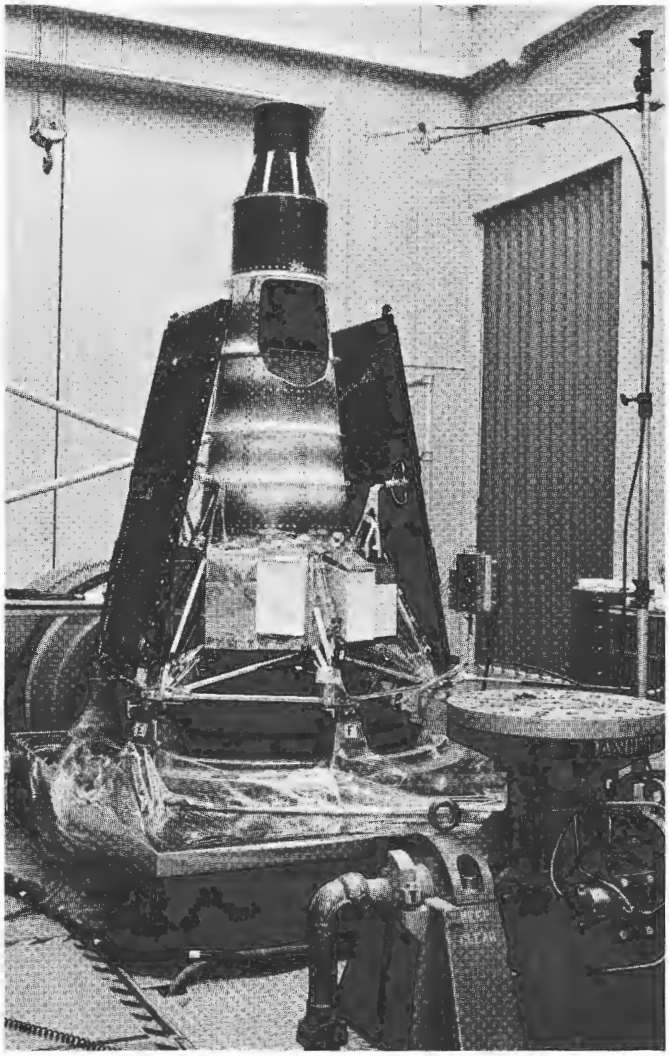

Fig. 1. *Ranger* spacecraft (Block III) undergoing vibration test

here were derived immediately following each flight. The selection of data for presentation was based on giving as complete a picture of the *Ranger* dynamic environment as possible with available data.

From the data package for each *Ranger* flight, the liftoff and transonic portions of random vibration and all available valid transient data were selected. Data which were reduced, but not presented here, include power spectral density of low-frequency channels, and some transient data which were of questionable validity or in a form not allowing direct comparison.

A considerable effort has been made to compress the data into a concise form. Both random vibration and transient data have been condensed to a form allowing a minimum of data review to define the flight environments.

In addition to defining the shock and vibration environment, acoustic measurements were made both on the launch pad and inside the spacecraft shroud. These measurements are included also.

In general, data quality is considered satisfactory. Some problems in interpretation developed due to lack of repetition of location, orientation, or mounting characteristics of transducers.

Section III briefly describes the environmental test program for the *Ranger* spacecraft. The test philosophy and test control techniques are discussed along with a comparison of typical test results and test specifications.

In Section IV the environmental measurements of Section II are interpreted and manipulated toward the end of making a postprogram comparison of the measured environment with the specification description of environmental test levels. Where transducer locations, orientations, and mounting characteristics allow direct comparison, the vibration environment appeared to be very repeatable from flight to flight, both in spectrum shape and level, with the highest wideband vibration always occurring at the transonic portion of flight.

Some general conclusions are drawn in Section V. Although the *Ranger* program came to a successful completion, the instrumentation and the application of measured data to environmental prediction did have known weaknesses. These are briefly discussed with the aim of improving techniques used in environmental engineering as related to spacecraft dynamic environments.

II. DEFINITION OF ENVIRONMENT

A. Data Acquisition

1. Instrumentation

The instrumentation system which was utilized to measure the *Ranger* spacecraft's dynamic environment consisted of transducers located in the *Agena-Ranger* interface area and in the spacecraft itself, the signal conditioning and telemetry equipment in the *Agena*, and the receiving stations of the Eastern Test Range. Data was received at JPL in the form of magnetic tape copies of the original recordings made at the receiving stations.

Transducers used were strain-gage type accelerometers (Statham), piezoelectric crystal accelerometers (Endevco), and piezoelectric type microphones (B and K).

Transducer locations are shown in Fig. 2 through 5. Nearly all flight measurements were made in the adapter connecting the *Agena* and the *Ranger*. The transducers in this area were mounted on the so-called "pork chop" fittings of the adapter, either directly or through use of a mounting bracket. Figure 6 illustrates the ground acoustic instrumentation. Figure 7 shows the mounting bracket used on *Ranger VI* for three transducers. Effects of a mounting bracket resonance in the frequency range of interest were especially noticeable on *Ranger VII*. This is discussed further in Section IV.

The only flight acoustic measurements were made on *Ranger VI* and *VII* with a microphone mounted on the inside of the spacecraft shroud. The *Ranger VI* microphone is shown in Fig. 8.

All flight transducers with orientations and nominal sensitivities are tabulated in Table 1. Frequency ranges as indicated here are those which were considered valid for data interpretation. Data-analysis frequency ranges are discussed below.

The flight data were telemetered in FM/FM multiplex on standard IRIG (Inter-Range Instrumentation Group) subcarrier bands. Bands utilized were 9, 10, 11, 12, 17, and 18.

Instrumentation frequency response is dependent on transducer frequency response, signal conditioning, and T/M characteristics and de-multiplexing effects. The most significant effect is probably the low-pass filter used in the output of the discriminator. Figure 9, taken from Ref. 1, indicates that nominal IRIG filtering may be

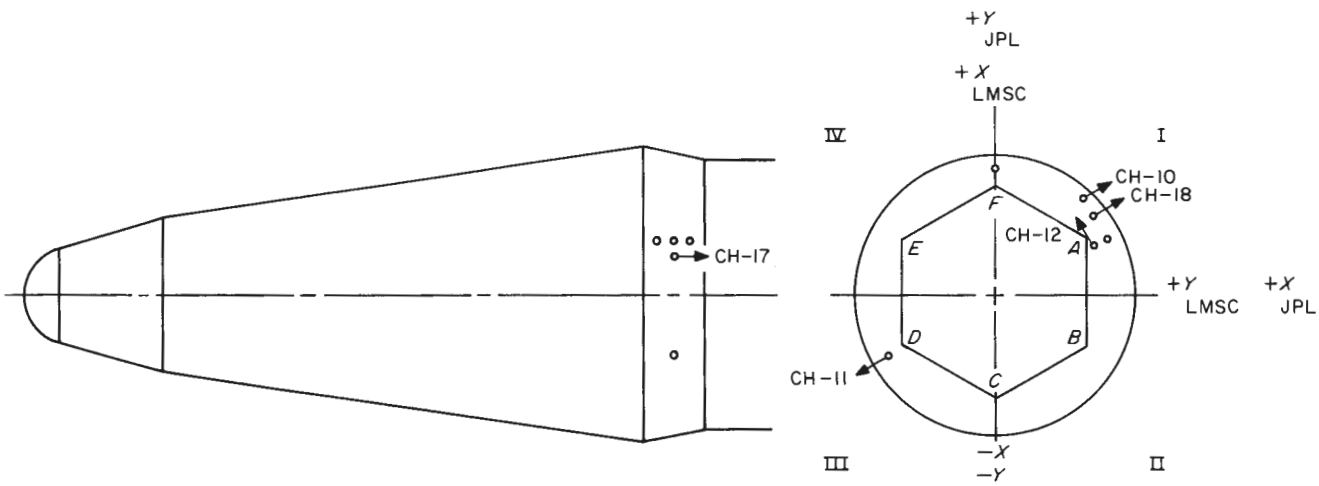

CHANNEL	ORIENTATION	TRANSDUCER RANGE
10	RADIAL	±5g
11	RADIAL	±5g
12	TANGENTIAL	±5g
17	AXIAL	±20g
18	RADIAL	±20g

Fig. 2. Dynamic instrumentation, *Ranger I*

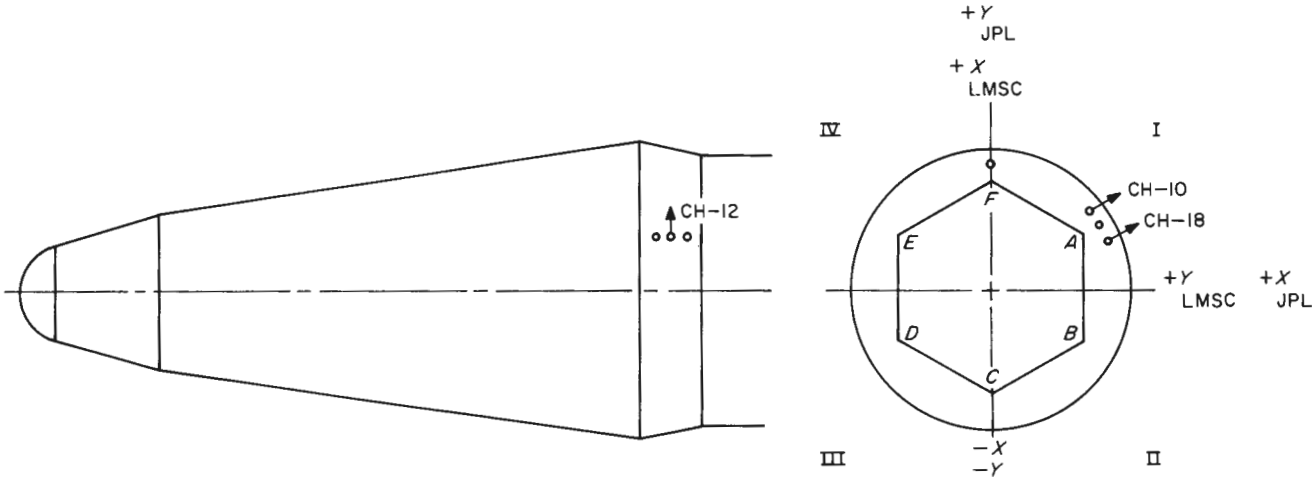

CHANNEL	ORIENTATION	TRANSDUCER RANGE
10	RADIAL	±5g *RANGER II, III* ±1.5g *RANGER IV*
12	TANGENTIAL	±5g *RANGER II, III* ±1.5g *RANGER IV*
18	RADIAL	±20g *RANGER II, III* ±10g *RANGER IV*

Fig. 3. Dynamic instrumentation, *Ranger II, III, IV*

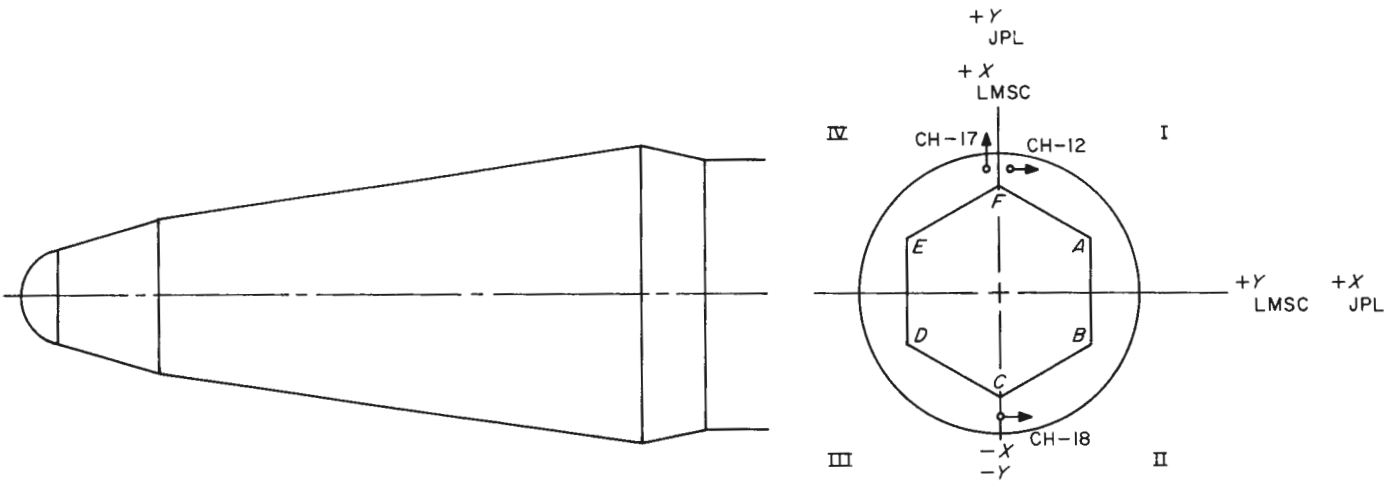

CHANNEL	ORIENTATION	TRANSDUCER RANGE
12	TANGENTIAL	±3g
17	RADIAL	±3g
18	TANGENTIAL	±3g

Fig. 4. Dynamic instrumentation, *Ranger V*

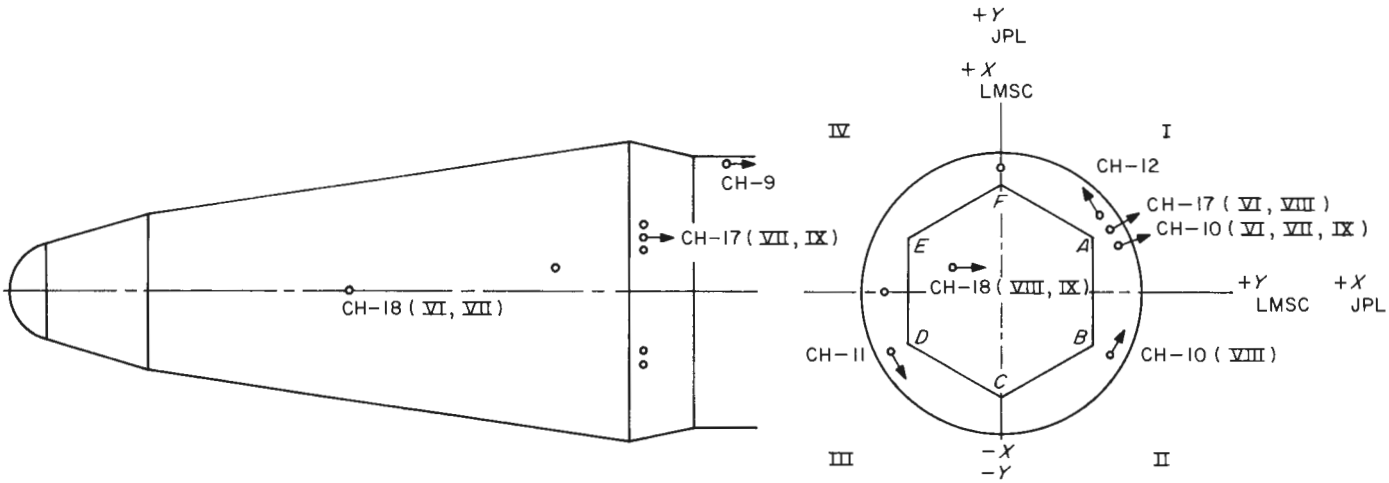

CHANNEL	ORIENTATION	TRANSDUCER RANGE	
9	AXIAL	−4 TO +12g	
10	TANGENTIAL	± 5g	*RANGER VIII*
10	RADIAL	± 1.5g	*RANGER VI, VII, IX*
11	TANGENTIAL	± 5g	
12	TANGENTIAL	± 5g	
17	RADIAL	± 15g	*RANGER VI*
	AXIAL	± 15g	*RANGER VII*
	RADIAL	± 25g	*RANGER VIII*
	AXIAL	± 25g	*RANGER IX*
18	OMNIDIRECTIONAL MICROPHONE	145.8 db	*RANGER VI, VII*
	PARALLEL JPL *X*	± 15g	*RANGER VIII, IX*

Fig. 5. Dynamic instrumentation, *Ranger VI, VII, VIII, IX*

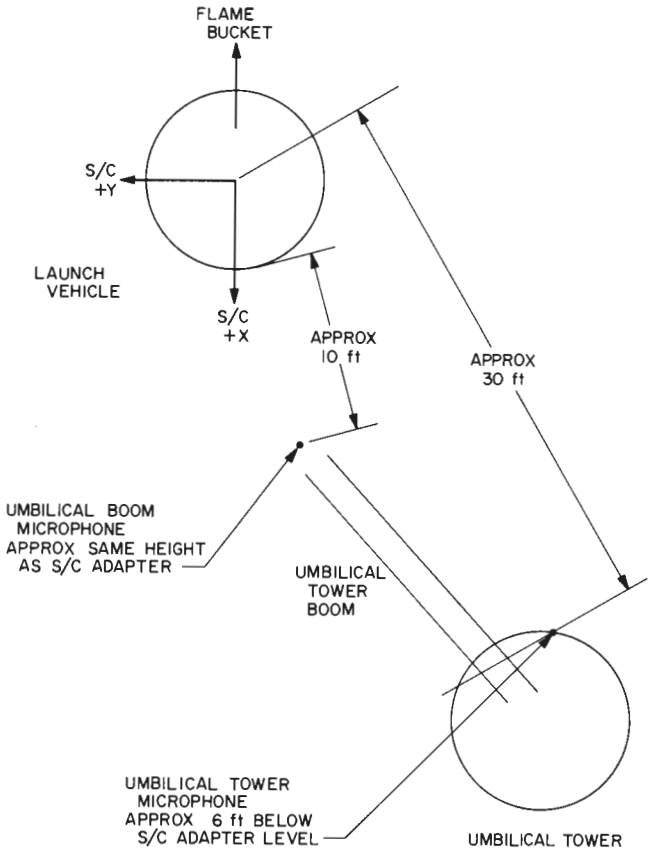

Fig. 6. Ground acoustic instrumentation

overly conservative for use with dynamic data. Sacrificing decreased signal-to-noise ratio at $f > f_0$, a low-pass filter having cutoff frequency above the nominal IRIG frequency was used in analysis of all data presented in this Report. Instrumentation noise level was checked to assure good data quality. The filters used in JPL's flight data reduction were the following:

Channel	*Cutoff Frequency*	*IRIG*
9	160	59
10	220	81
11	330	110
12	450	160
17	2100	790
18	3000	1050

Ideally, an end-to-end calibration would provide complete gain-and-phase information as a function of frequency for each channel. Such end-to-end calibration was performed on *Ranger VIII* and *IX*. Figures 10 through 15 show channel frequency response as determined from these end-to-end calibrations. These curves were derived from a discrete frequency sine-wave excitation test by comparing a reference transducer measurement or standard to the telemetered and discriminated signal. Thus, "end-to-end" includes everything between transducer and plotted data including JPL's playback.

If it is assumed that *Ranger VIII* and *IX* end-to-end calibration information is representative of all *Ranger* flights, then all flight data presented in this Report may be considered to be attenuated by approximately the frequency responses of Fig. 10–15. No correction for instrumentation frequency response has been applied to data presented here, since all channels were flat within approximately 1 db to twice IRIG cutoff frequencies.

2. Data Analysis and Compression

Several types of analysis have been applied to the raw flight data. Those types which are presented here include:

a. Oscillogram of raw-data signals

b. Wideband average vs time

c. Spectral density analysis

d. Shock spectrum analysis

A brief description of each type of analysis follows.

Data Playback. In recovering the data signals from the magnetic tape, discriminator low-pass filters as described in Section II-A-1 were used for all types of analysis.

Oscillogram Presentation. All data channels plus time-code and signal-strength indication are recorded on an oscillogram for visual evaluation of the data. Invalid data as a result of instrumentation or transmitting and receiving problems are often easily detected by such visual inspection. Also, it is from oscillogram records that time portions for spectrum analysis and shock analysis are selected. Galvanometer frequency responses were sufficient to record data to the maximum frequency compatible with the system frequency response. Typically, the complete flight record was made at a paper speed of 6.4 in./sec with transient events of interest also recorded at a paper speed of 64 in./sec.

Wideband Average vs Time. Another time-history presentation is data average (or rms) as a function of time. This form of analog analysis also contributes to the selection of time portions for more detailed analysis. Typically,

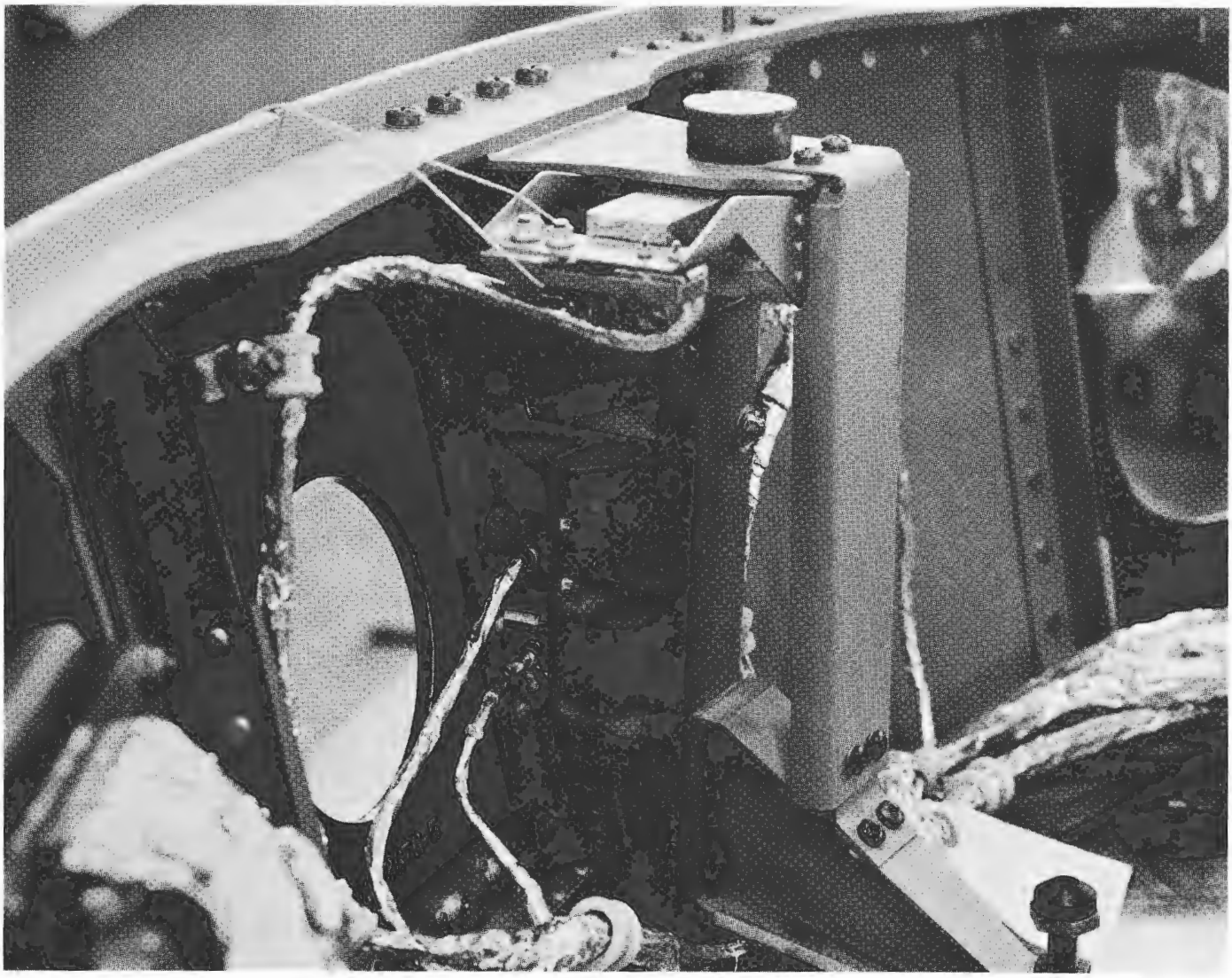

Fig. 7. Mounting block for channels 10, 12, and 17, *Ranger VI*

Fig. 8. Flight microphone, *Ranger VI*

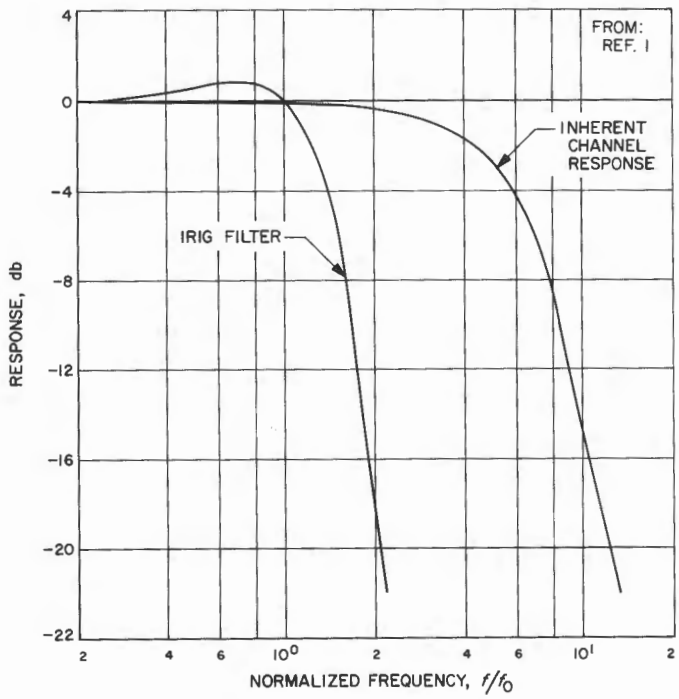

Fig. 9. Frequency response of an FM/FM telemetry channel

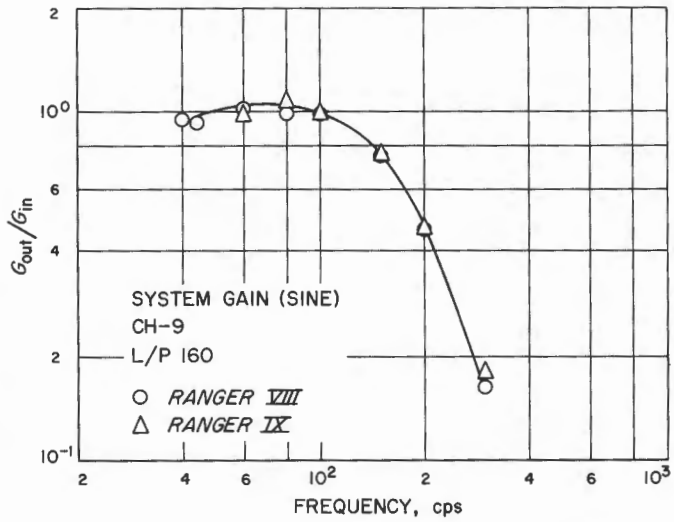

Fig. 10. Frequency response, end-to-end, channel 9

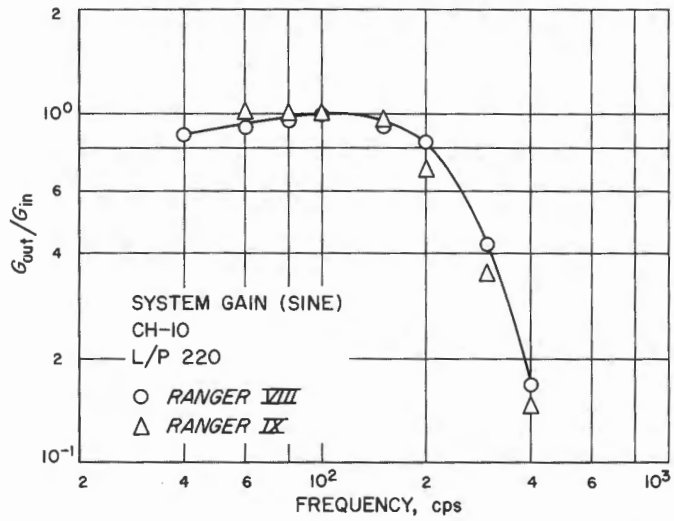

Fig. 11. Frequency response, end-to-end, channel 10

these records were made using an averaging time constant of 0.3 sec and plotted with a time scale of 10 sec/in.

Spectral Density Analysis. All spectral density data presented here were derived, using a digital technique of power spectral density analysis. Typically, two second-data portions were analyzed. Analysis parameters consisted of the following:

Resolution: 20 cps

Low-pass filter: 2.2kc (for Channel 17 and 18)

Digitizing sample rate: 5000 sample/sec

Table 1. *Ranger* dynamic instrumentation

Channels	CH-9	CH-10	CH-11	CH-12	CH-17	CH-18	Comments
Frequency Range	0–150	0–150	0–320	0–320	10–2000	10–2000	
Ranger I		Radial ±5g	Radial ±5g	Tangential ±5g	Axial ±20g	Radial ±20g	
Ranger II		Radial ±5g		Tangential ±5g		Radial ±20g	
Ranger III		Radial ±5g		Tangential ±5g		Radial ±20g	
Ranger IV		Radial ±1.5g		Tangential ±1.5g		Radial ±10g	
Ranger V				Tangential ±3g	Radial ±3g*	Tangential ±3g*	*Low freq. transducers; valid range approx. 150 cps
Ranger VI	Axial +12 to −4g	Radial ±1.5g	Tangential ±5g	Tangential ±5g	Radial ±15g	Omnidirectional microphone 145.8 db	
Ranger VII	Axial +12 to −4g	Radial ±1.5g	Tangential ±5g	Tangential ±5g	Axial ±15g	Omnidirectional microphone 145.8 db	
Ranger VIII	Axial +12 to −4g	Tangential ±5g	Tangential ±5g	Tangential ±5g	Radial ±25g	S/C Lateral* ±15g	*Parallel to S/C X axis
Ranger IX	Axial +12 to −4g	Radial ±3.5g	Tangential ±5g	Tangential ±5g	Axial ±25g	S/C Lateral ±15g	

Notes:

1. Data are assumed valid over the above frequency ranges. Frequency responses of transducer, amplifier, and T/M channel have been considered.
2. Amplitude ranges are nominal values. Amplifier gains are typically set so that these levels deviate T/M channel to 90% of full bandwidth.

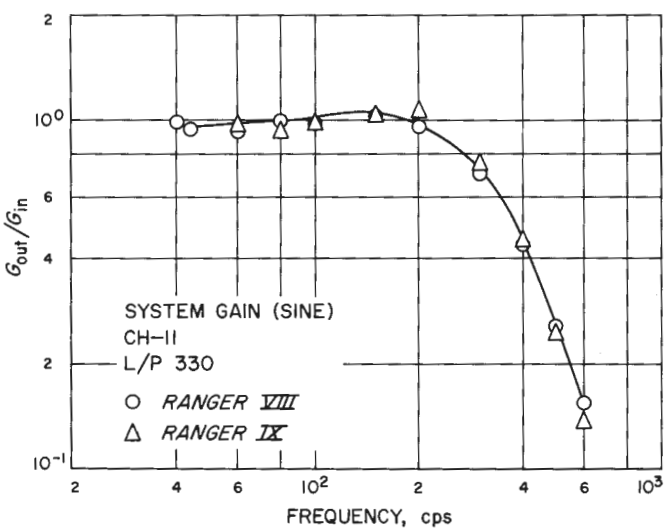

Fig. 12. Frequency response, end-to-end, channel 11

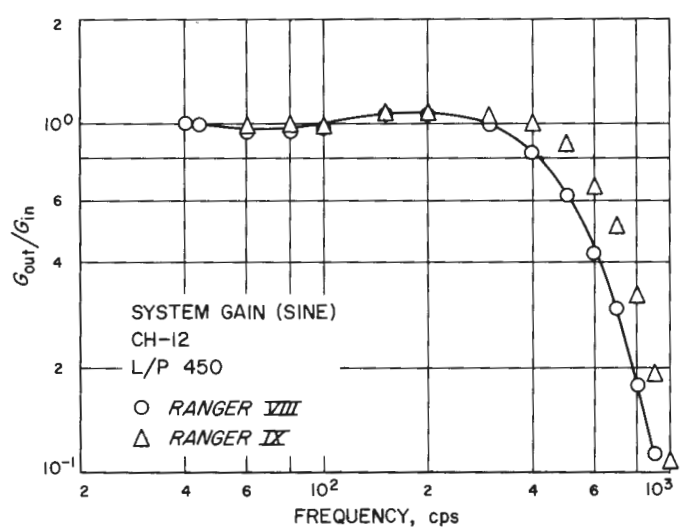

Fig. 13. Frequency response, end-to-end, channel 12

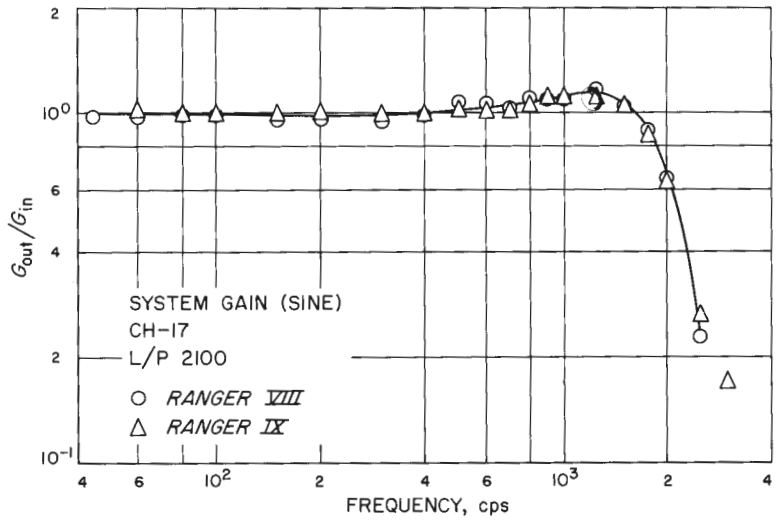

Fig. 14. Frequency response, end-to-end, channel 17

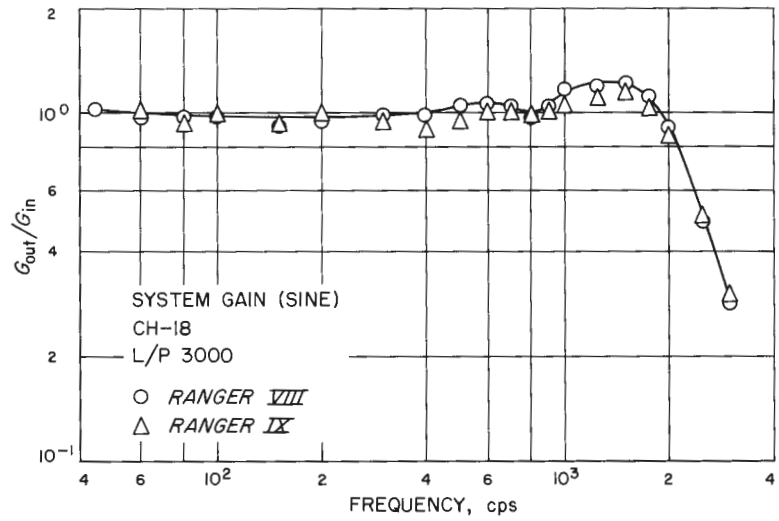

Fig. 15. Frequency response, end-to-end, channel 18

The computational portion of the analysis was performed on an IBM 7094 digital computer. Analysis output consists of plots of the autocorrelation function and the spectral density function. In addition the spectrum values for each plot were stored on cards for later manipulation.

Shock Spectrum Analysis. Where transient vibration or shock occurred and was not of sufficient duration for a spectral density analysis, a shock-spectrum analysis was made. This analysis is also done digitally following analog-to-digital conversion of the data signal.

The shock spectrum presents the peak response to the transient (applied as a base acceleration) of a single-degree-of-freedom spring-mass-damper system as a function of system natural frequency and damping.

The computation of the shock spectrum is performed on an IBM 7094 computer. The computed spectrum is presented in plotted form. Spectrum values are also stored on cards for later manipulation.

The frequency range of the analysis is selected to be compatible with the transmission-playback frequency range and with a visual estimate of frequency range of interest. Sample rates for the analog-to-digital conversion were typically selected to be at least eight to ten

times the highest frequency content. All spectra presented were made with a $Q = 20$ ($Q = 1/2\zeta$, where ζ = percent of critical damping). Additional spectra were calculated for a $\zeta = 0$ and $\zeta = 0.05$, but are not included here.

In addition to the above basic data-analysis techniques, some further data evaluation capability was utilized. This capability was developed from the need to review a large amount of data (power spectral density, PSD, or shock spectra), especially in connection with evaluating ground environmental-test results. This evaluation utilizes a digital computer and the spectral data stored on cards to perform simple arithmetic computations on sets of data. Operations available to the user include:

1. Maximum and/or minimum envelope
2. Average levels
3. Percentile level estimation
4. Ratio between spectra
5. Product of a spectrum and a spectra-ratio
6. One-third octave conversion
7. Plot overlay

B. Random Vibration Environment

The complete flight dynamic environment has been subdivided into three areas, each of special interest. These are (1) the wideband random vibration environment, (2) the acoustic environment, and (3) the transient vibration or shock environment.

The random vibration environment has two time portions of special interest. These occur at liftoff (L/O) and at the transonic-maximum q region. As a description of the time variation of vibration level, Fig. 16 shows the wideband acceleration in g_{rms} as a function of flight time. Two particular flights, *Ranger IV* and *IX*, were selected as being representative of all flights. Time portions other than L/O and transonic show random signal levels which are not appreciably above the instrumentation noise level. Consequently, little detailed analysis was done on random data except in the L/O and transonic regions.

Presented here as typical of all flights are portions of the *Ranger IX* oscillogram. All events of interest for all data channels are shown in Fig. 17 through 28. More detailed description of both random vibration and shock data for *all* flights is shown in power spectral density and shock spectrum format.

From wideband average vs time records and oscillograms for each flight, time portions of two-second duration are selected for power spectral density (PSD) analysis. For the liftoff and transonic time portions containing the highest wideband level, the PSD's from high-frequency channels (IRIG subcarrier 17 or 18) are

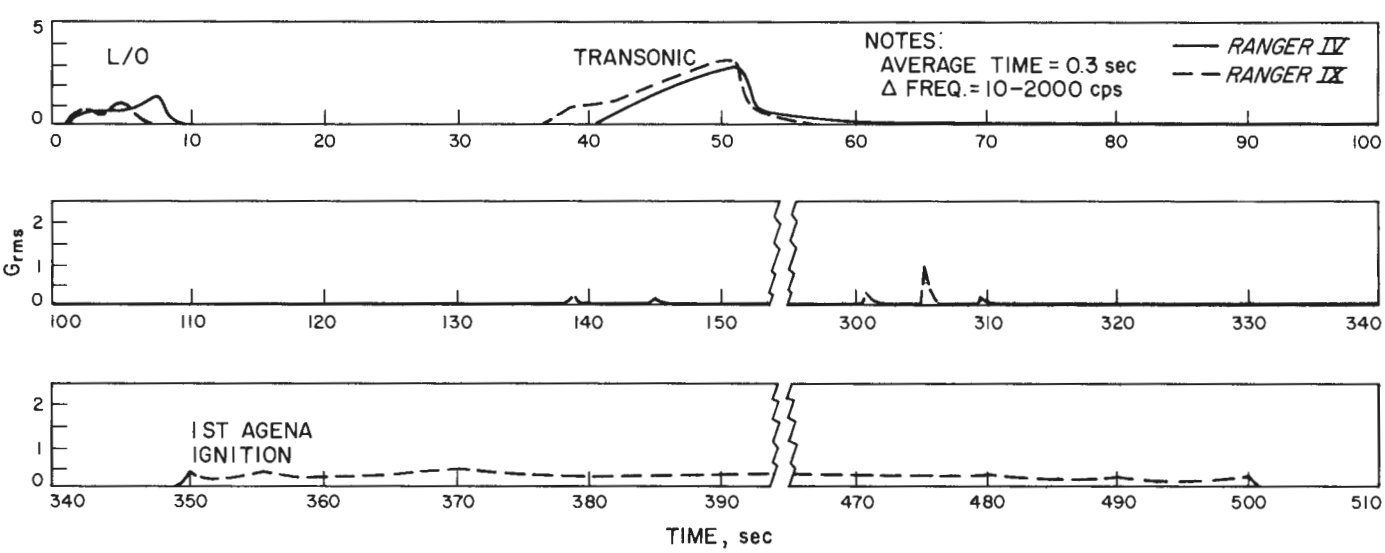

Fig. 16. Wideband vibration time history, *Ranger IV* and *IX*

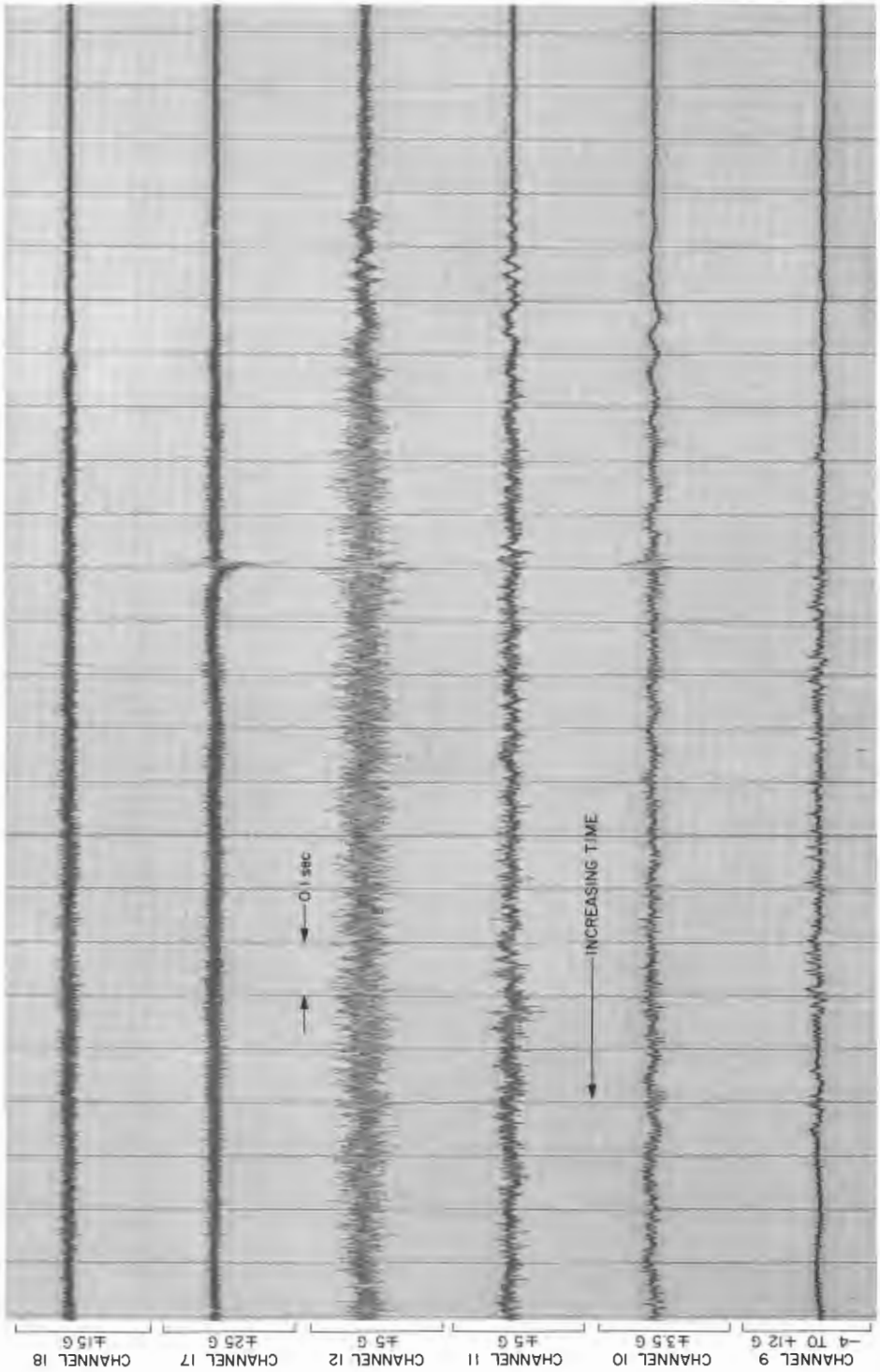

Fig. 17. Oscillogram, *Ranger IX*, liftoff

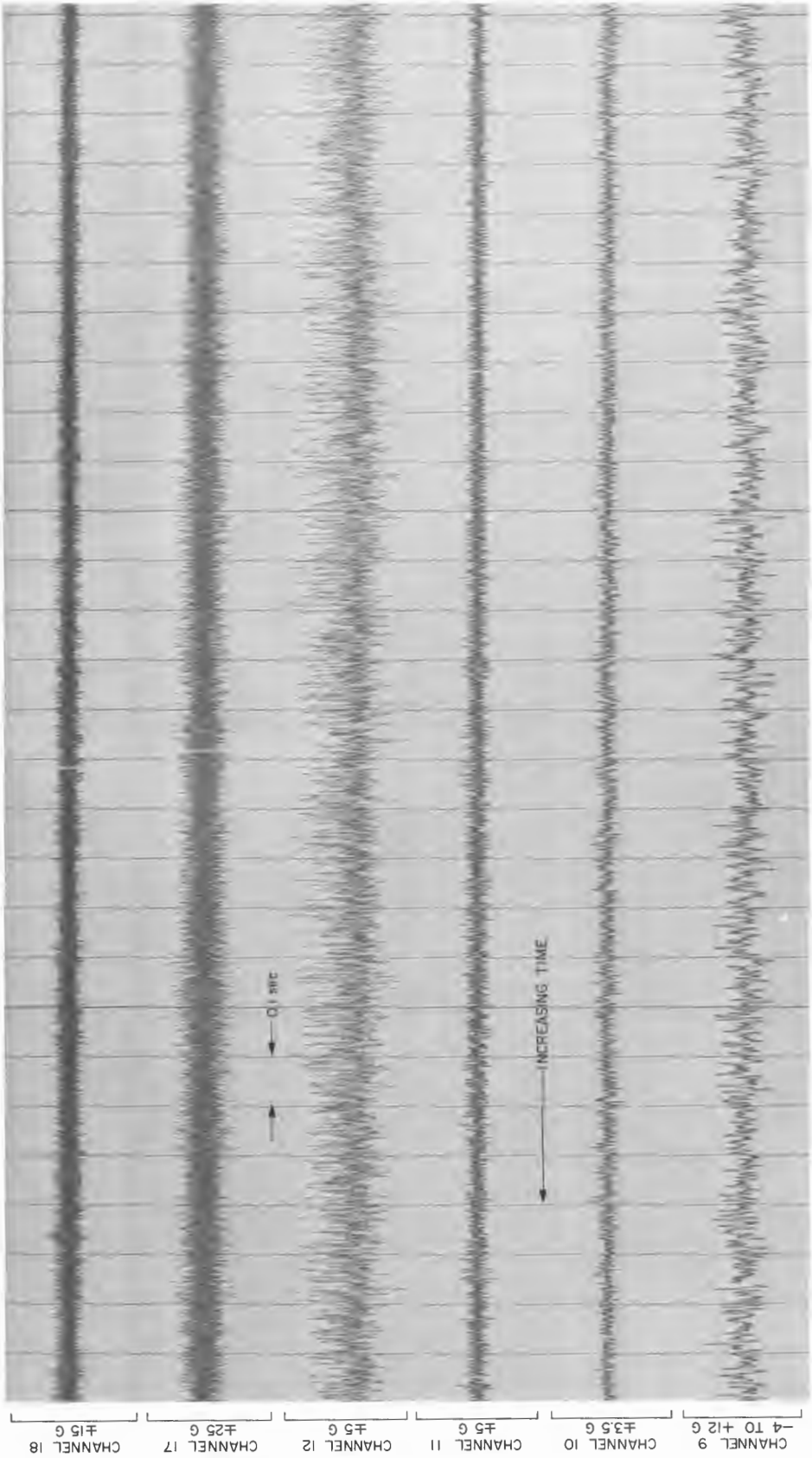

Fig. 18. Oscillogram, *Ranger IX*, transonic

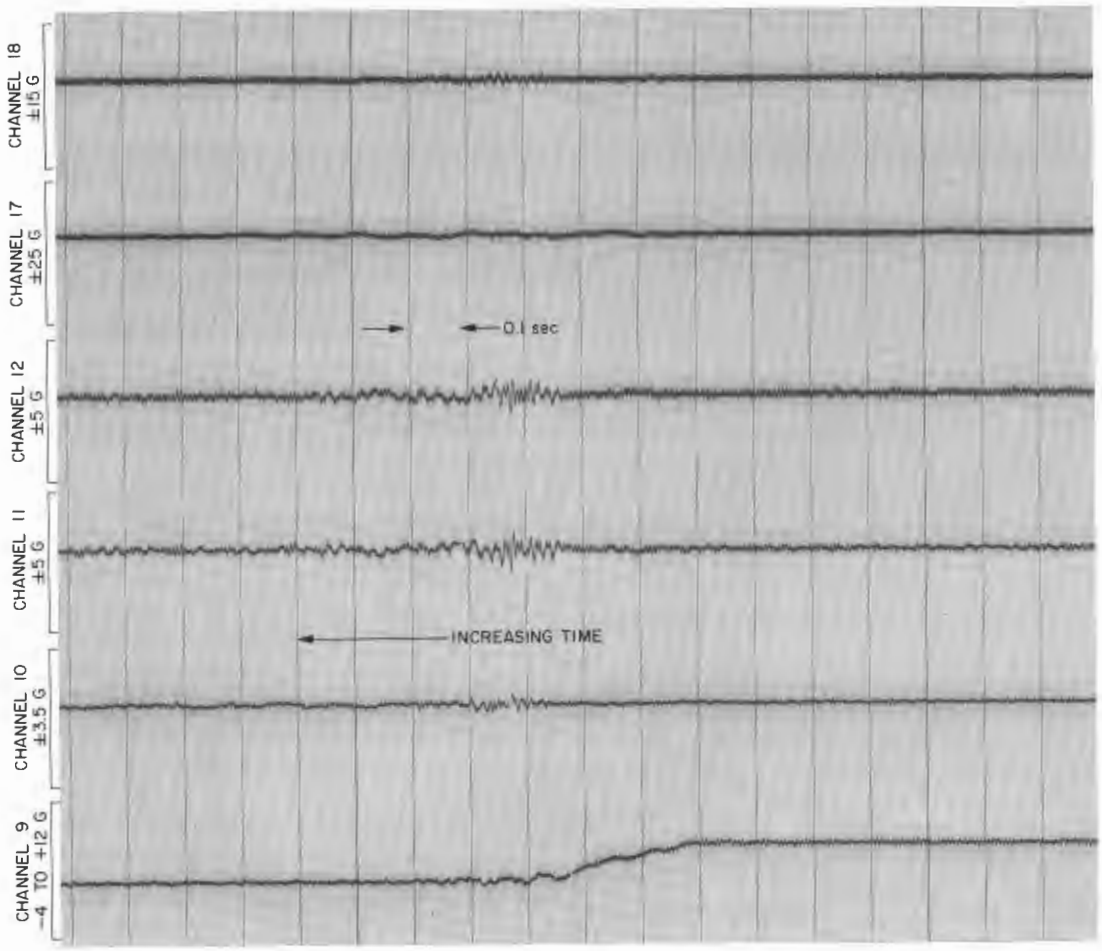

Fig. 19. Oscillogram, *Ranger IX*, BECO (booster engine cutoff)

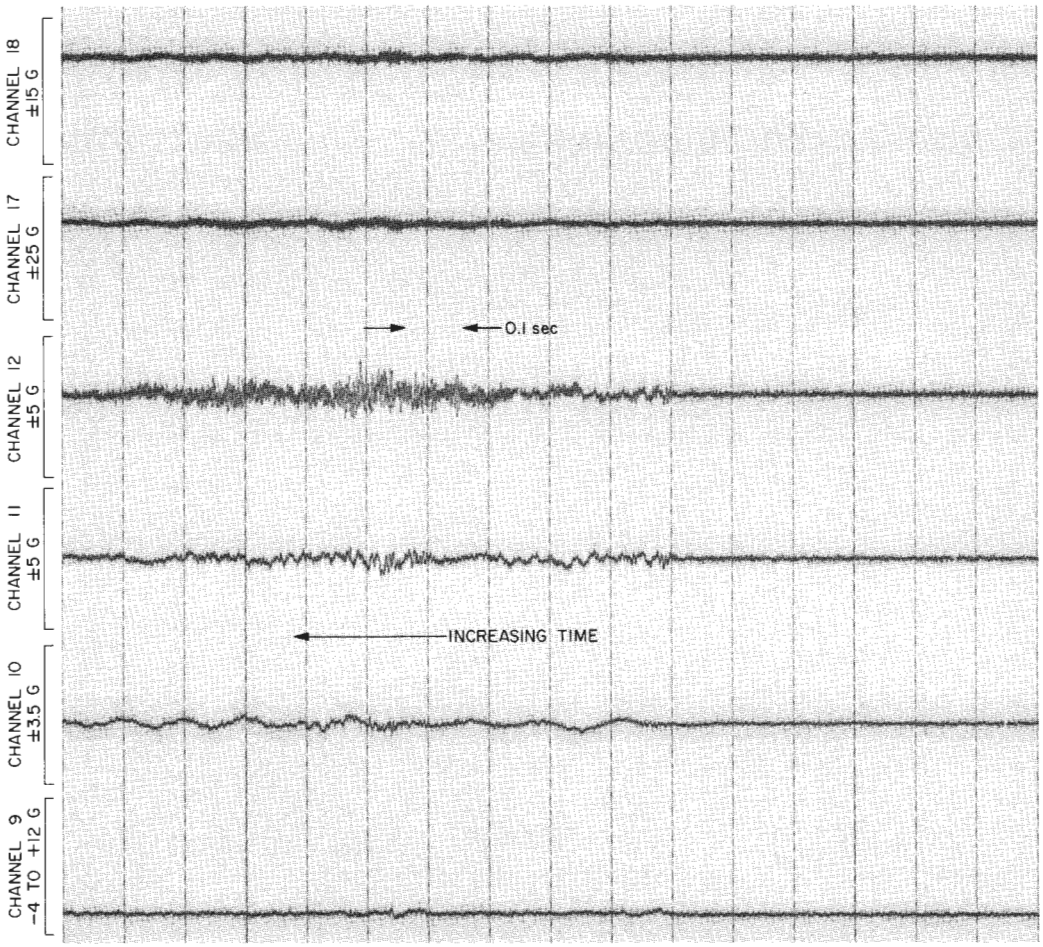

Fig. 20. Oscillogram, *Ranger IX*, booster separation

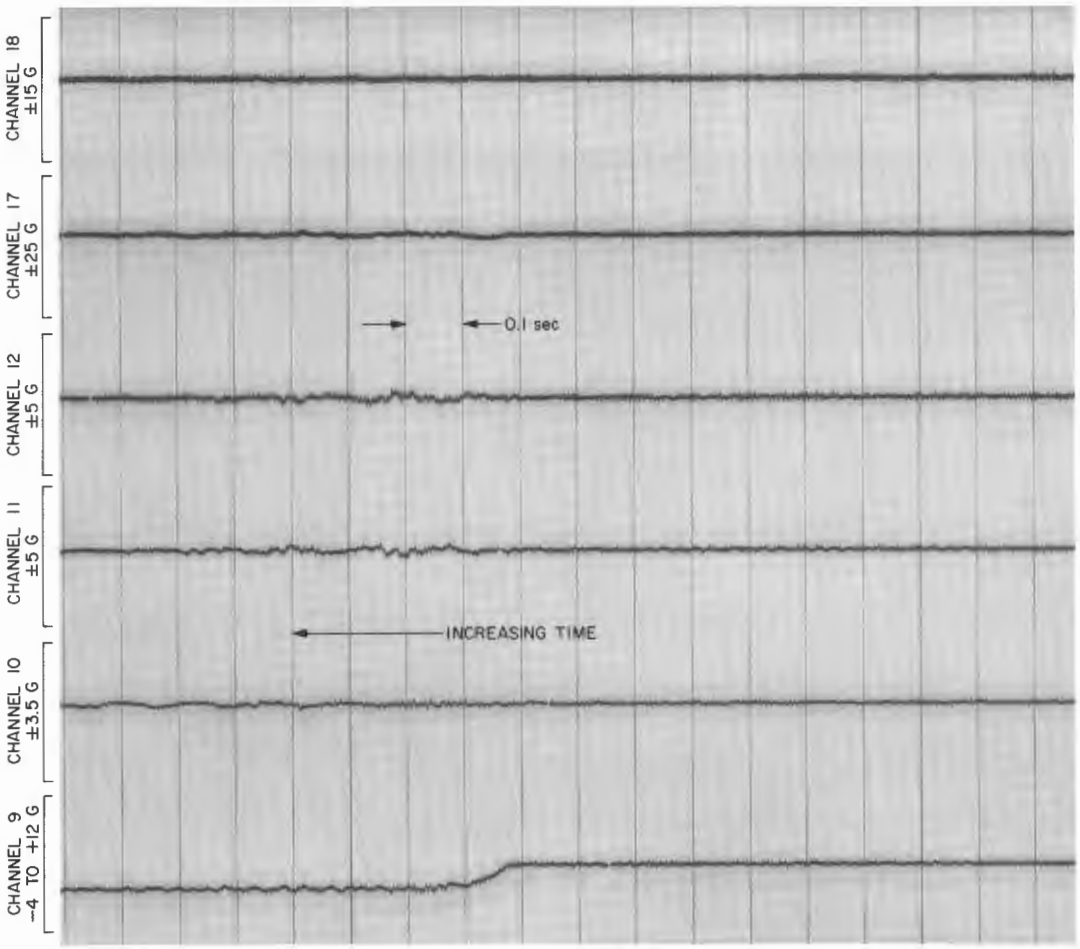

Fig. 21. Oscillogram, *Ranger IX*, SECO (sustainer engine cutoff)

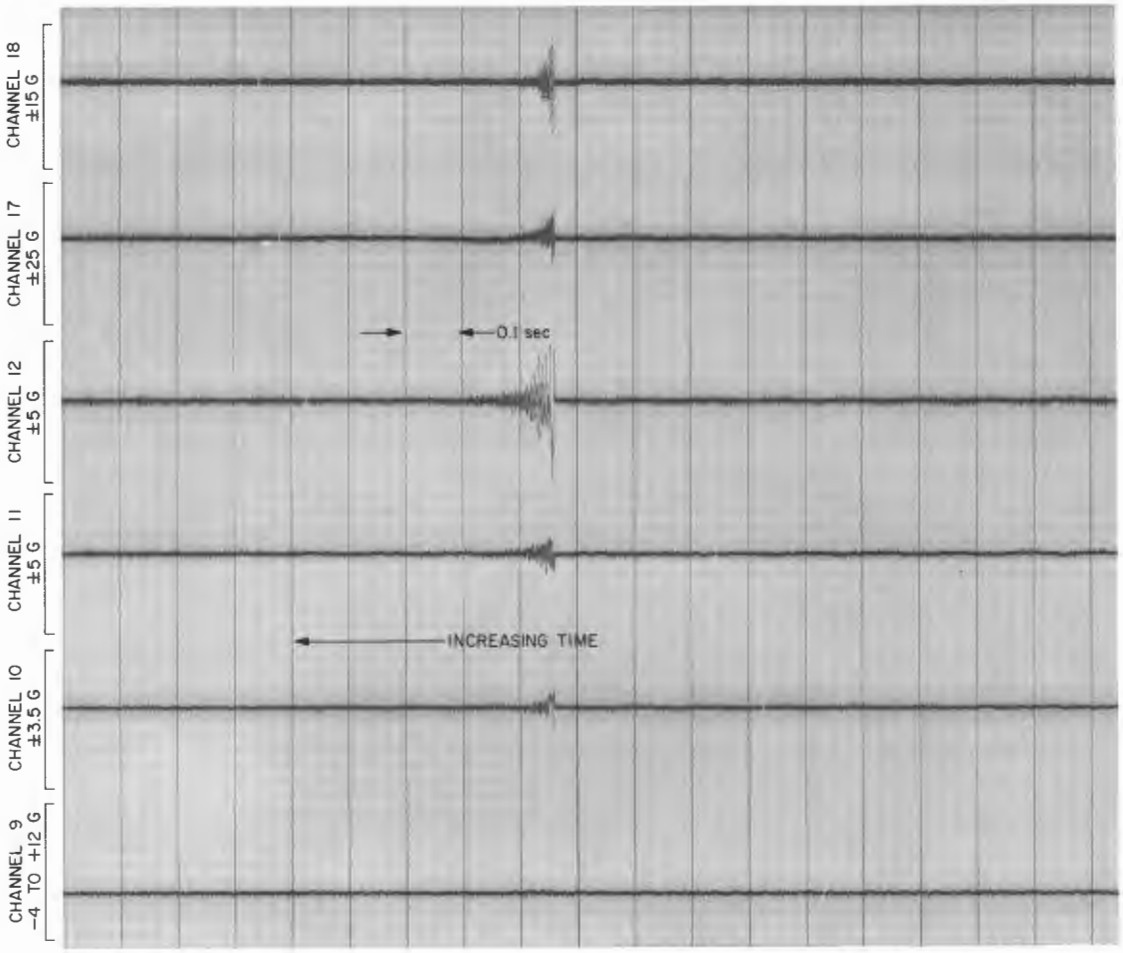

Fig. 22. Oscillogram, *Ranger IX*, jettison horizon-sensor fairing

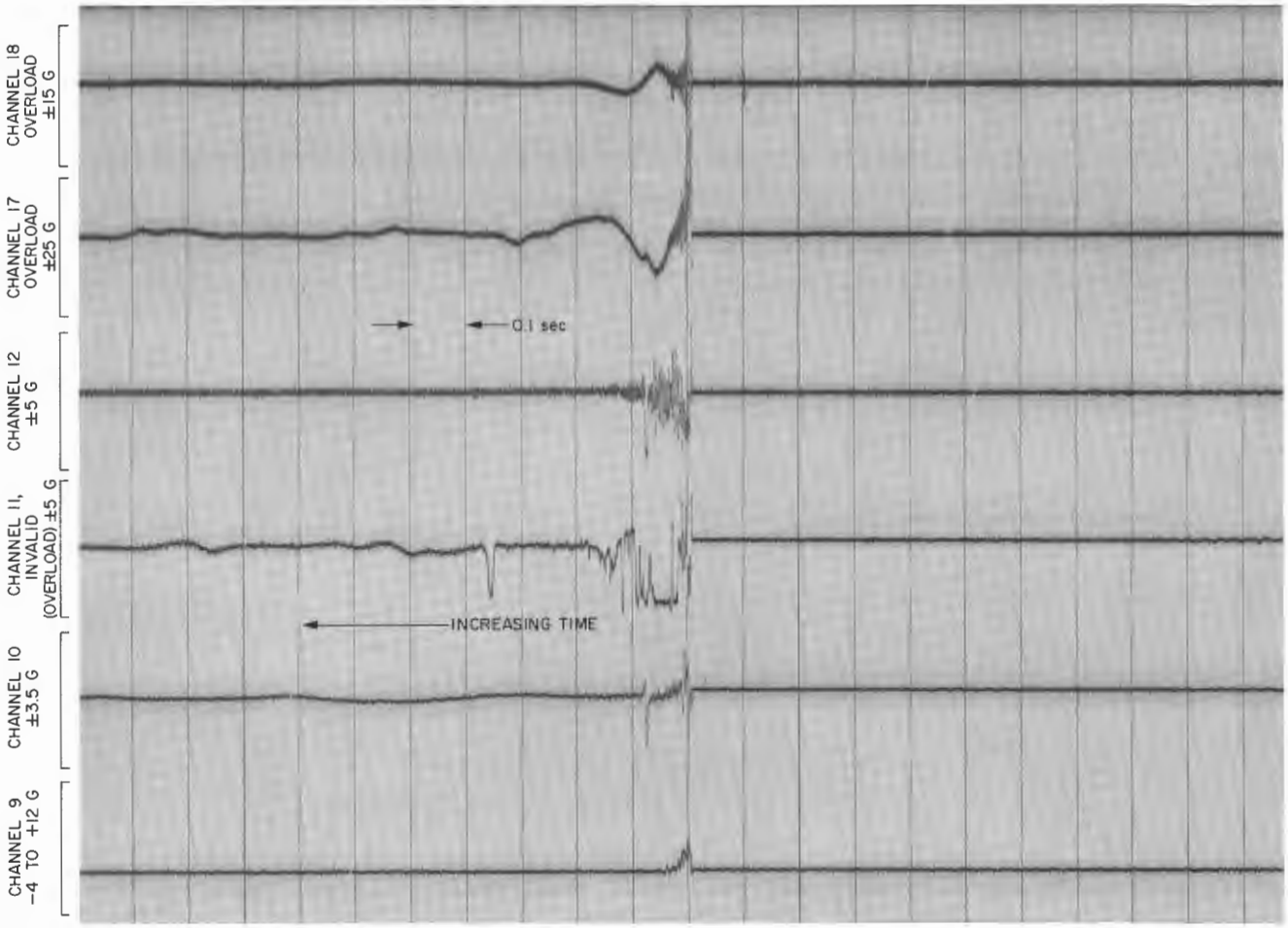

Fig. 23. Oscillogram, *Ranger IX*, shroud separation

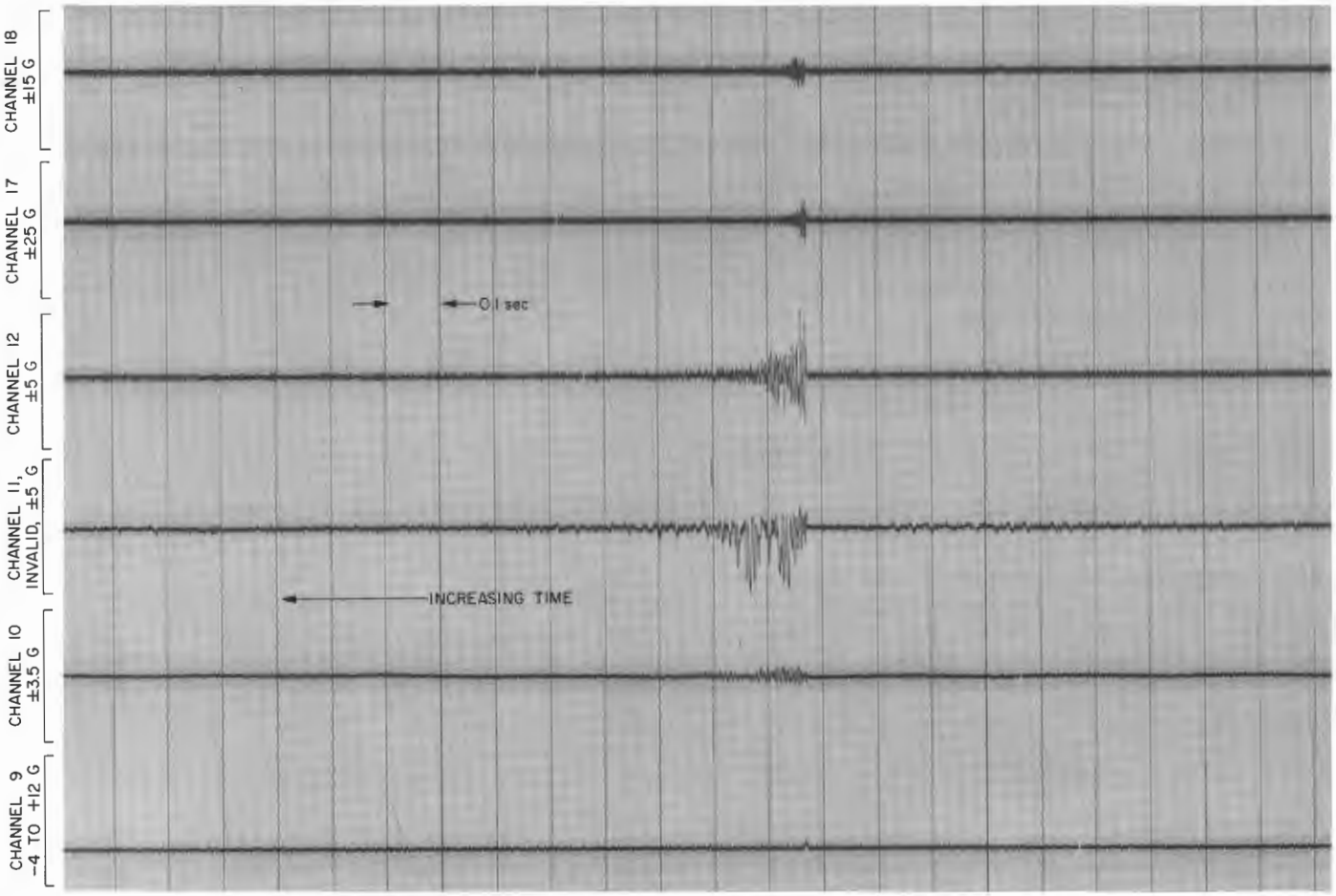

Fig. 24. Oscillogram, *Ranger IX, Atlas–Agena* separation

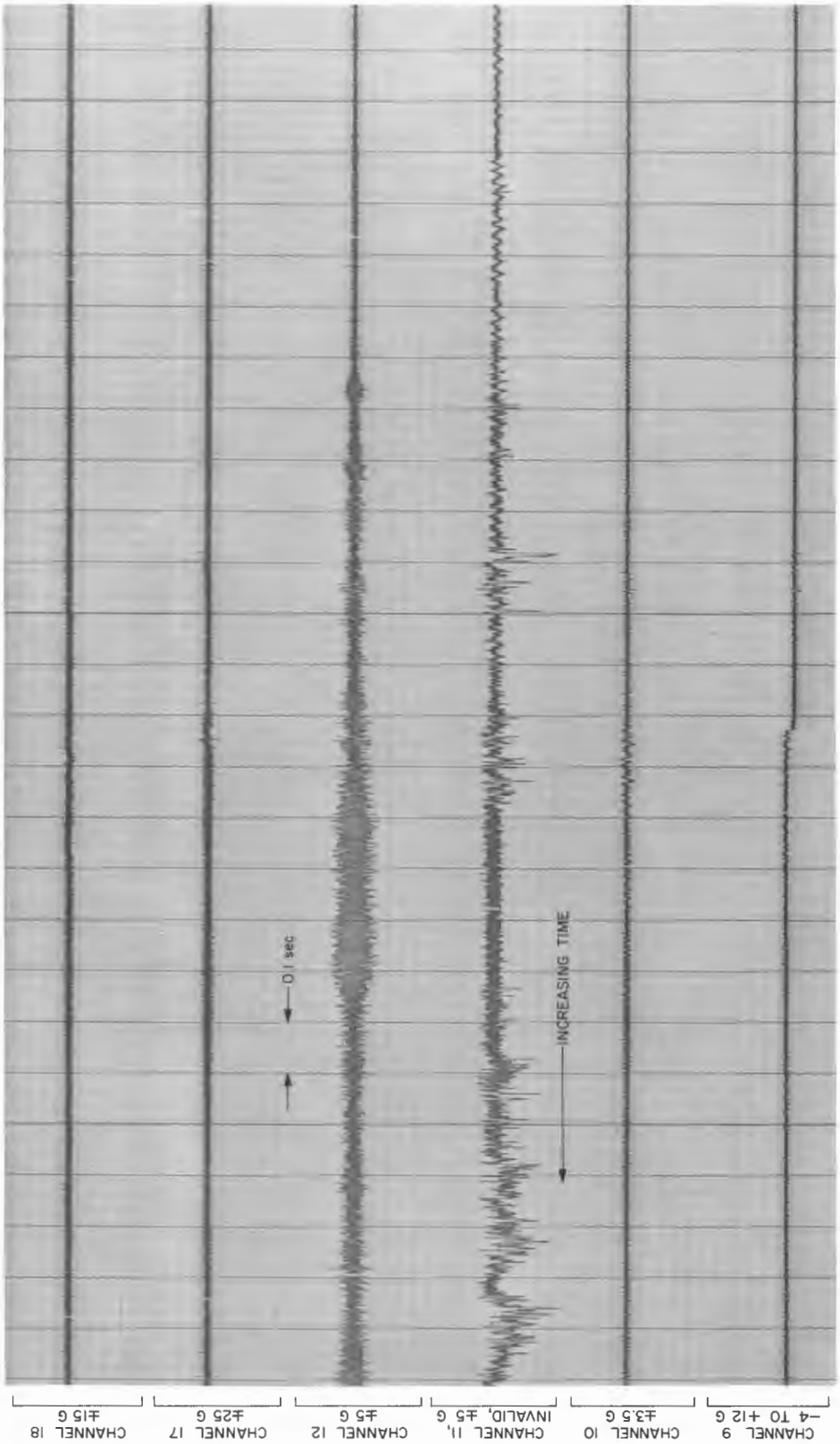

Fig. 25. Oscillogram, *Ranger IX*, 1st *Agena* ignition

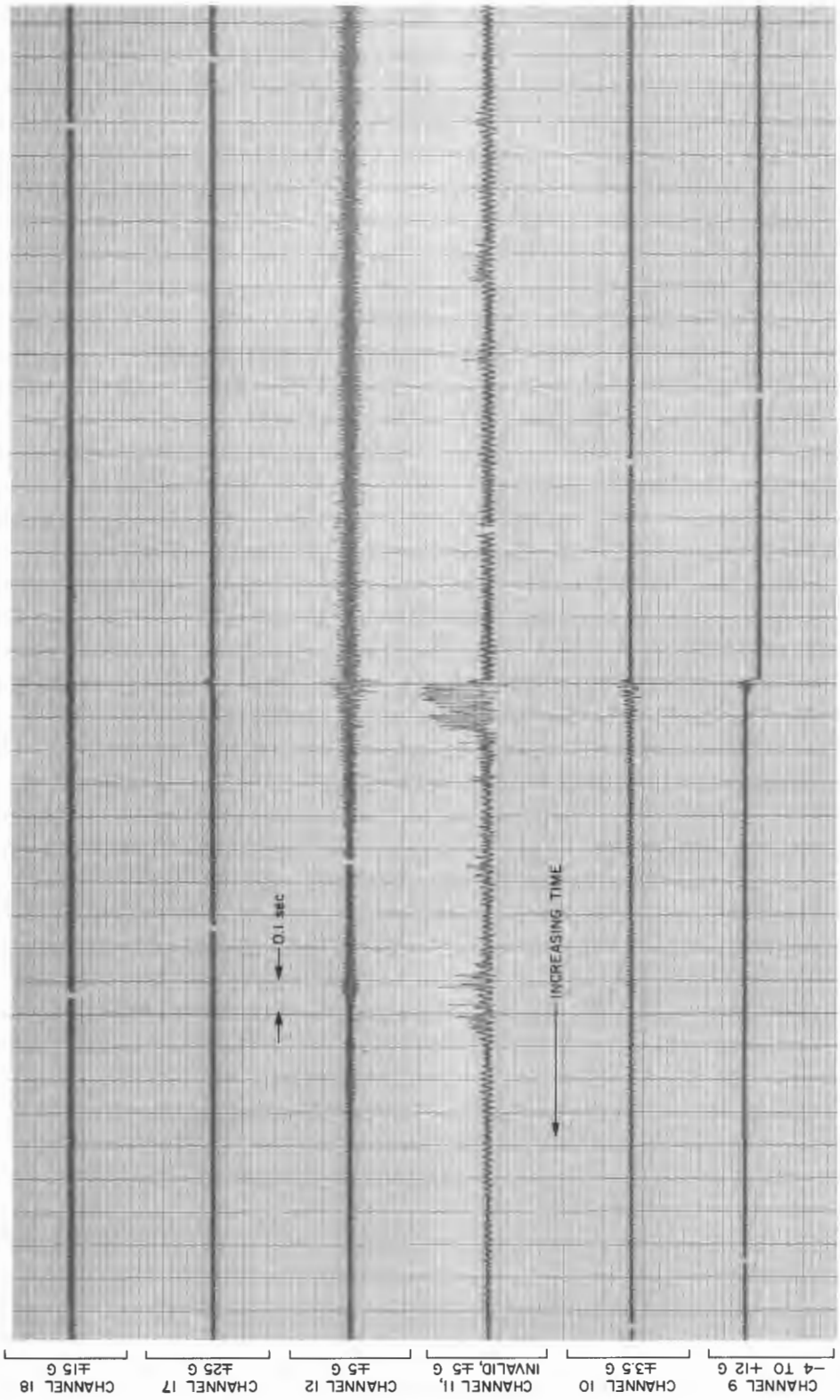

Fig. 26. Oscillogram, *Ranger IX*, 1st *Agena* cutoff

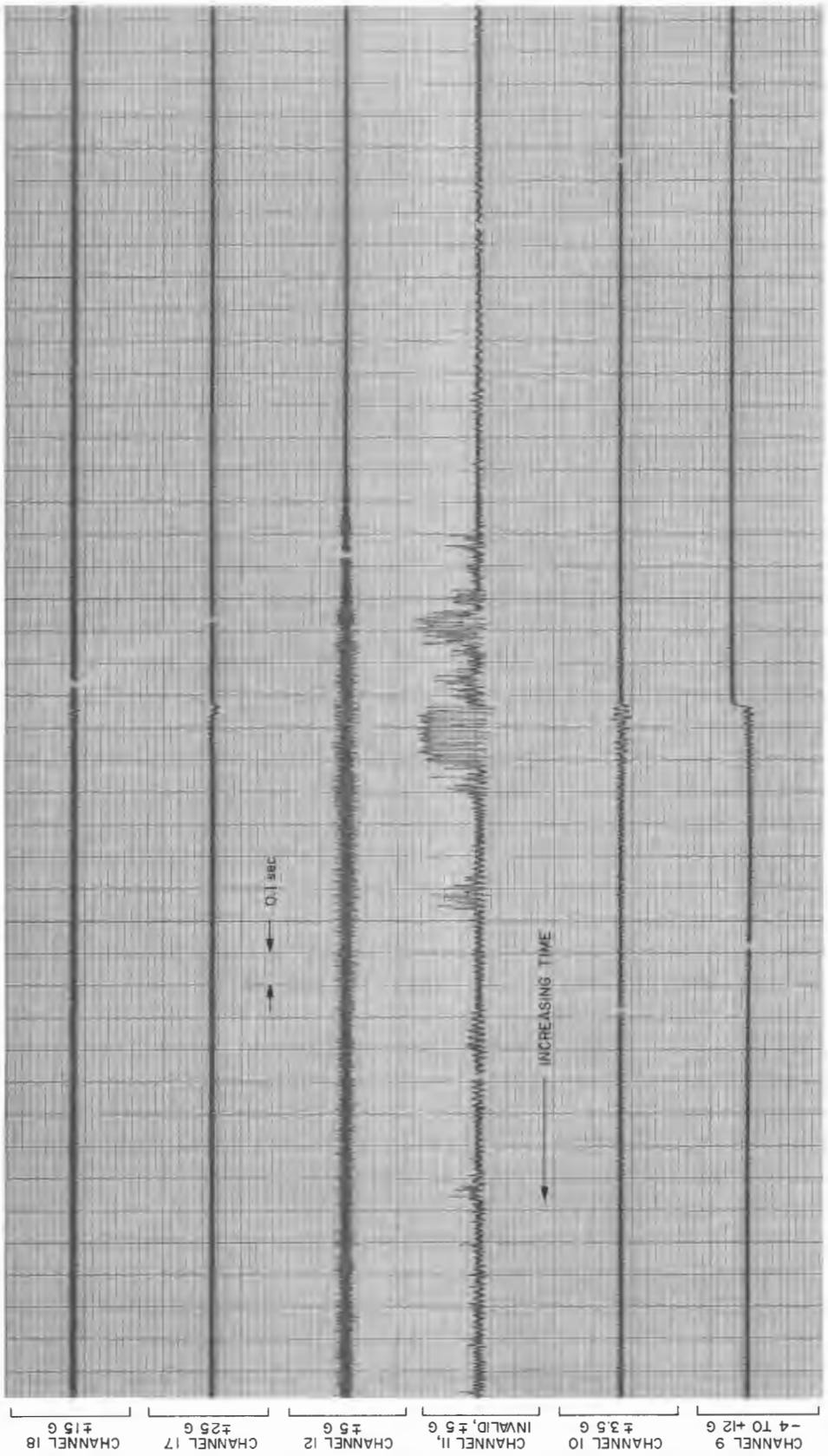

Fig. 27. Oscillogram, *Ranger IX*, 2nd *Agena* ignition

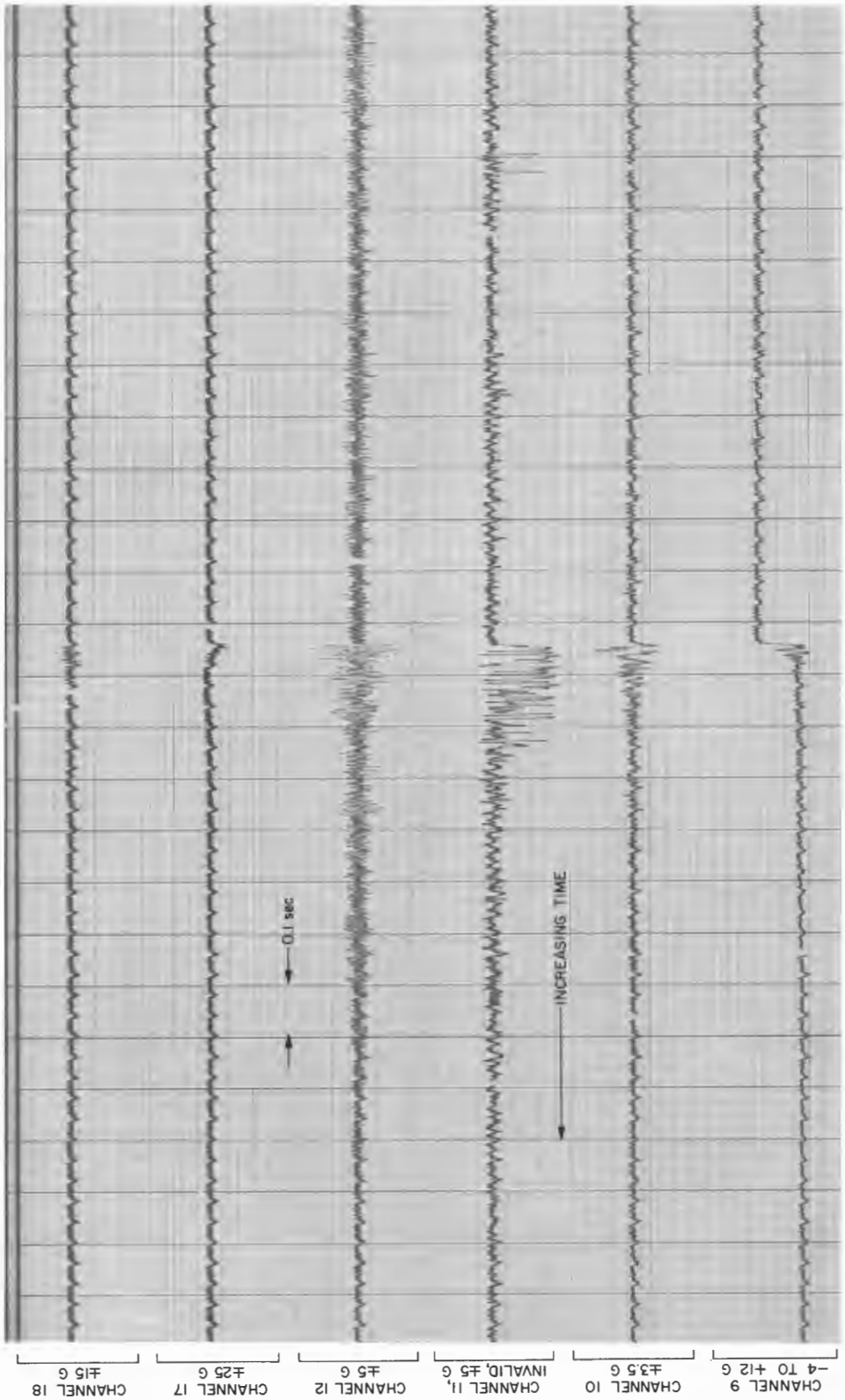

Fig. 28. Oscillogram, *Ranger IX*, 2nd *Agena* cutoff

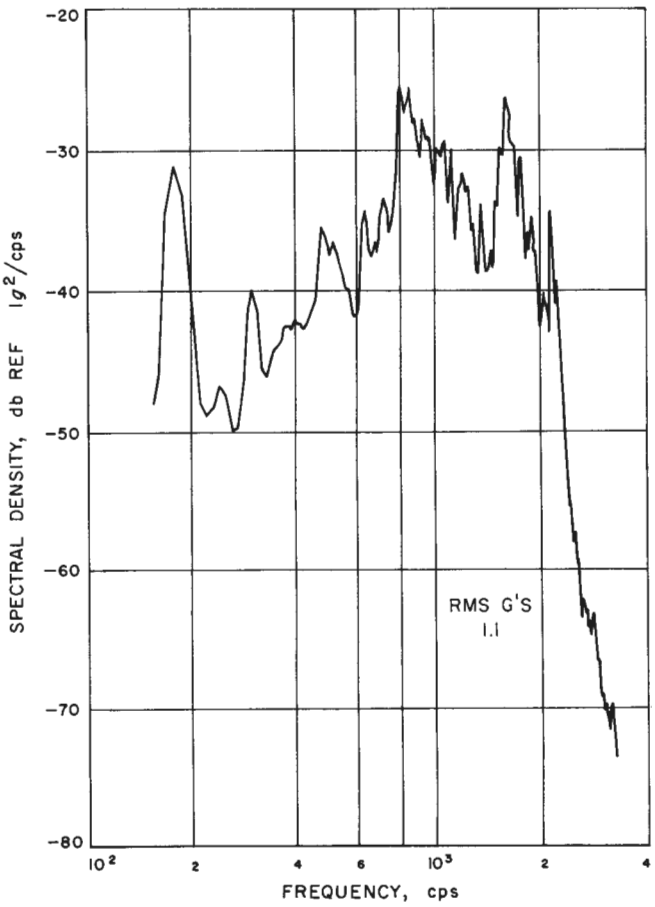

Fig. 29. Acceleration spectral density, *Ranger I*, axial, liftoff

Table 2. Wideband high-frequency vibration levels

Flight	Liftoff, g rms	Transonic, g rms
1	1.5	2.8
2	1.8	3.1
3	1.7	3.5
4	1.7	3.1
5	*	*
6	4.0	8.6
7	2.6	8.0
8	3.2	6.2
9	1.7	4.2

*No high-frequency transducer.

shown for all flights in Fig. 29 through 38. Wideband average levels for liftoff and transonic have been tabulated in Table 2 for all *Ranger* flights.

For purposes of comparison, the data have been grouped and presented in sets. The grouping places data which should be similar (when considering *Ranger–Agena* structure, and transducer location, orientation and mounting) on the same plot.

Structural changes affecting vibration, including removal of the sterilization diaphragm, occurred between Block I and II (*Ranger I, II, III,* and *IV*) and Block III (*Ranger VI, VII, VIII,* and *IX*). Table 3 defines the data sets. Considering the factors shown in Table 3 the most comparable data would appear to be radial *Ranger I, II, III,* and *IV* sets. Indeed, Fig. 30 and 34 do show very repeatable results. However, *Ranger VI, VII, VIII,* and

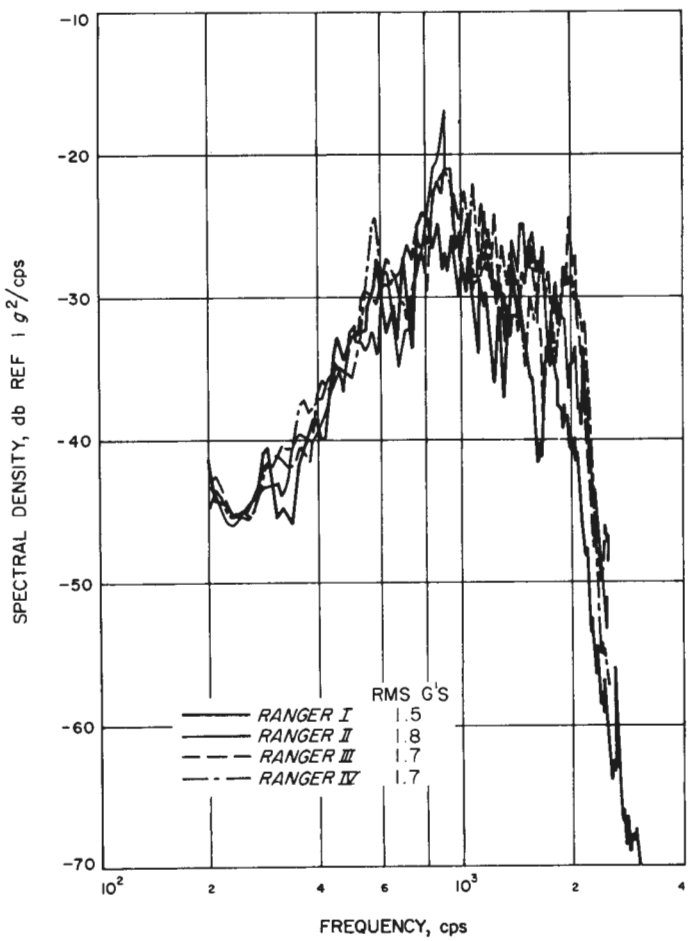

Fig. 30. Acceleration spectral density, *Ranger I, II, III, IV*, radial, liftoff

IX measurements are generally similar with some exceptions in the 1000-cps area.

Table 3. Grouping of *Ranger* flight vibration measurements

Data	Sensitive Axis	Type of Bracket	Comment
Ranger I	Axial	Block I, II	Sterilization diaphragm used
Ranger I, II, III, IV	Radial	Block I, II	Sterilization diaphragm used
Ranger VI, VIII	Radial	Block III	No diaphragm Bracket slightly closer to S/C
Ranger VII, IX	Axial	Block III	Bracket stiffened on *Ranger IX*

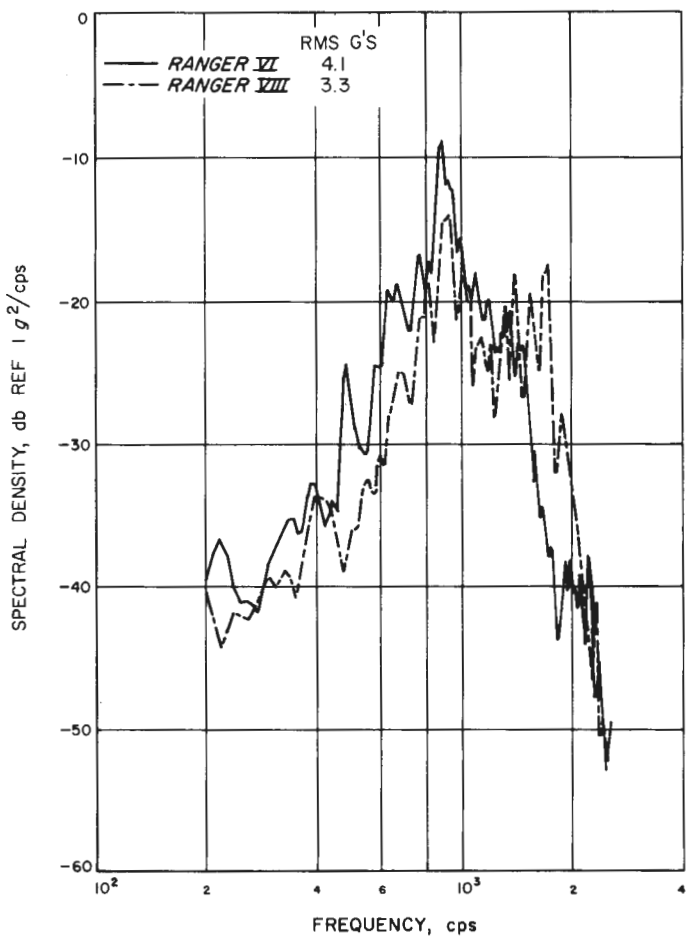

Fig. 31. Acceleration spectral density, *Ranger VI, VIII*, radial, liftoff

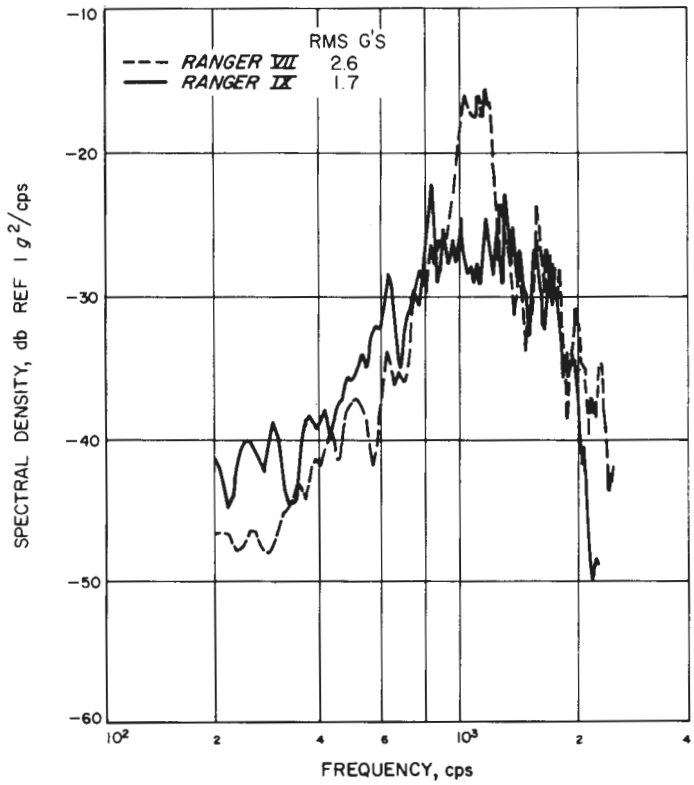

Fig. 32. Acceleration spectral density, *Ranger VII, IX*, axial, liftoff

It has been established that the accelerometer mounting bracket used on *Ranger VI*, *VII*, and *VIII* had a resonant frequency in the 1000-cps area affecting both radial and axial measurements. This effect is discussed further in Section IV.

The only vibration measurements made on the actual spacecraft structure were made on the *Ranger VIII* and *IX* flights. Data from liftoff and transonic for these measurements is shown in Fig. 37 and 38.

The data signals from low-frequency transducers (Channels 9, 10, 11, 12) were also reduced to power spectral density plots; however, because of the limited frequency range, little application of this data to environmental definition was possible and the data is not included here.

C. *Acoustic Environment*

Data defining the acoustic environment were collected during the final four flights, *Ranger VI*, *VII*, *VIII*, and *IX*. Measurements made consisted of a flight microphone

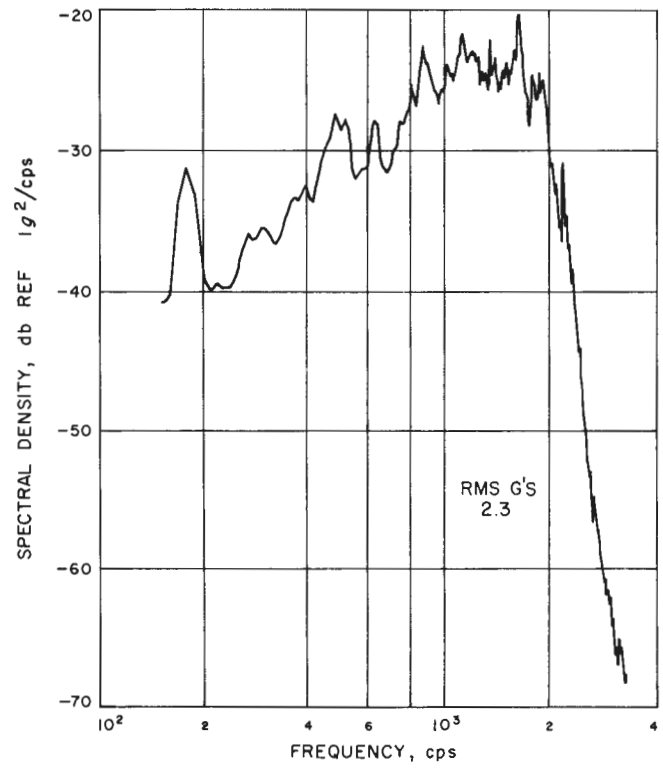

Fig. 33. Acceleration spectral density, *Ranger I*, axial, transonic

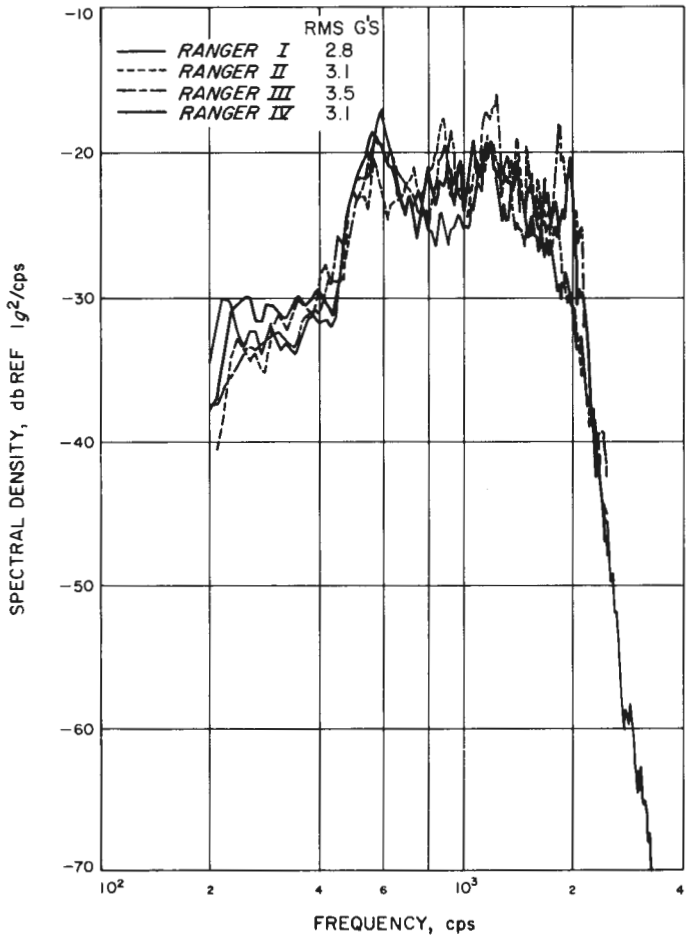

Fig. 34. Acceleration spectral density, *Ranger I, II, III, IV*, radial, transonic

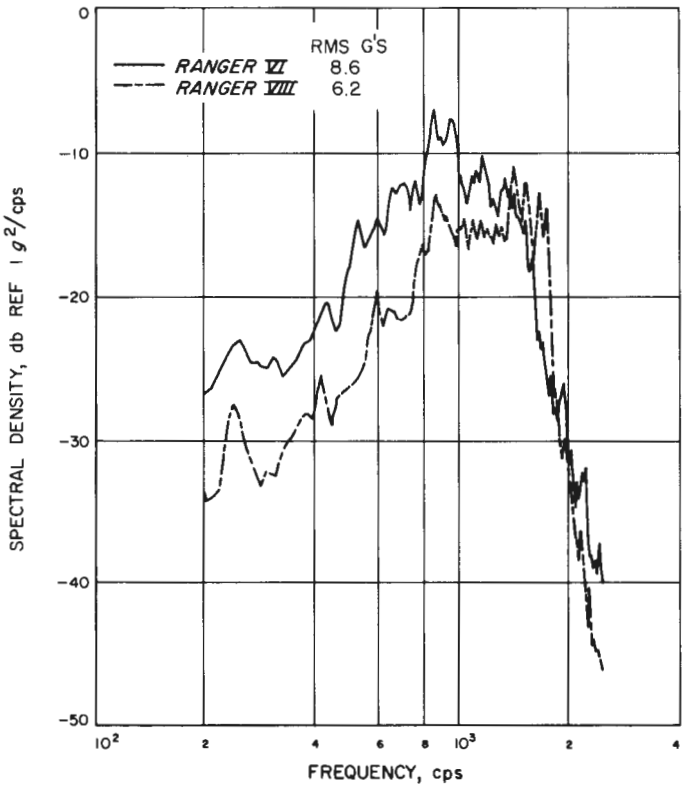

Fig. 35. Acceleration spectral density, *Ranger VI, VIII*, radial, transonic

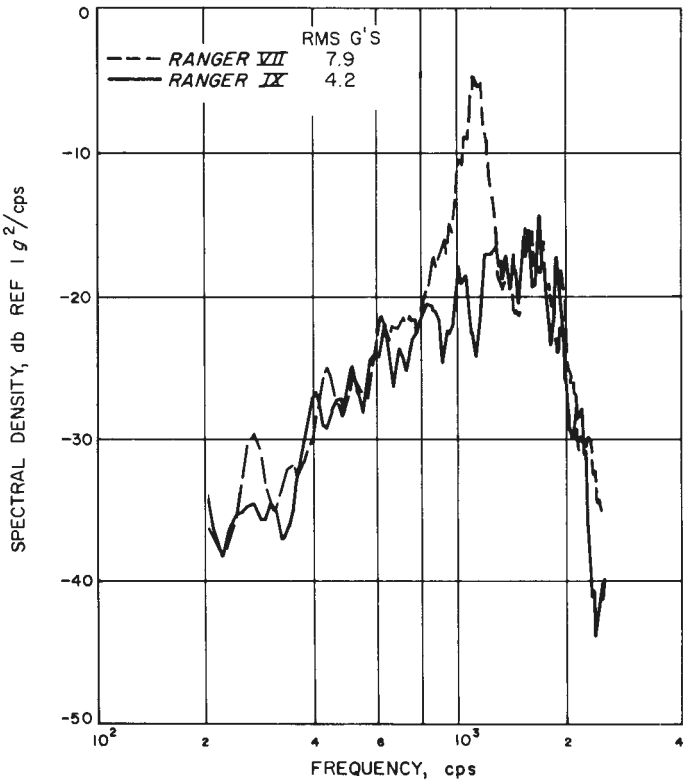

Fig. 36. Acceleration spectral density, *Ranger VII, IX,* axial, transonic

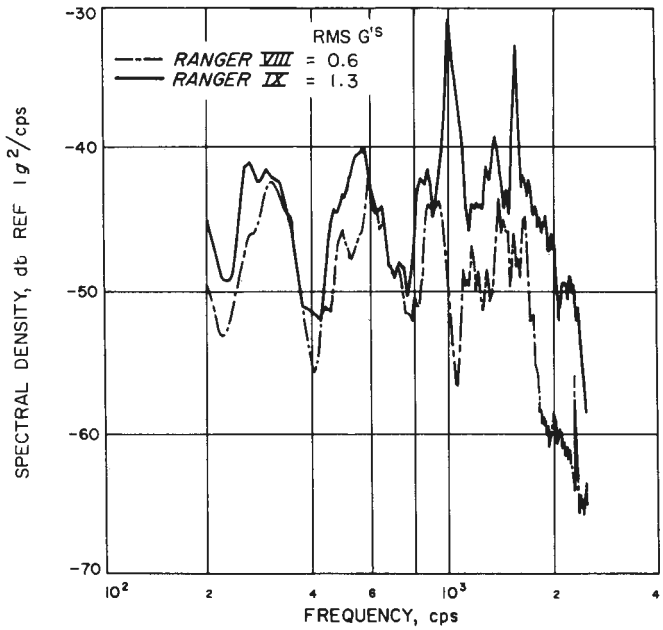

Fig. 38. Acceleration spectral density, *Ranger VIII, IX,* spacecraft lateral, transonic

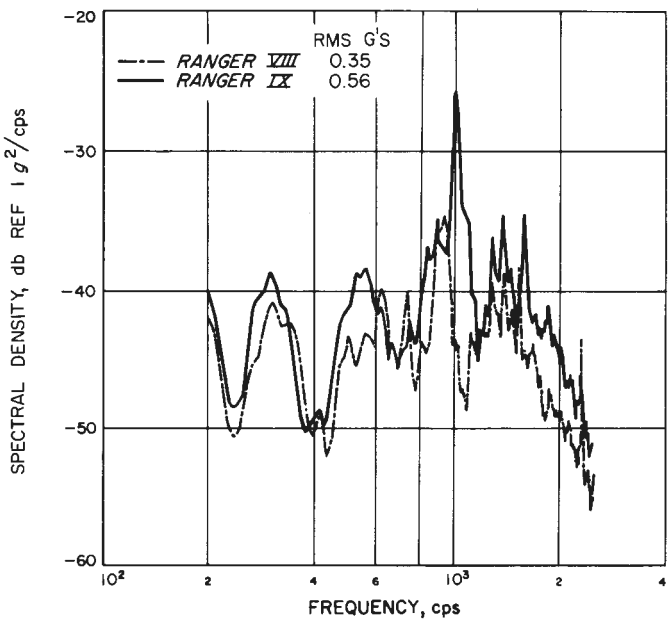

Fig. 37. Acceleration spectral density, *Ranger VIII, IX,* spacecraft lateral, liftoff

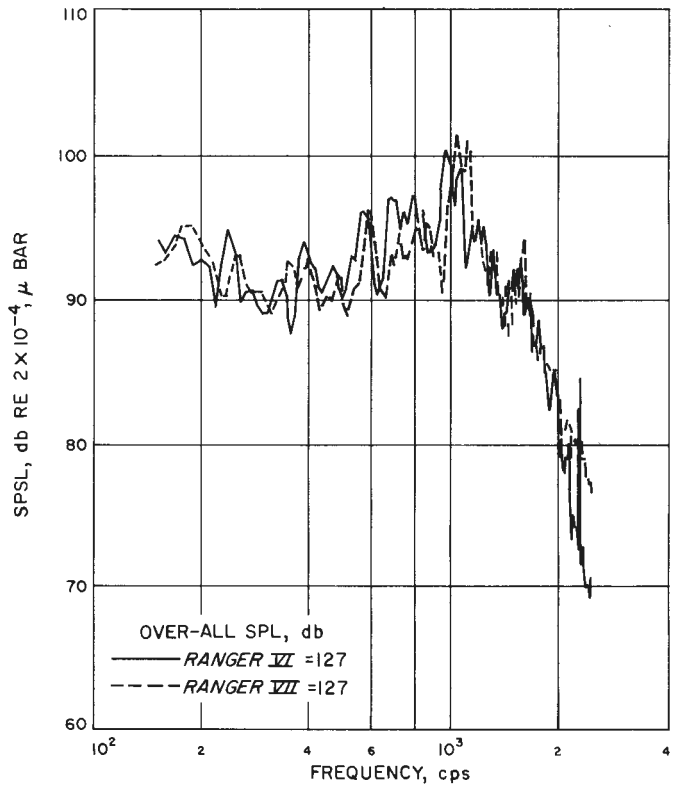

Fig. 39. Sound pressure spectrum level, *Ranger VI, VIII,* liftoff

flown on *Ranger VI* and *VII* and ground measurements made with microphones in the launch pad–umbilical tower area.

The flight microphones used on *Ranger VI* and *VII* were mounted in the spacecraft (S/C) shroud (Fig. 8). Sound-pressure spectrum levels from these measurements are shown for liftoff and transonic in Fig. 39 and 40. The same data shown as sound pressure level in ⅓ octave bands are shown in Fig. 41 and 42.

The ground acoustic measurements which are presented here consist of one measurement from each of *Ranger VI* through *IX*. The *Ranger VI*, *VII*, and *VIII* measurement locations on the umbilical tower are identical while the *Ranger IX* measurement is somewhat nearer the spacecraft on the umbilical tower boom. Results of these measurements are shown in Fig. 43 and 44. These measurements were made at approximately −0.5 to 1.5 sec relative to $T = 0$ (liftoff). Good agreement between all four flights is seen with the exception of the 550-cps notch which is missing on the *Ranger IX* measurement, probably an effect of launch-pad geometry on a slightly different microphone location.

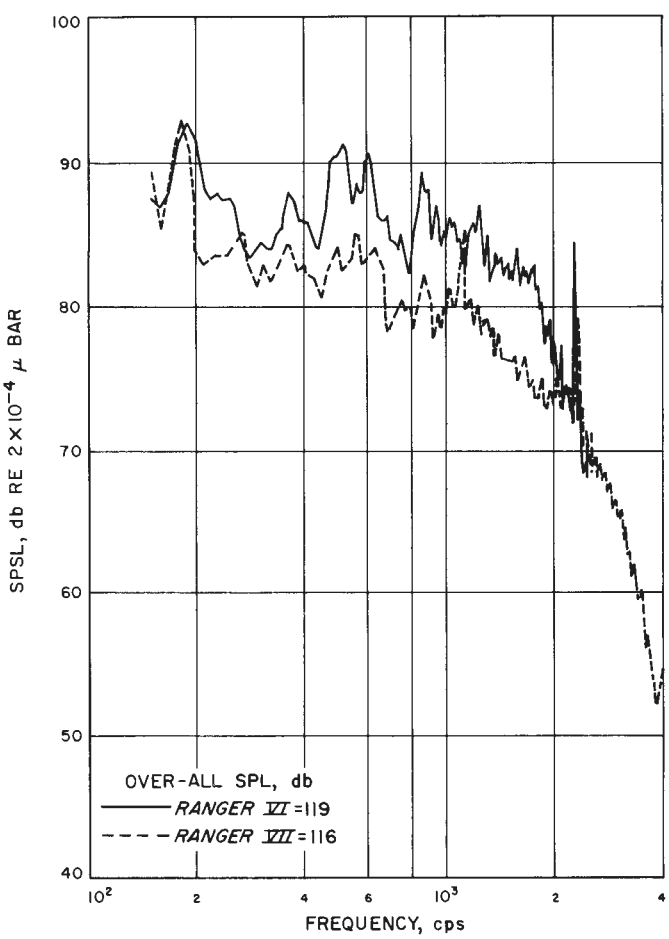

Fig. 40. Sound pressure spectrum level, *Ranger VI, VII,* transonic

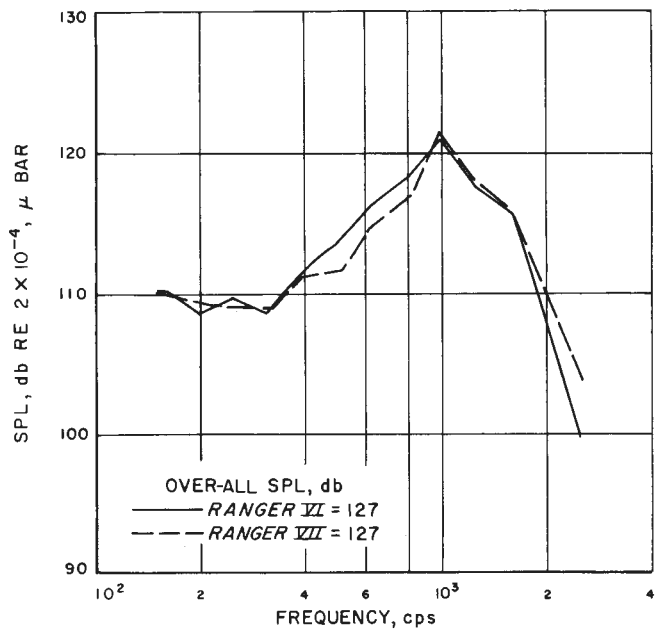

Fig. 41. Sound pressure level, ⅓ octave bands, *Ranger VI, VII,* liftoff

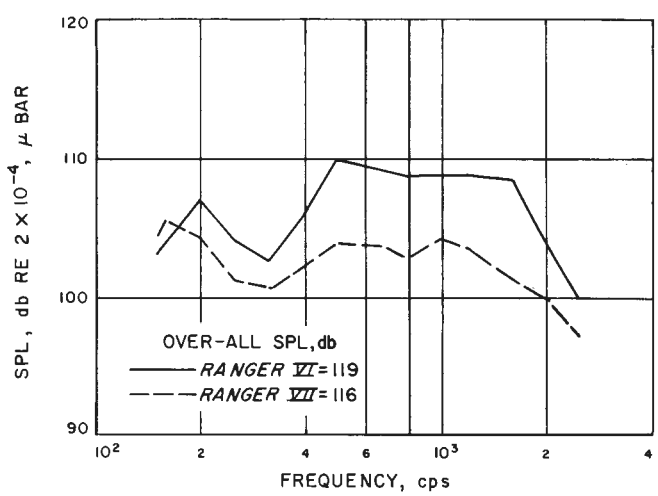

Fig. 42. Sound pressure level, ⅓ octave bands, *Ranger VI, VII,* transonic

D. Shock Environment

Transient vibration or shock data are presented in this section. The data presentation is in the form of the time

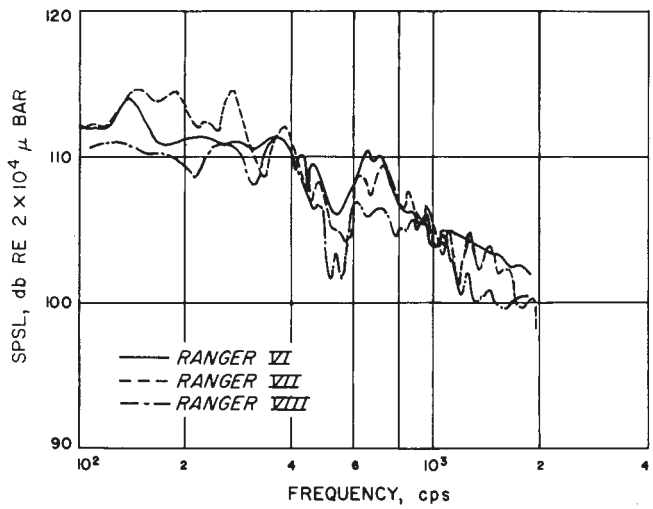

Fig. 43. Sound pressure spectrum level, umbilical tower microphones, *Ranger VI, VII, VIII*

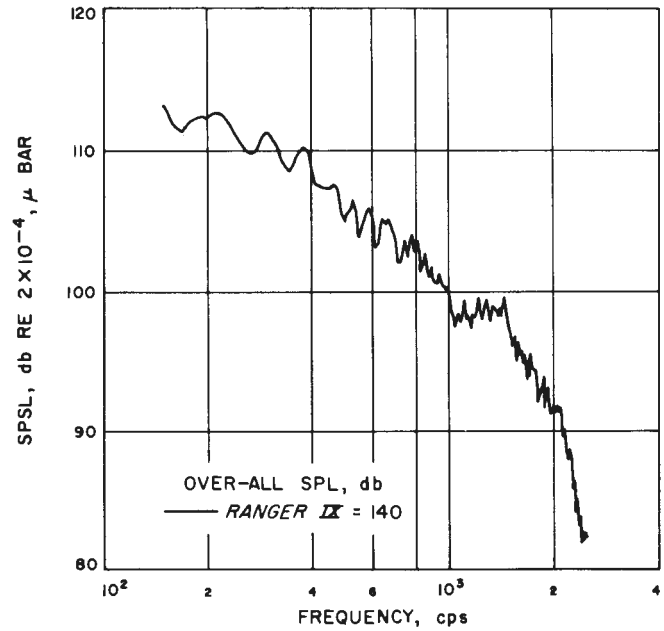

Fig. 44. Sound pressure spectrum level, umbilical boom microphone, *Ranger IX*

history of the transients and the associated shock spectra. Both high-frequency and low-frequency events are included. The data presentation shows superimposed spectra for similar events and measurement locations. The selection of data to be presented here was accomplished by reviewing all flight data which had been analyzed with shock spectrum analysis, choosing those waveforms which appear to be valid data signals, and grouping the spectra into equivalent sets. While not all data from all flights are included, the data presented are the best available and are considered to be representative of the various transients which occur. All shock spectra presented were computed with a damping factor of 2.5% of critical damping ($Q = 20$). Figures 45–57 illustrate the shock spectra for the various events of the *Ranger* Block I, II, III flights.

The transient event which is most thoroughly described in this section is booster engine cutoff (BECO). This event received special attention during the *Ranger* program because of the torsional nature of the excitation at the *Ranger–Agena* interface. Data from all flights are included for this event.

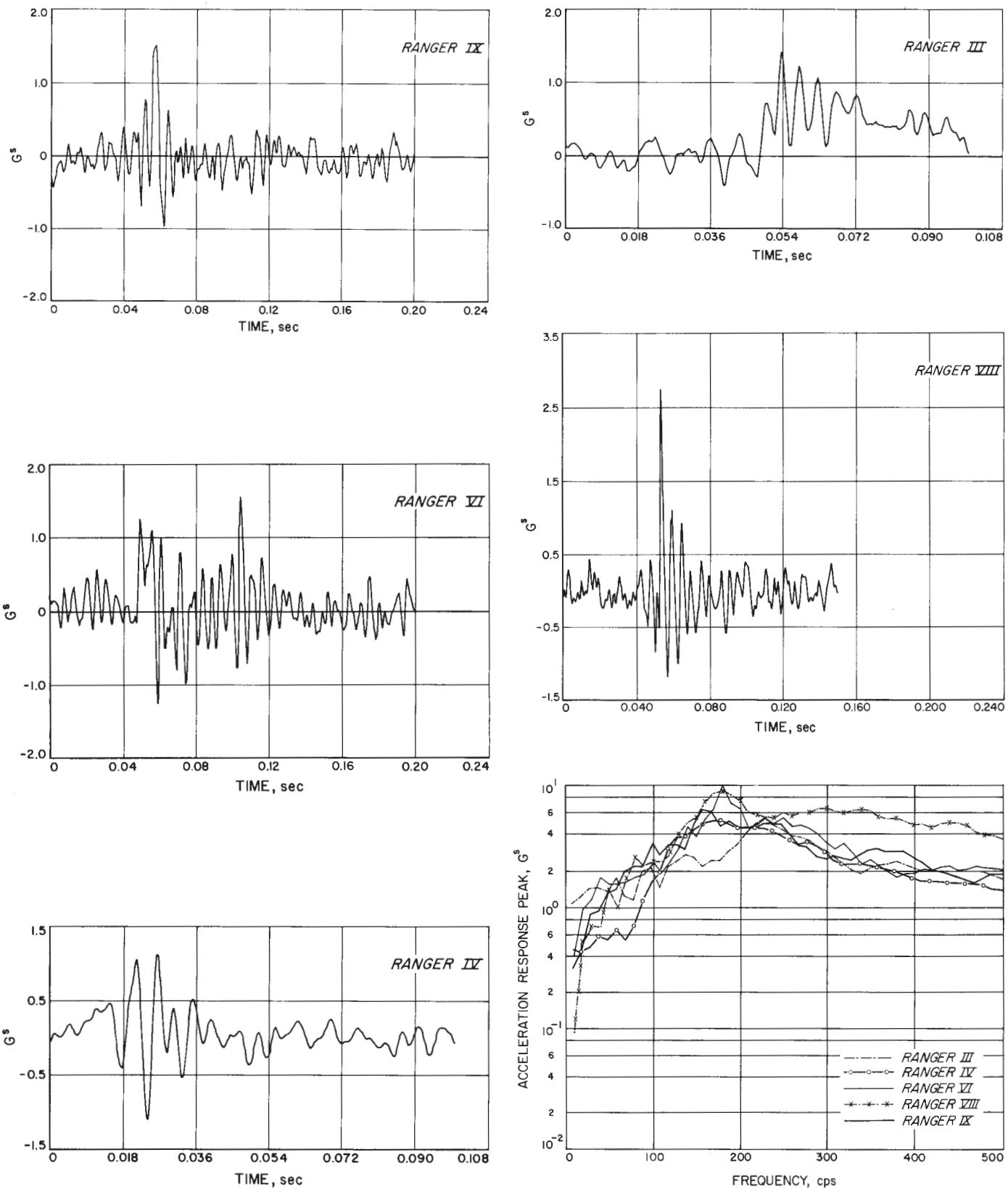

Fig. 45. Shock spectra, liftoff transient, radial, channel 10

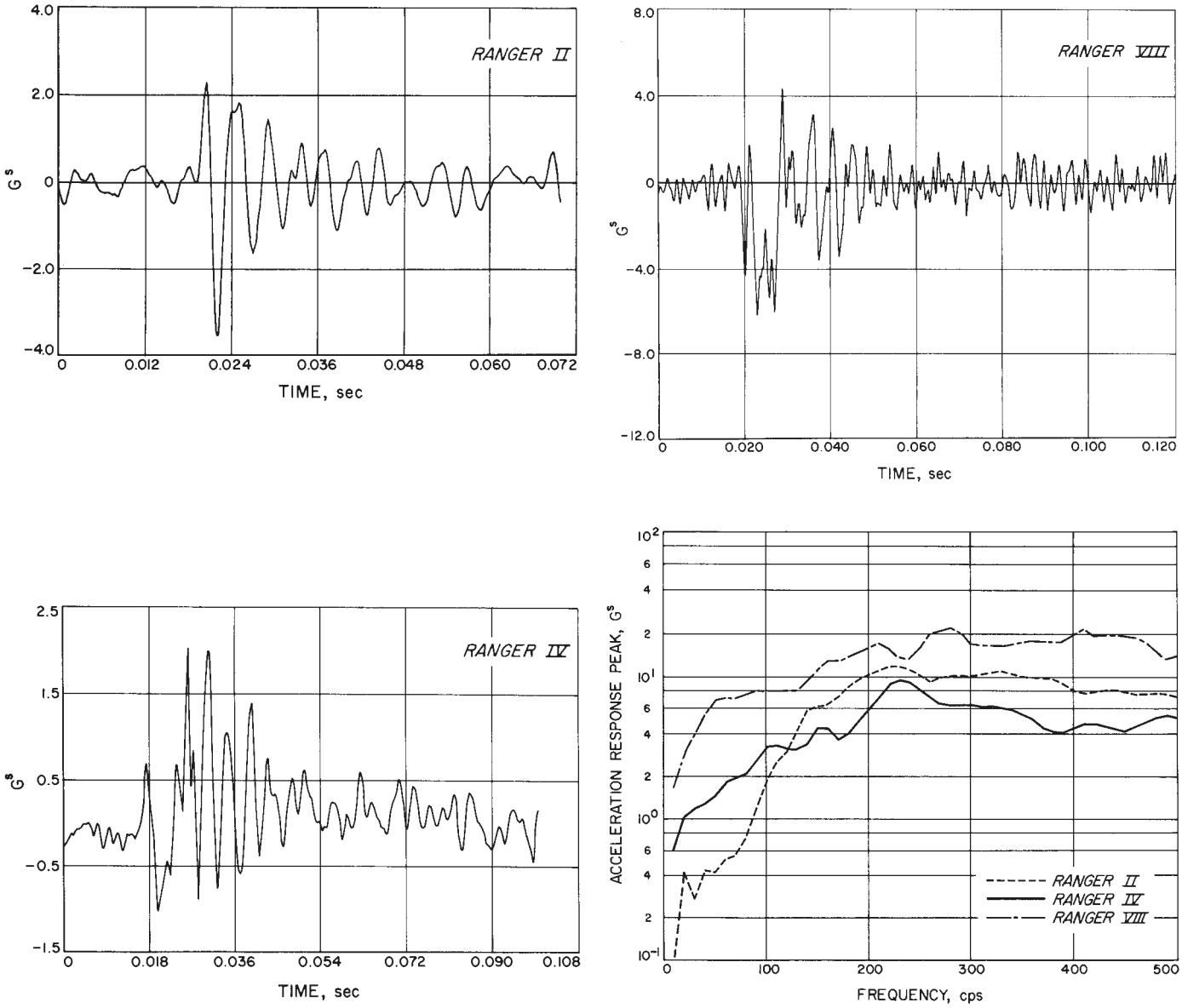

Fig. 46. Shock spectra, liftoff transient, tangential, channel 12

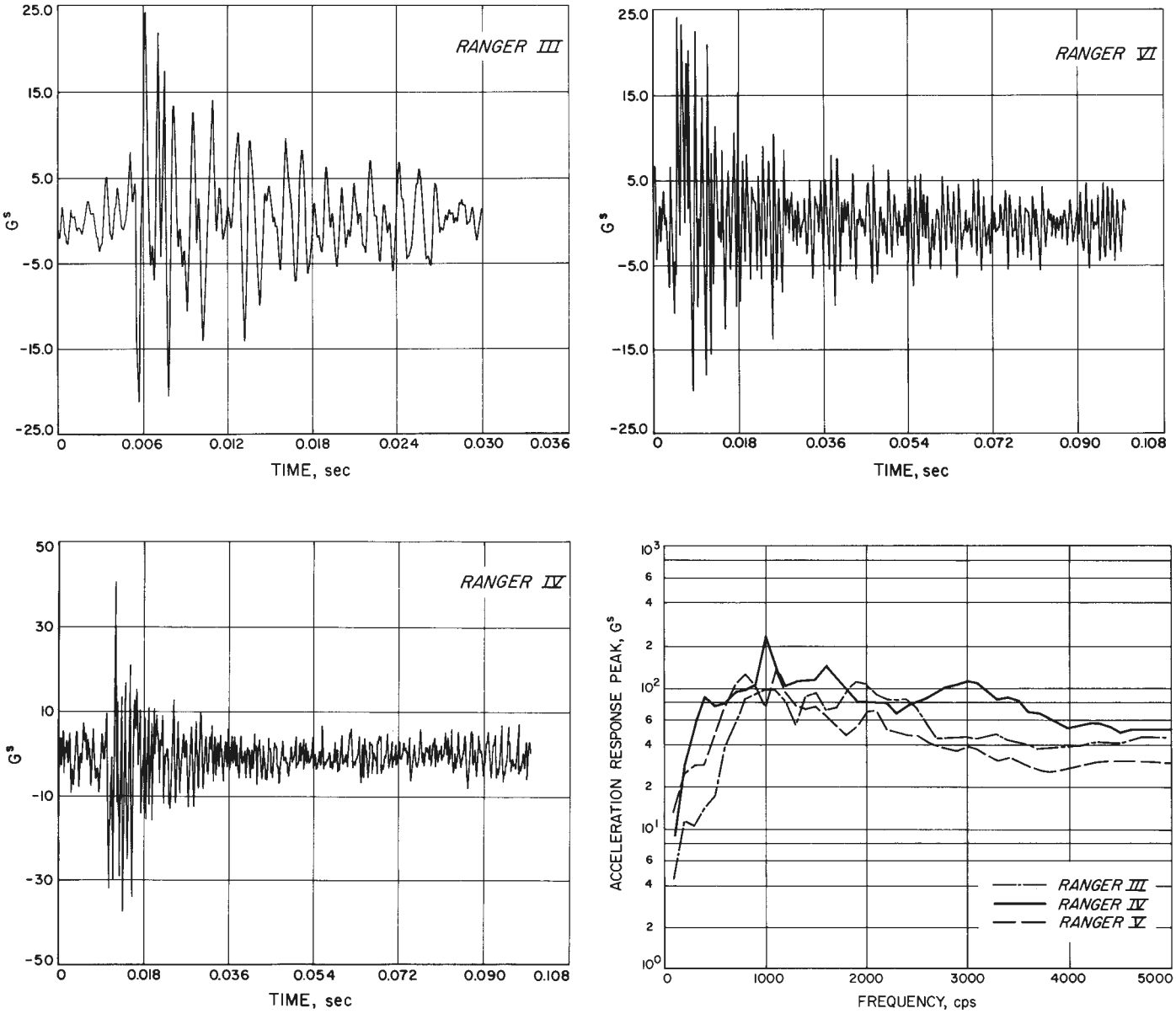

Fig. 47. Shock spectra, liftoff transient, radial, channel 17, 18

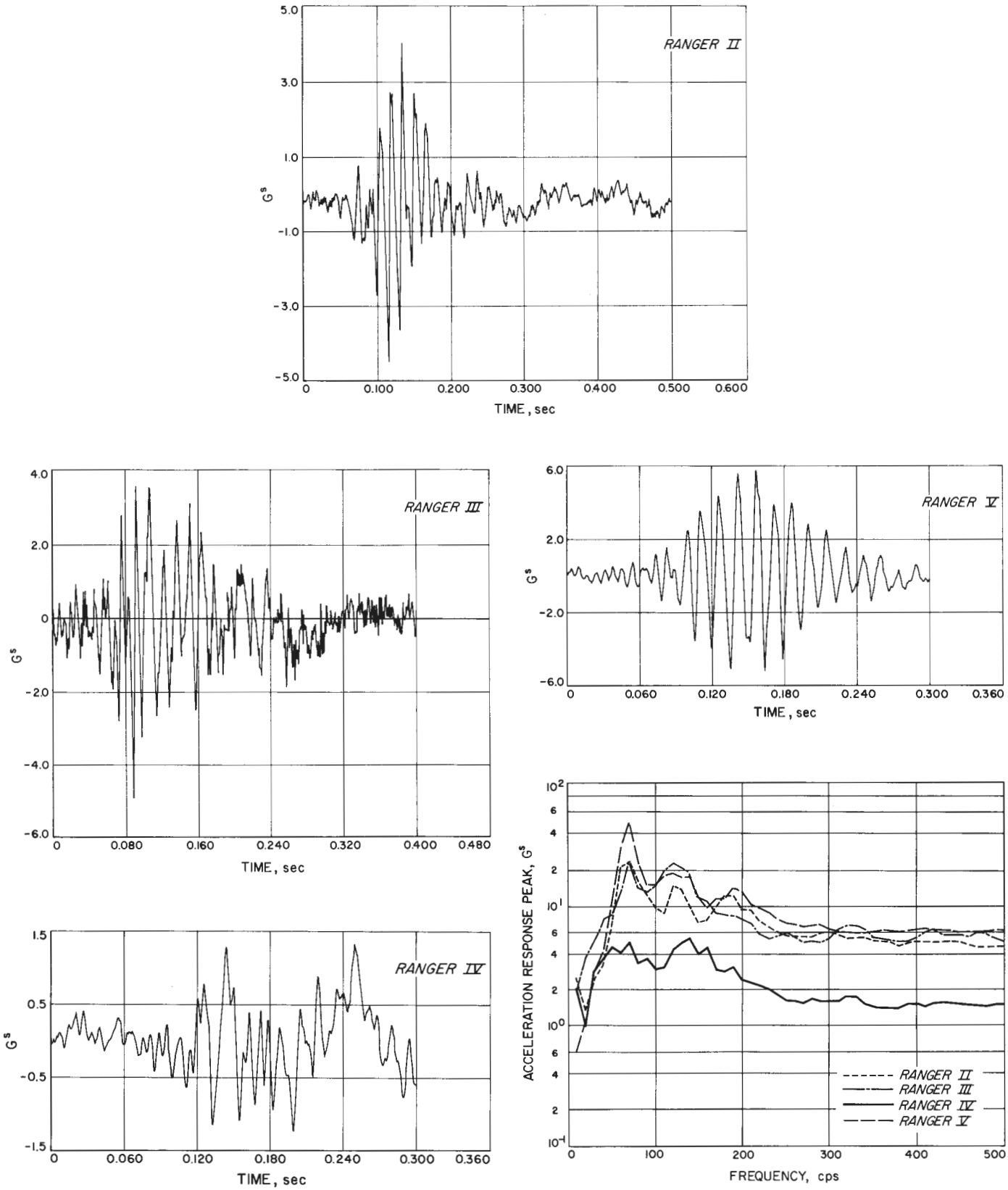

Fig. 48. Shock spectra, BECO, tangential, channel 12, Block I and II

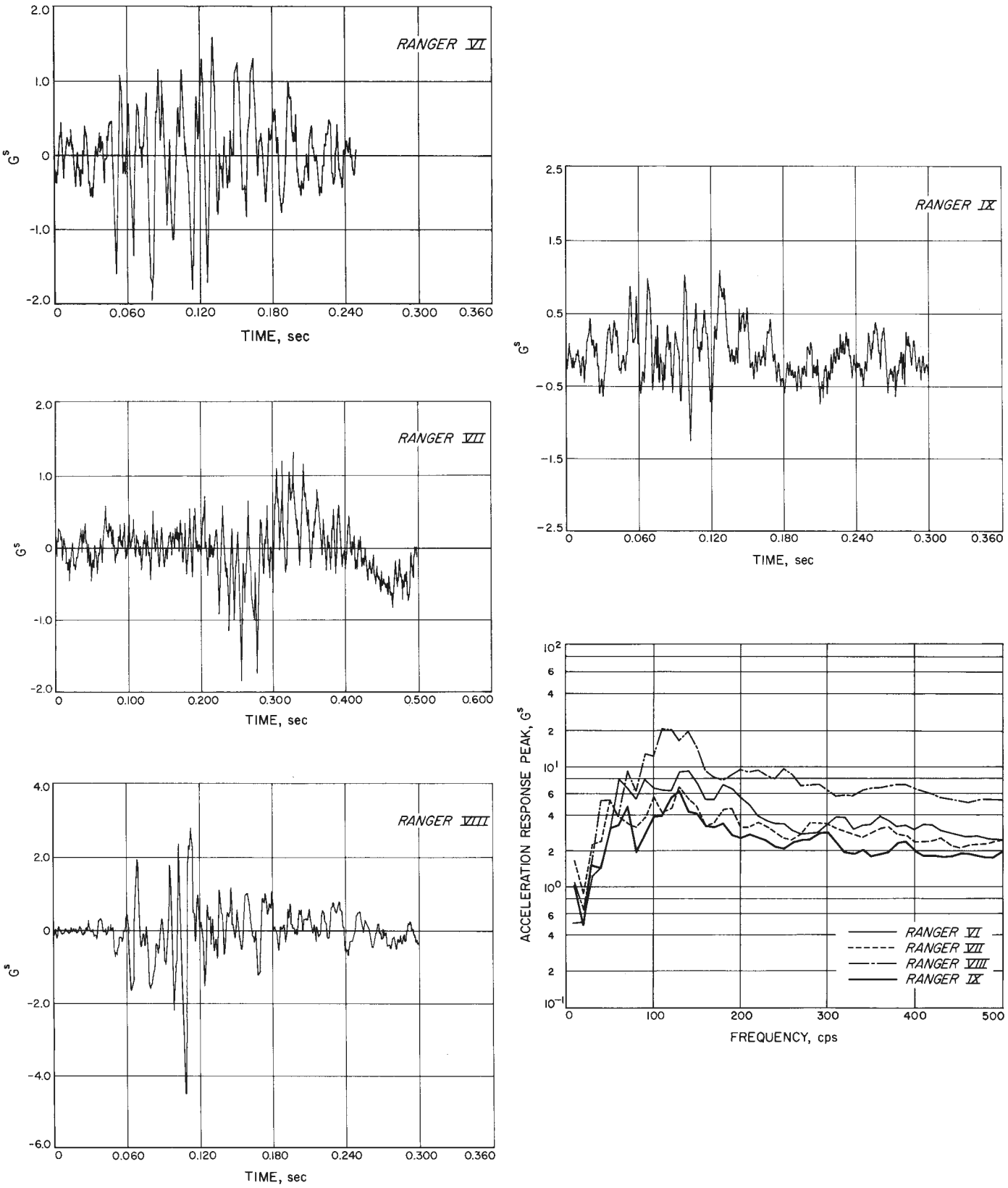

Fig. 49. Shock spectra, BECO, tangential, channel 12, Block III

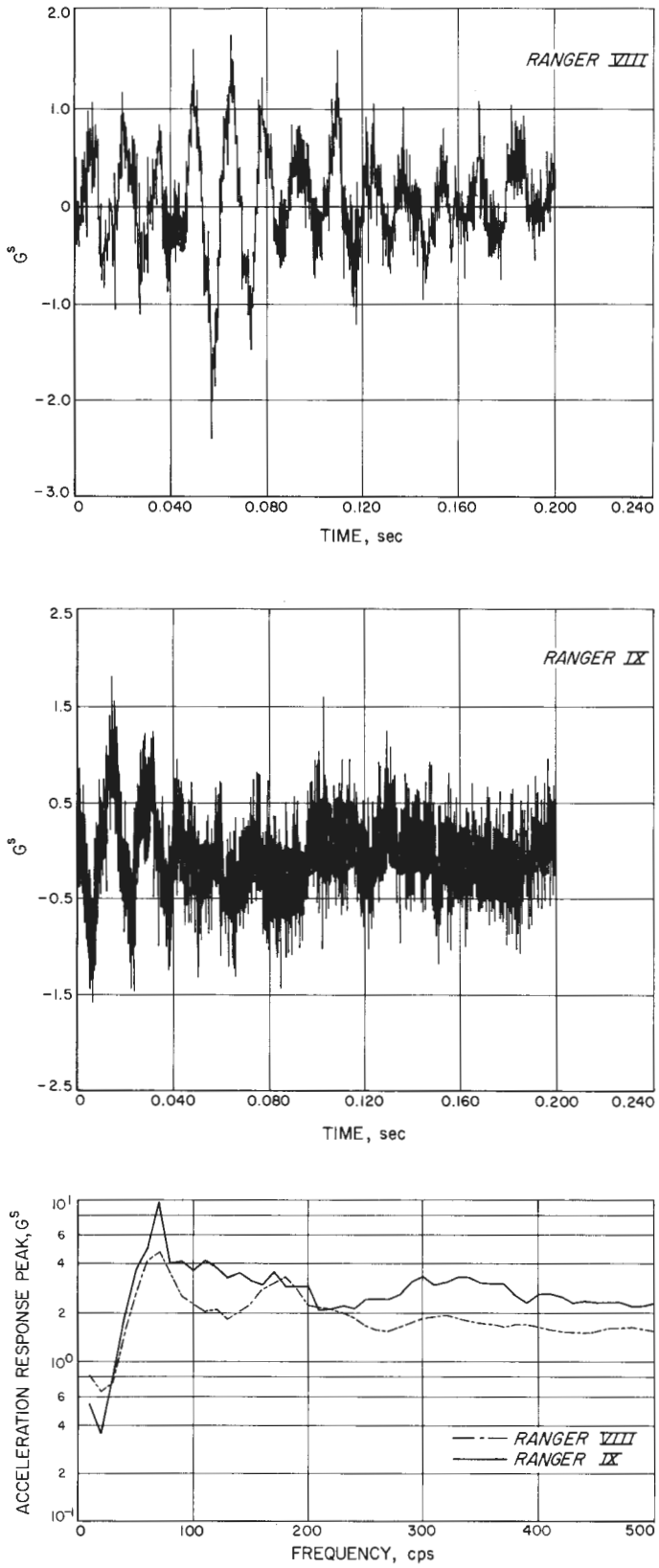

Fig. 50. Shock spectra, BECO, spacecraft lateral, channel 18

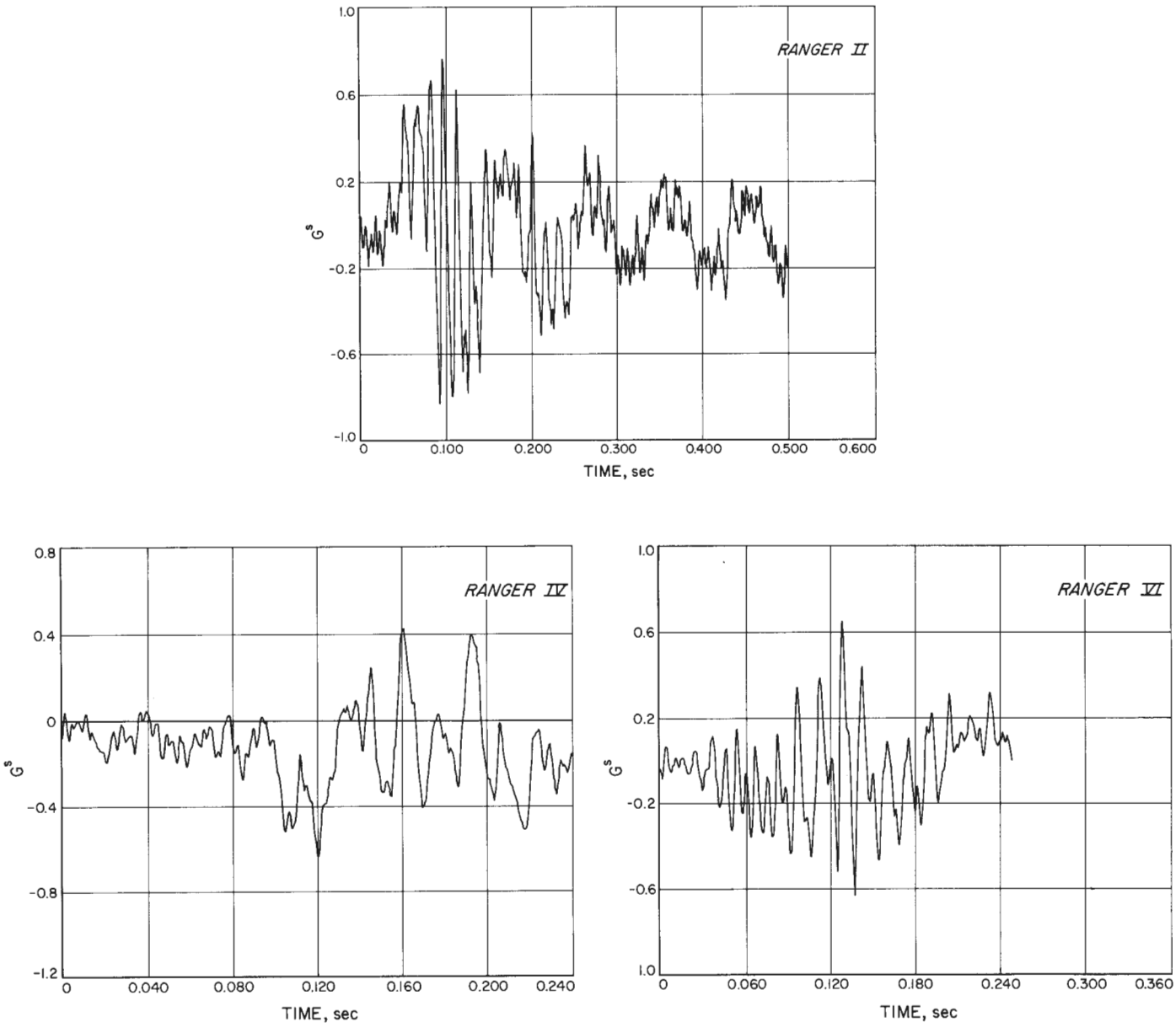

Fig. 51. Shock spectra, BECO, radial, channel 10

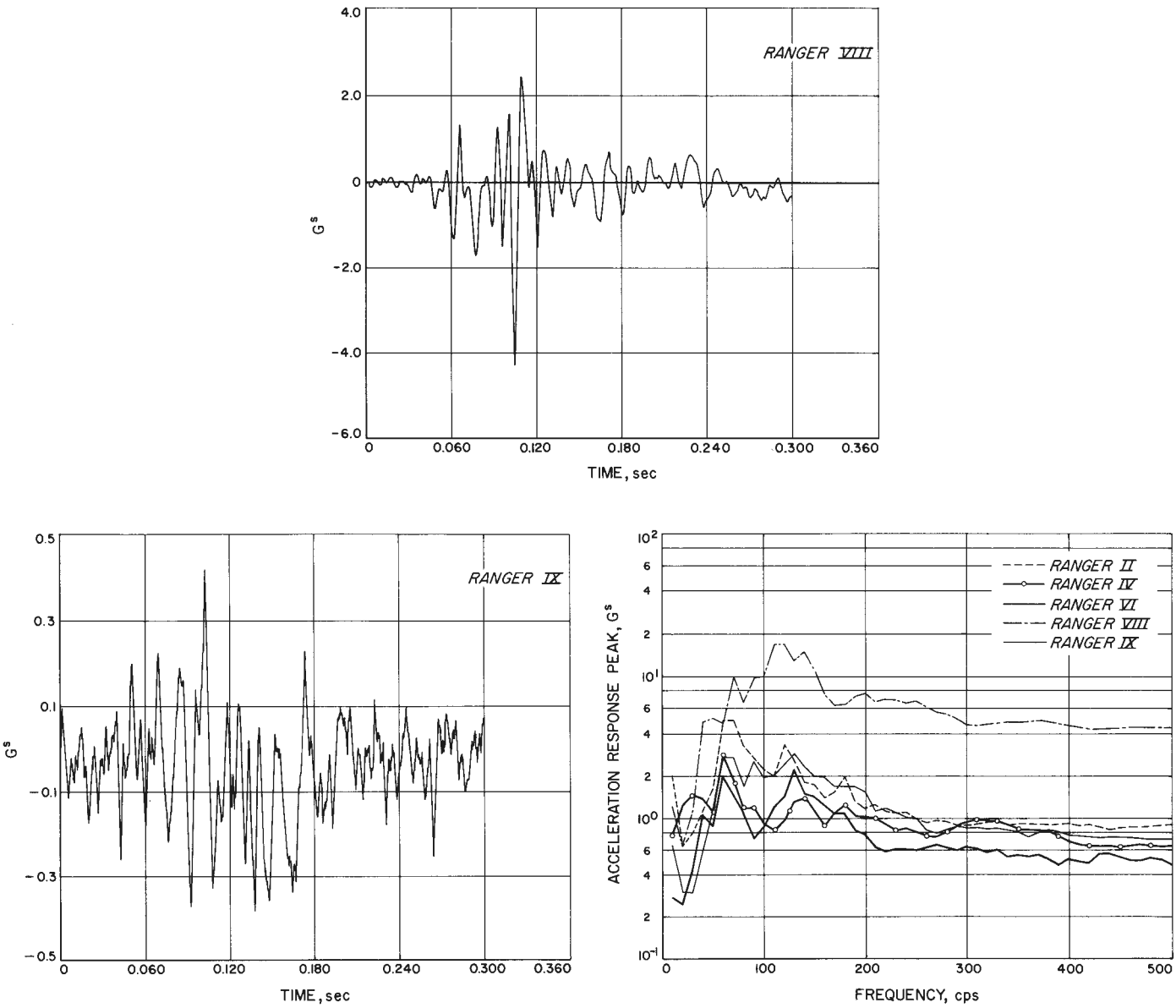

Fig. 51. Shock spectra, BECO, radial, channel 10 (cont'd)

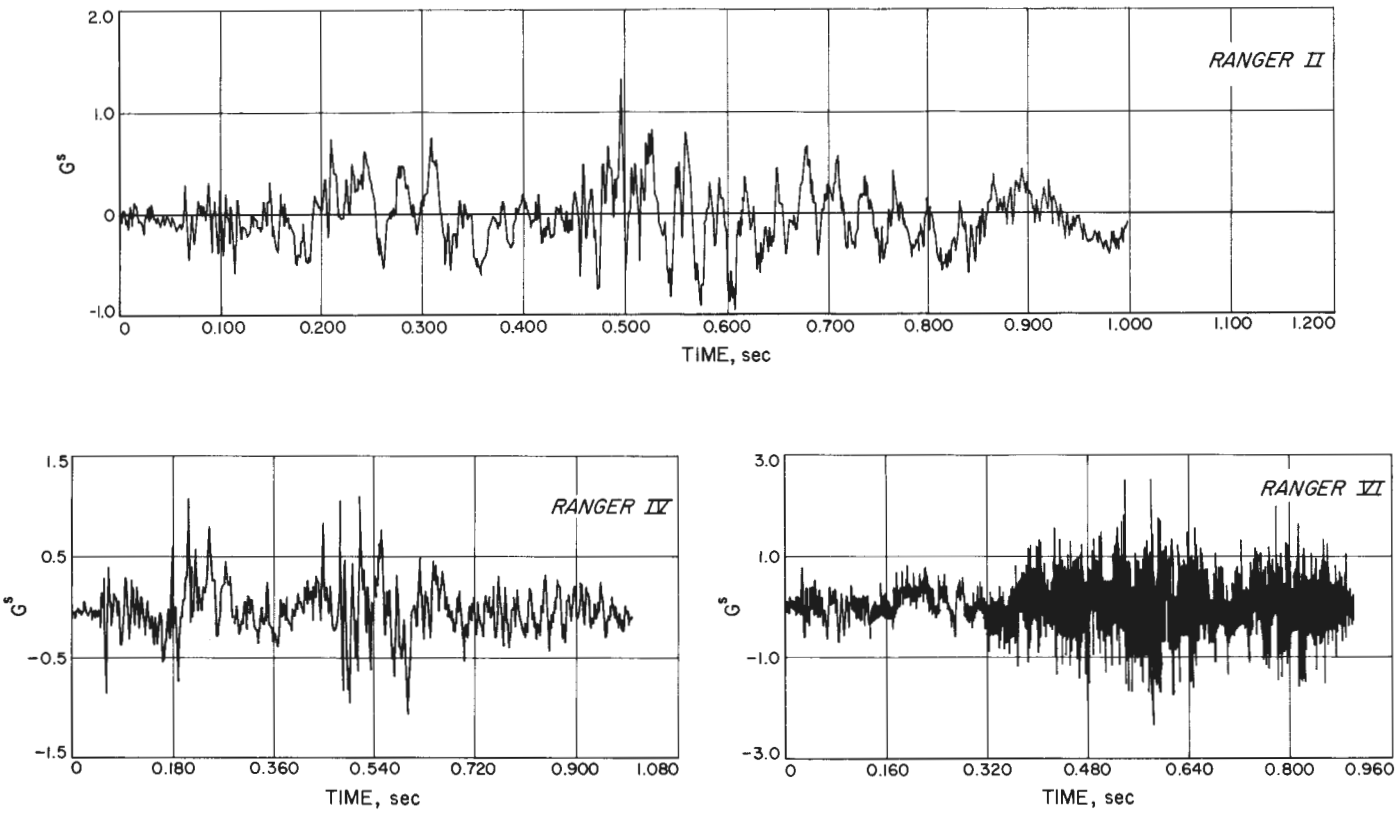

Fig. 52. Shock spectra, booster separation, tangential, channel 12

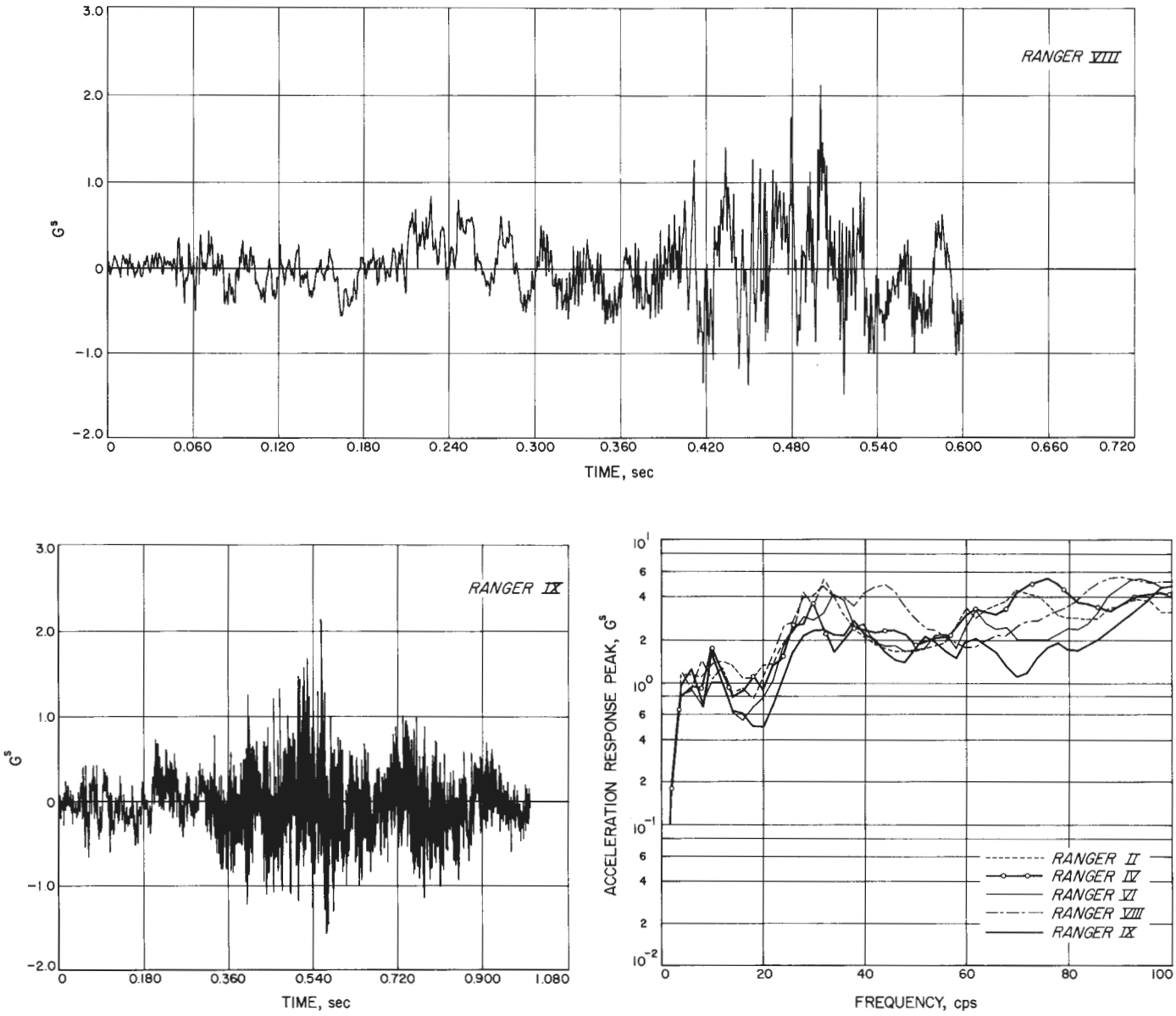

Fig. 52. Shock spectra, booster separation, tangential, channel 12 (cont'd)

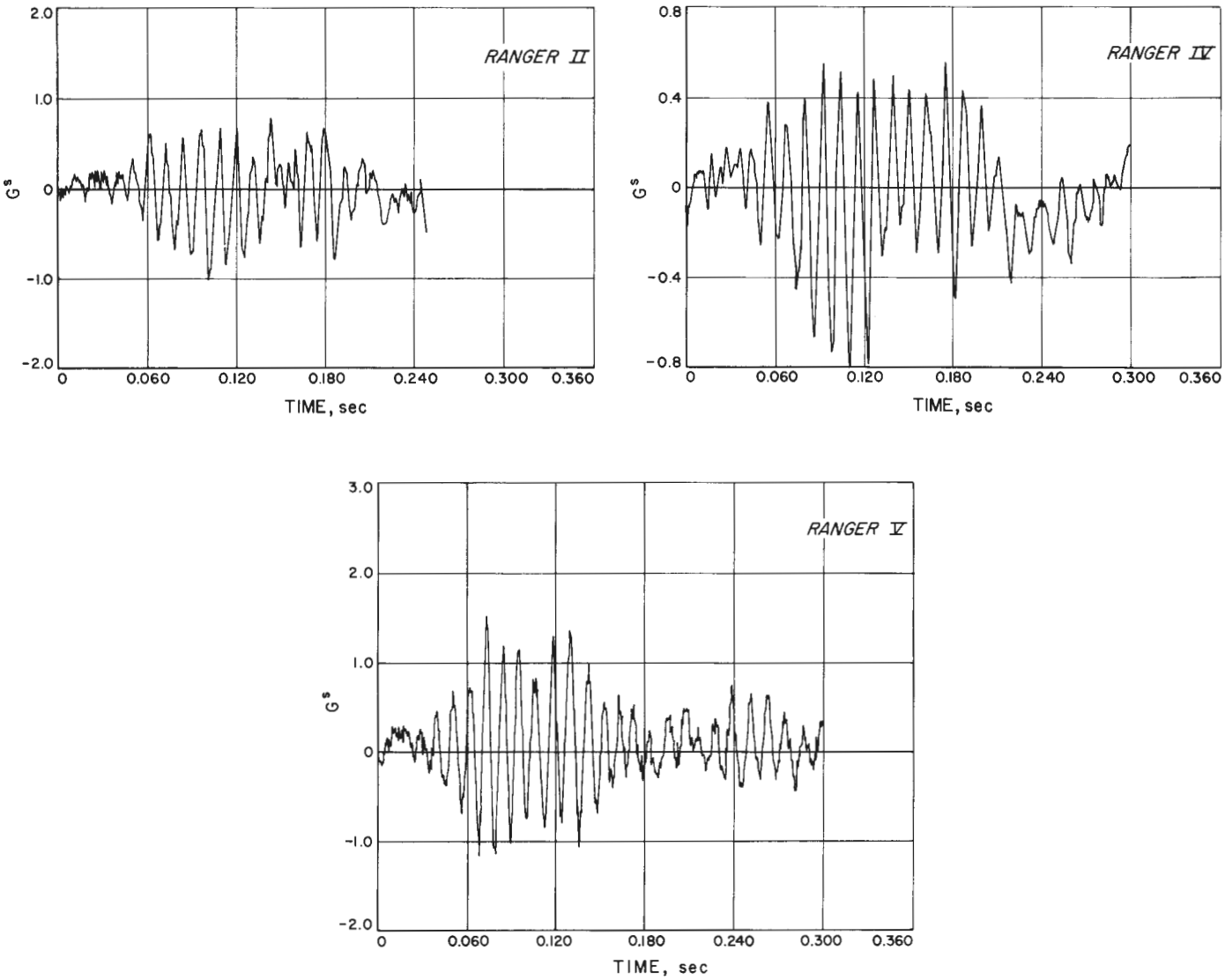

Fig. 53. Shock spectra, SECO, tangential, channel 11, 12

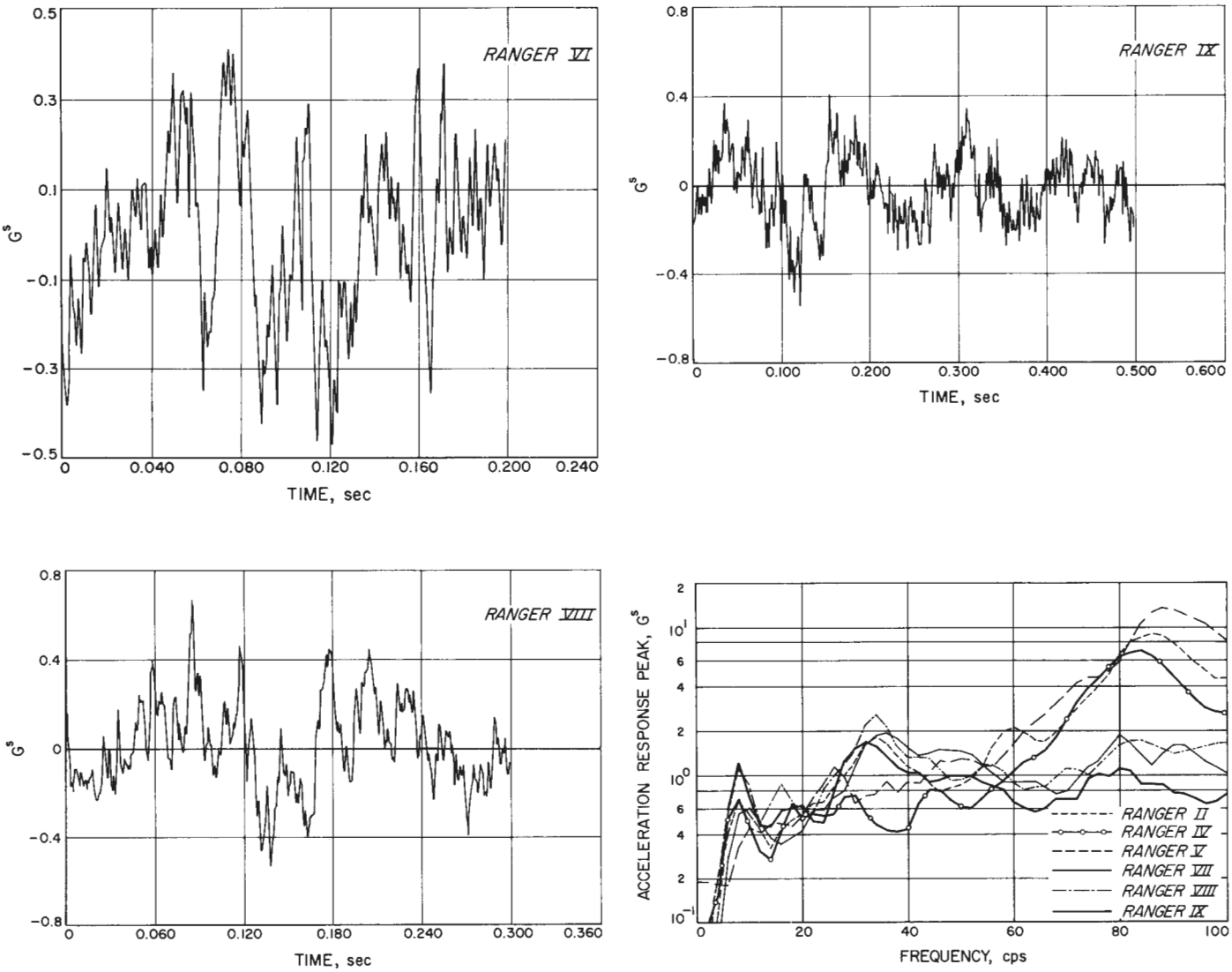

Fig. 53. Shock spectra, SECO, tangential, channel 11, 12 (cont'd)

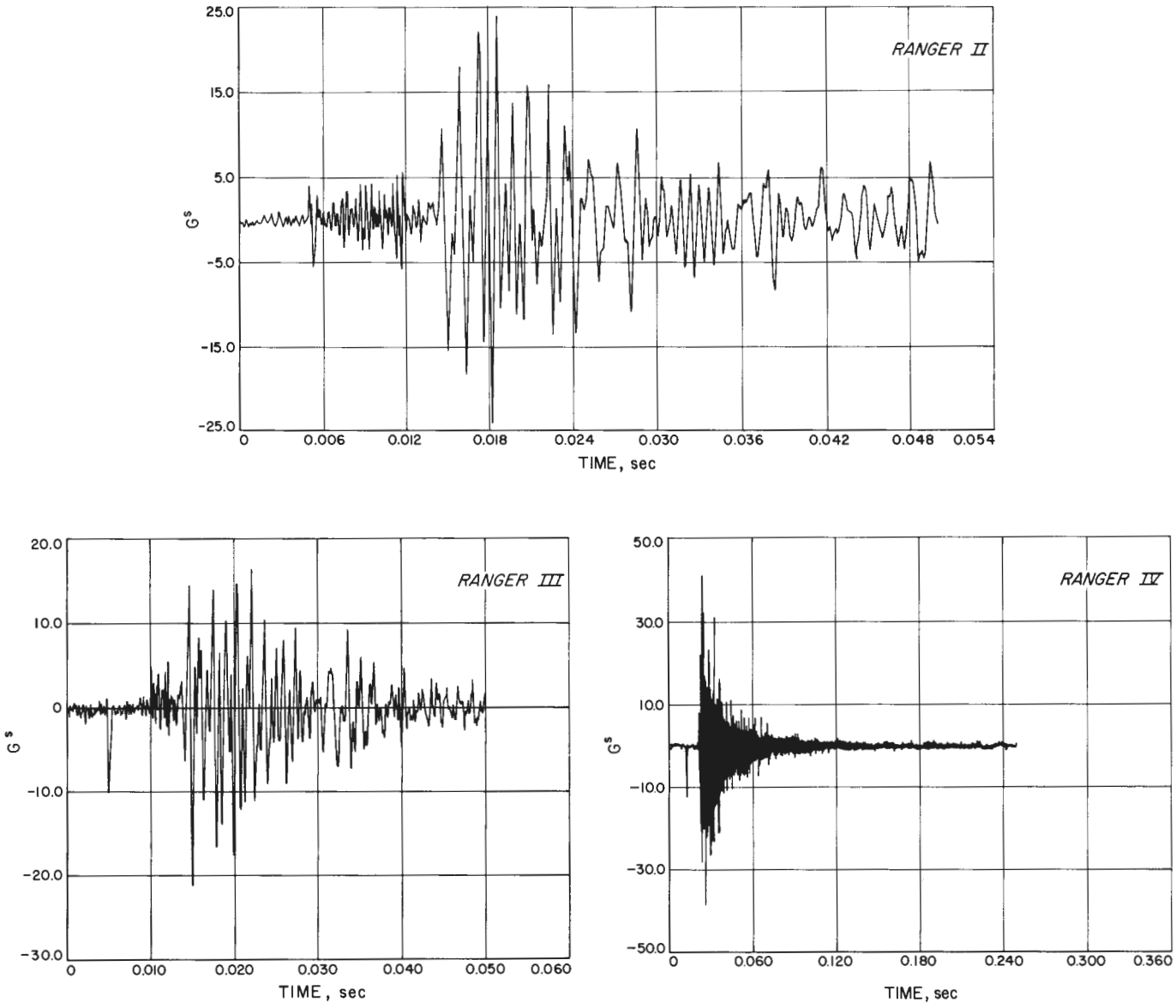

Fig. 54. Shock spectra, jettison horizon-sensor fairing, channel 17, 18

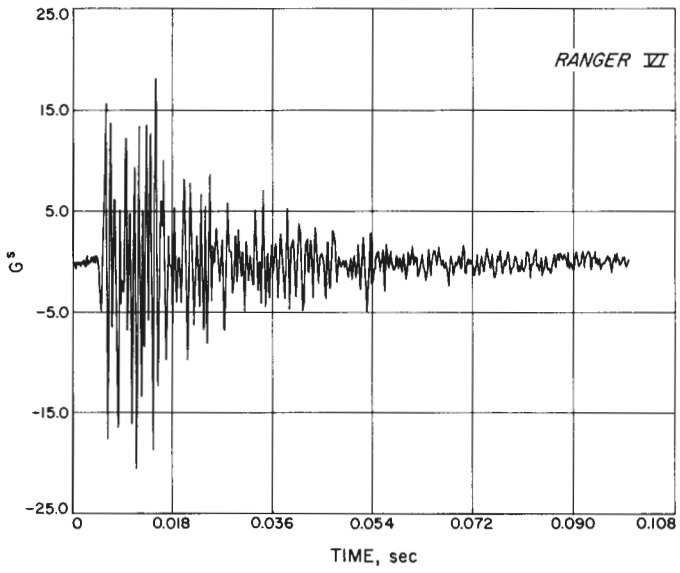

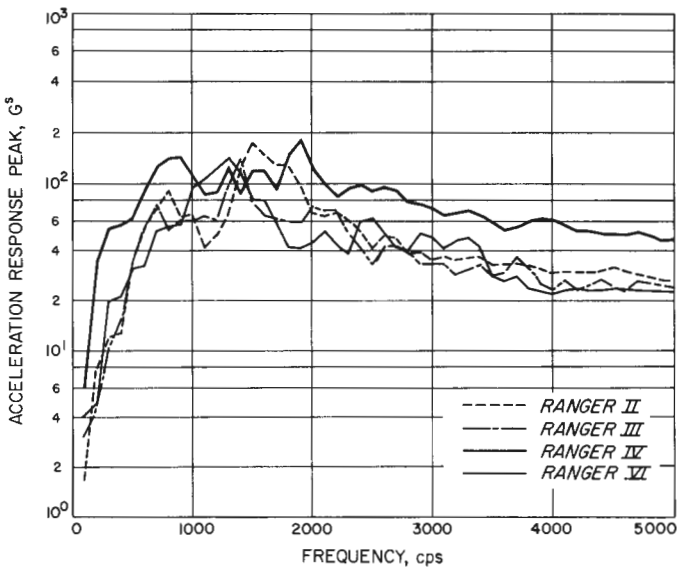

Fig. 54. Shock spectra, jettison horizon-sensor fairing, channel 17, 18 (cont'd)

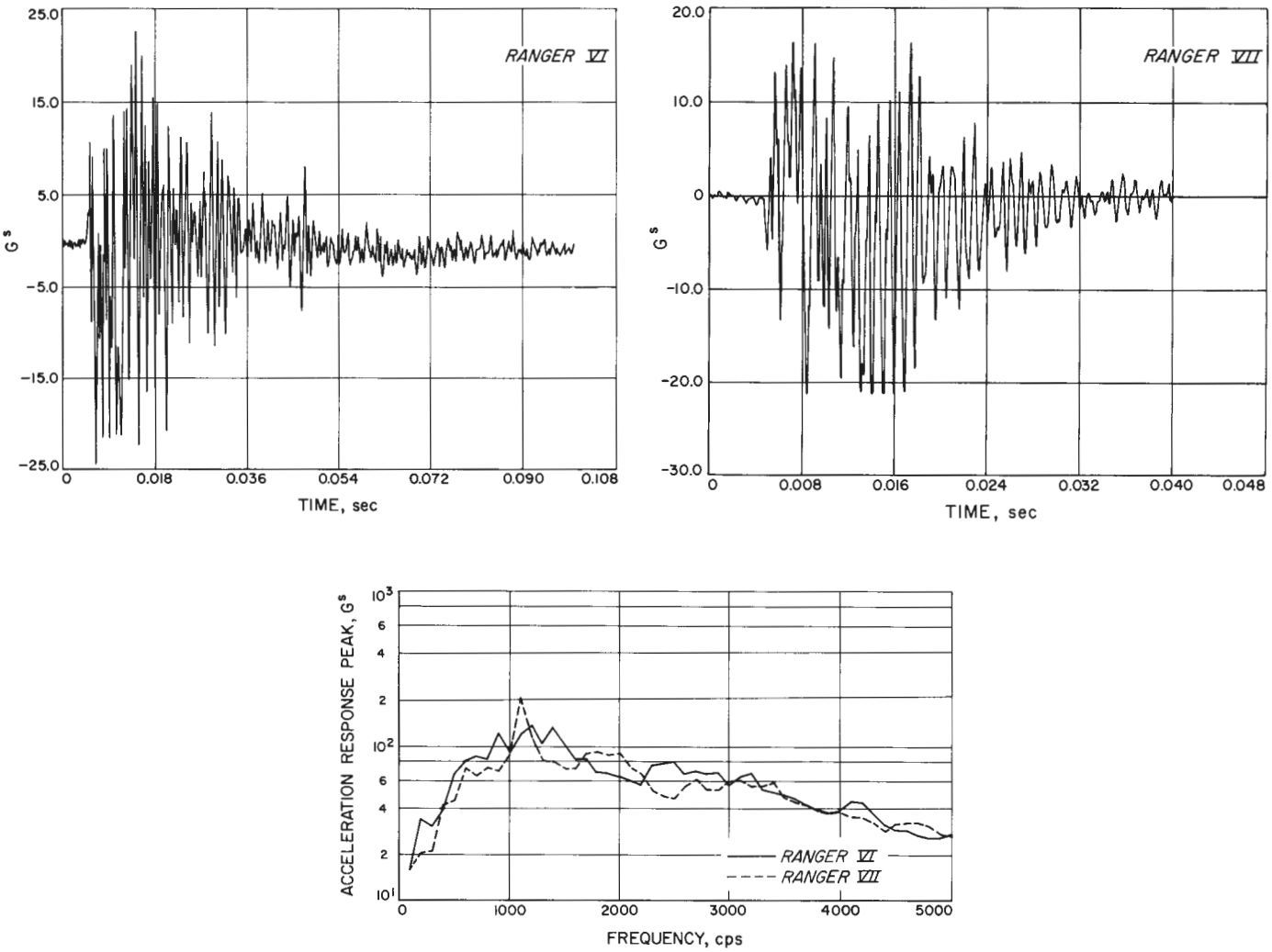

Fig. 55. Shock spectra, shroud separation, channel 17

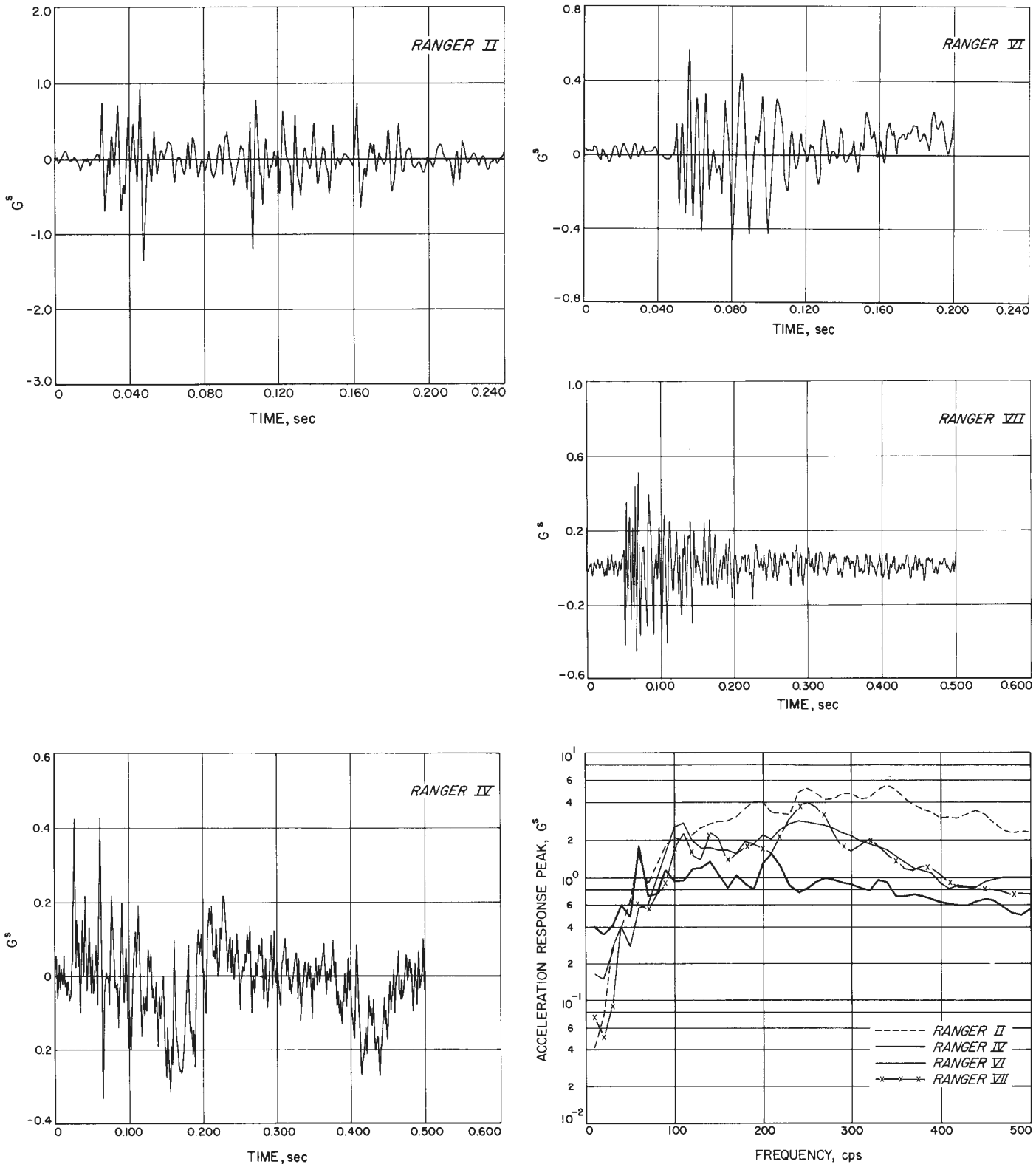

Fig. 56. Shock spectra, *Atlas–Agena* separation, radial, channel 10

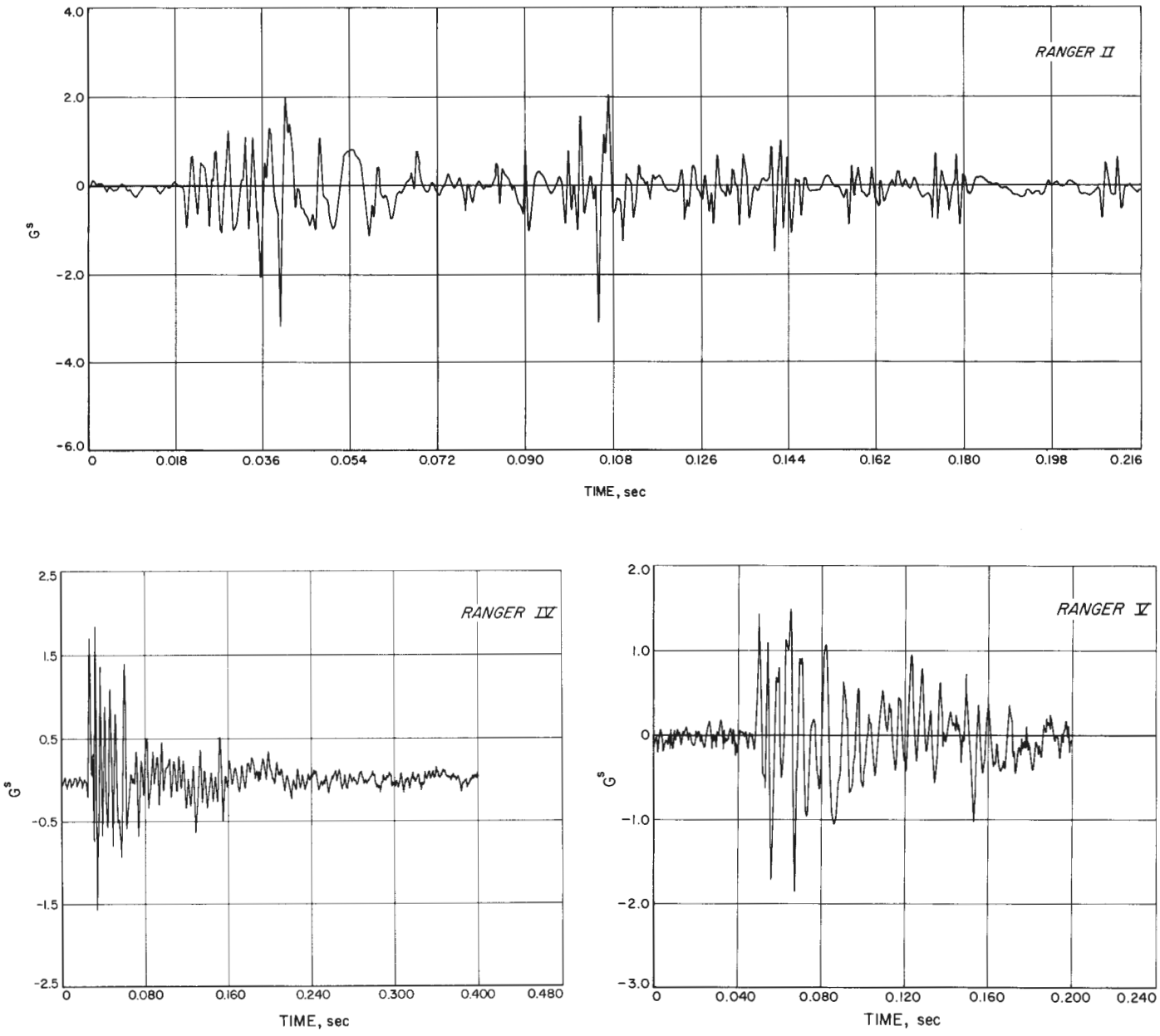

Fig. 57. Shock spectra, *Atlas–Agena* separation, tangential, channel 12

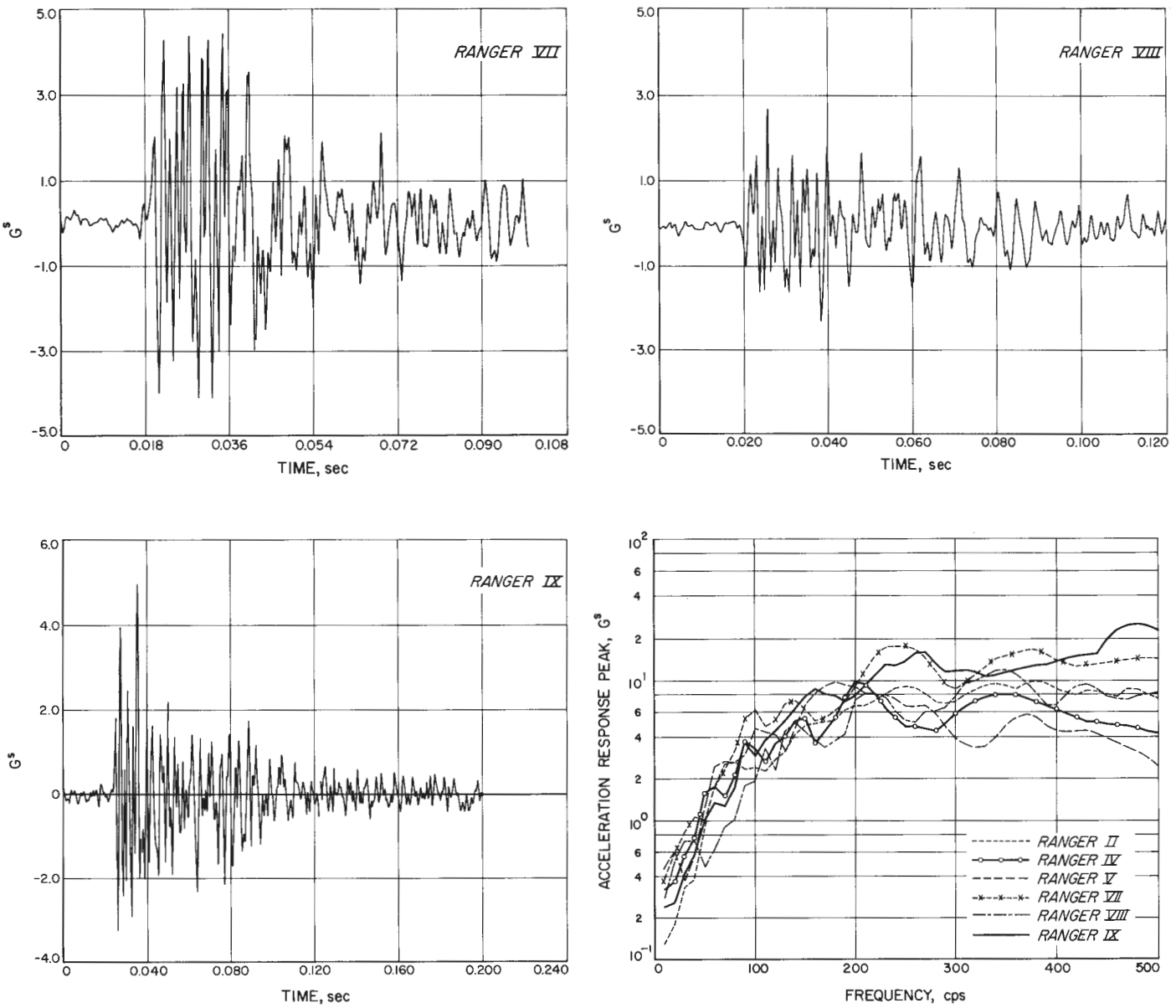

Fig. 57. Shock spectra, *Atlas—Agena* separation, tangential, channel 12 (cont'd)

III. VIBRATION TESTING

A. Historical Comments

JPL vibration test specifications were continuously revised and updated as additional knowledge of the actual environment was gathered and as vibration test techniques were refined or more completely understood. The test specification referred to in the following section of this Report is the most up-to-date version; it, however, does not include as base material all *Ranger* flight data. In actuality, the final test requirements were based on the Block I and II flights and a review of the *Ranger VI* data. The only really significant tests of the adequacy of the spacecraft requirements were the actual successful launches themselves. The results of the *Ranger VII*, *VIII*, and *IX* flights serve to demonstrate graphically this adequacy. In retrospect, an estimate based on flight environment of all *Ranger* launches will be defined as the "best test."

B. Test Philosophy

1. Qualification and Acceptance Testing

Vibration tests were conducted at two levels: the lower level test called "Flight Acceptance" (FA) is performed on actual flight equipment and is intended to simulate a 95th percentile flight; the higher level test (3 db above FA) called "Type Approval" (TA) is performed on special flight-type equipment and is intended to demonstrate equipment design margins above the expected flight environment and above the FA test level.

The performance of an FA test on the flight spacecraft itself provides confidence that it will survive in the flight environment. The performance of a TA test on a flight type of spacecraft (at a higher level than the FA test) provides confidence that the FA test has not measurably degraded spacecraft performance and that the spacecraft design was not marginal at FA levels.

2. Assembly Level and System Level Tests

Environmental tests are performed on equipment at both the assembly level and at the system level (complete spacecraft). Both tests are necessary as they have separate but required functions. The assembly level tests are performed early in the development of the spacecraft equipment. They provide confidence that a design will be adequate when tested at the system level and when actually flown. The levels of these tests are controlled both by vibration expected in flight and vibration produced by the system level tests. The system level FA test is the final vibration test prior to flight. It provides a large fraction of the confidence that the spacecraft will successfully survive launch.

C. Control Techniques

Early spacecraft tests were performed by controlling the input at *one* location. It was soon apparent that this procedure was inadequate and methods were improved and refined (and additional equipment designed and developed) until the final method was settled upon. In the final test method the input was specified as some combination of the input at all six spacecraft feet. For the low-frequency sine test, the level is the maximum at any of the six feet; for the high-frequency sine test and the random noise test, the specified input is the average of the mean square inputs at the six feet. For noise testing equalization, the test system gains are adjusted to produce a flat (within $\pm$ 3 db) average mean square response of 1 g_{rms} at the six feet for a constant voltage sinusoidal-signal input to the vibration exciting system. Then an input noise with the desired test spectrum (using magnetic tape input) is used. The over-all (wideband) response is adjusted with the intent of producing the required PSD input levels which are the ultimate measure of test adequacy.

D. Resultant Tests Compared with Specified Tests

The actual attained tests are not identical with the ideal specified tests. The tests themselves allow for a deviation within a specified tolerance, usually $\pm$ 3 db. The following discussion describes some typical actual test inputs compared with the specified inputs.

1. Sine Wave: High and Low Frequency

Figures 58 and 59 show the actual spacecraft input attained during the high- and low-frequency sine-wave portions of a vibration test. For the high-frequency sine test, the desired level is maintained by servo-controlling the output of an electronic device which computes the square root of the average of the square at the input of each at the six spacecraft feet. The low-frequency sine test was controlled electronically to limit the input at any one of the six spacecraft feet to the desired maximum level. This particular example shows the actual test to be reasonably close (within tolerance) to the specified test.

During other tests, however, some excessive deviations were noted and as such had to be analyzed in detail before the test could be judged acceptable or not.

2. Random Noise Test

Figure 60 is the *X*-axis noise test input PSD's from the *Ranger VII*, *VIII*, and *IX* FA tests. Unlike the test control input which is a root average square of six wideband inputs at the six feet, the composite PSD plot used as the final measure of the test adequacy is determined by averaging the PSD's at each of the six feet. The PSD resolution used is 20 cps. The indicated results are typical of the obtained test spectra in the other two test axes. The deviations from the desired spectra are due to nonlinearities resulting in the vibration exciter-spacecraft system responding differently to the noise test input than it does to the lower level sinusoidal signal used for equalization. The figure illustrates the test to test variation; the *Ranger VIII* and *IX* tests are almost overlays, while the *Ranger VII* test shows some significant deviation at 700 and 800 cps. The better repeatability of *Ranger VIII* and *IX* may be due to the continued improvement in test procedures.

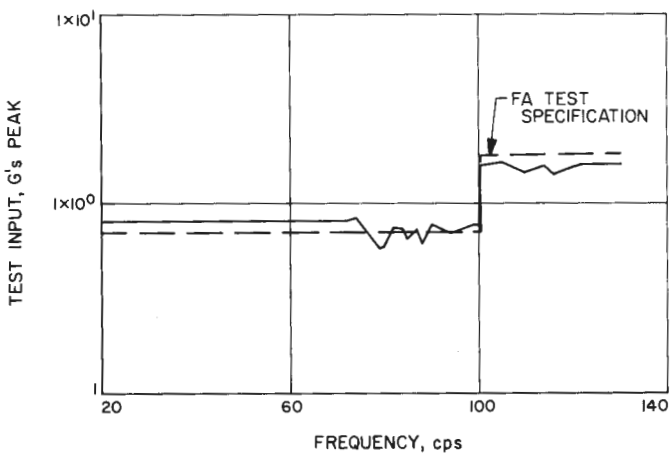

Fig. 58. Specification vs vibration test, low-frequency sine

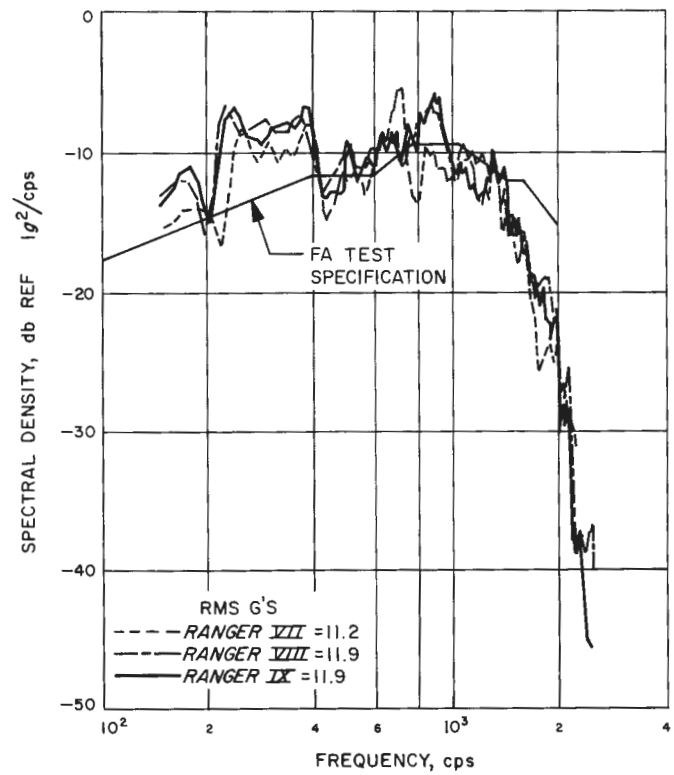

Fig. 60. Specification vs vibration test, *Ranger VII, VIII,* and *IX* FA (flight approval) random vibration

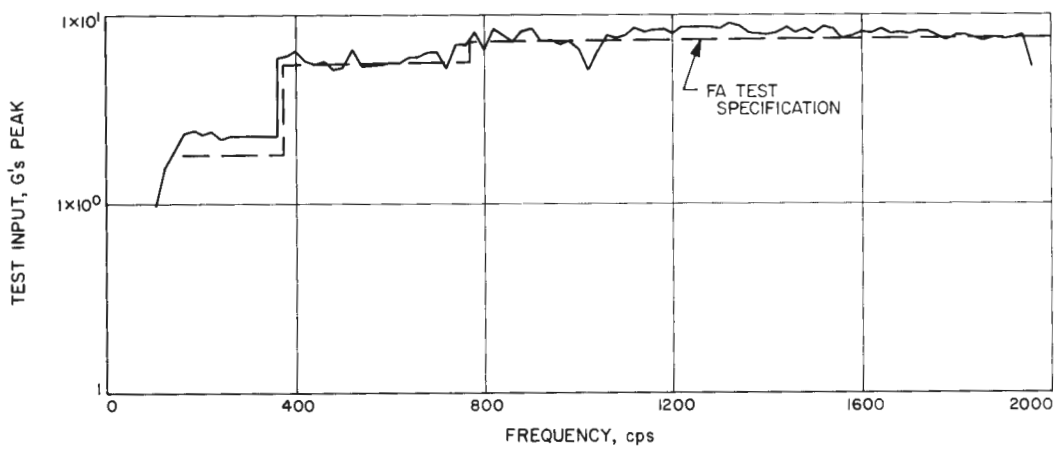

Fig. 59. Specification vs vibration test, high-frequency sine

3. Torsional Tests

The torsional test is in two parts: (1) a servo-controlled sinusoidal sweep from 50 to 300 cps, and (2) pulse inputs. Figure 61 is a typical sine sweep; good agreement with the specification levels is noted. It was more difficult to produce the desired pulse as its frequency content (69 cps) lies between a spacecraft anti-resonance and a shaker-spacecraft resonance. The pulse is produced by equalizing the system (as for the noise test) and then playing the recorded pulse signal (see Fig. 62) into the exciter system "open-loop." Nonlinearities in the spacecraft shaker system, coupled with the proximity of the system resonances, then resulted in large changes in the system "equivalent" mass (probably due to nonlinear structural damping) and a poorly controlled input. Table 4 shows the obtained magnitude of the pulse test for the *Ranger VII*, *VIII*, and *IX* spacecraft. Better test procedures (involving lower-level pulse inputs) resulted in a more controlled test on the *Ranger IX* spacecraft.

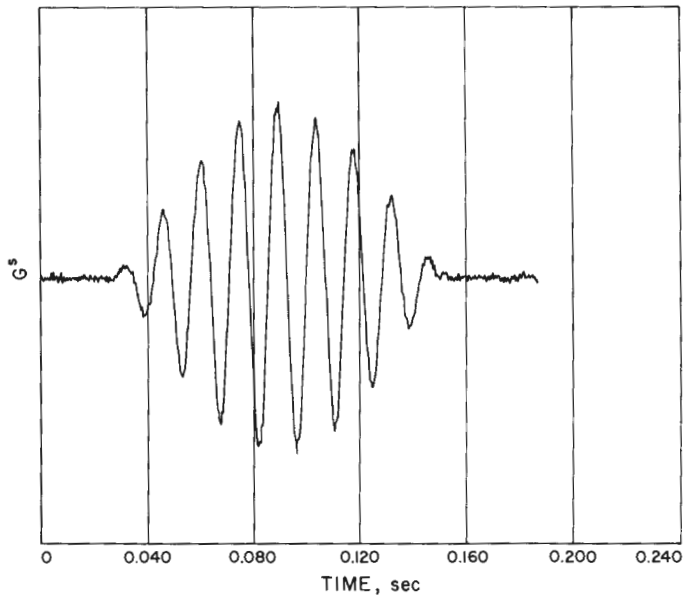

Fig 62. Torsional test pulse

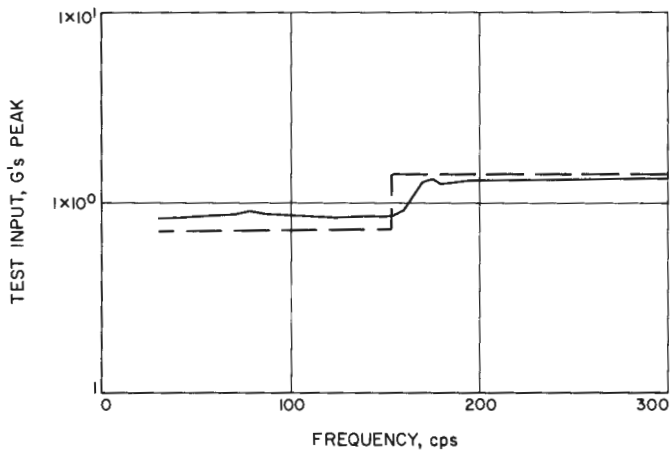

Fig. 61. Specification vs vibration test, torsional sine

Table 4. Torsional pulse test levels

Spacecraft	Pulse No.	Foot	
		A (g peak)	D (g peak)
Ranger VII	1	4.0	3.5
	2	3.0	3.0
Ranger VIII	1	13.0	12.0
	2	12.5	12.0
Ranger IX	1	8.0	7.5
	2	7.7	7.0
Specified value	1	6.0	6.0
	2	6.0	6.0

IV. COMPARISON OF TEST SPECIFICATIONS AND FLIGHT ENVIRONMENTS

The environments of shock, vibration, and acoustics were estimated early in the *Ranger* project. These estimates were used to establish test specifications which defined random vibration tests, sine-sweep vibration tests, and acoustic tests to be performed on test models or flight spacecraft. During the program as flight data were accumulated, the test specifications were modified and updated. The comparisons which are made in this section use the most recent version of the test specifications.

Comparisons are made of both the complete spacecraft tests and of assembly level tests. In either case, use of some type of prediction technique has been required to estimate the flight environment at the location of the defined test environment. The techniques which were used are described and comparisons are made between environmental levels and test levels.

A. *Flight Data vs Spacecraft Test (Random Vibration)*

A review of the flight data shown in Section II leads to the following observations:

1. The transonic vibration environment is nearly always higher in all frequency bands than the liftoff environment.
2. Data offering the best comparison between flights are those from the radial measurements of *Ranger I, II, III,* and *IV*.
3. The *Ranger VII* and *IX* measurements compare well, except near 1000 cps. It has been demonstrated that the *Ranger VII* mounting bracket was resonant at this frequency.
4. The *Ranger VI* measurements are approximately 2 to 5 db higher than the *Ranger VIII* measurements. This difference is unexplained. Structure and mounting characteristics were nominally the same.

Due to the differences observed, some care must be taken in choosing pieces of data for making detailed comparisons.

1. Comparison of S/C FA Specifications to *Ranger I, II, III, IV* Flight Data

The spacecraft test is defined as an input vibration level at the spacecraft feet. The measurements used to estimate this environment in each flight were Channel 18 on *Ranger I, II, III, IV* and Channel 17 on *Ranger VI, VII, VIII, IX*. A difficulty arising in making a straightforward comparison results from the detailed differences in location and mounting characteristics of the flight transducer. The transducer location in each flight is in the adapter joining the spacecraft to the *Agena* (see Section II–A). To estimate the vibration level at the S/C foot, some relation between the flight transducer vibration and the S/C foot vibration must be assumed.

The assumed relation between flight transducer and S/C foot vibration levels is based on measurements of vibration levels during ground acoustic tests on an STM (structural test model) spacecraft, see Ref. 2. Measurements made at the spacecraft feet and at the flight location during these tests have been reduced to power spectral density (PSD) plots. The ratio between the average foot PSD and the flight location PSD was determined. This ratio between spectra has then been applied to the flight measurements resulting in an estimate of the spectral density level at the spacecraft feet during flight.

Two assumptions have been made in use of this spectra ratio approach to the estimation of vibration levels at locations which were not instrumented. The first assumption is that the excitation mechanism is similar in flight and ground test. The second is that over some range of vibration levels, including the flight test and ground test, the spectra ratios are approximately constant (i.e., the structure is approximately linear over this range).

Since structural changes and transducer mounting location changes were made between the Block II and Block III phases of the *Ranger* program and mounting block changes and transducer orientation were not consistent within the Block III models (*Ranger VI, VII, VIII, IX*), the spectra ratios used to estimate spacecraft foot environment must differ from flight to flight. Unfortunately, ground tests on all versions of structure and mounting arrangement were impossible to make. Thus, spectra ratio information required to estimate spacecraft foot environment is not available for all flights.

The best available spectra ratio data are applicable to the *Ranger I, II, III, IV* radial measurements. It was also these measurements which were used to establish the flight acceptance (FA) test specification levels for the

random vibration test applicable to the Block III spacecraft (see Ref. 3).

Using the *Ranger I, II, III, IV* transonic measurements and estimating the spacecraft foot environment, as described above, give the levels shown in Fig. 63 and 64.

The FA test specification* which was derived from these four flight measurements and actually incorporated into the *Ranger* test program during *Ranger VII* testing is shown superimposed on Fig. 63 and 64.

Some use of percentile level estimation has been made in summarizing sets of data. It has not yet been used in this section because of the limited amount of data under discussion; however, it is interesting to note that with the four measurements, considered thus far, the practical effect of using a 95% level instead of actual data is small. This is due to the good comparison between flights. The small variation (3 to 5 db) is demonstrated in Fig. 65 where the mean, the 95% level, and the maximum envelope of estimated spacecraft foot environment are superimposed. The percentile level estimate shown here and used later in this Report is based on an assumed log normal distribution for the spectral values.

*JPL Spec. RCO-50107-FAT-A, "Environmental Test Specification, *Ranger* Block III Flight Equipment; Spacecraft Flight Acceptance, *Ranger VIII* and *IX*," November 13, 1964.

2. Comparison of S/C FA Specifications to *Ranger VI, VII, VIII, IX* Flight Data

The high-frequency vibration measurements made on *Ranger VI, VII, VIII, IX* (*Ranger V* had no high frequency measurements) demonstrated poor repeatability as might be expected when considering transducer orientation and mounting-block characteristics. Unfortunately, the mounting-block resonance problem was not completely corrected until the *Ranger IX* flight and was not evaluated in the system configuration.

For the purpose of making some comparison with previous flights, and test specifications, the same spectra-ratio approach as described above has been used on *Ranger VI, VII, VIII, IX* flight data, attempting to estimate the vibration at the spacecraft feet. However, the results are not considered to be useful in the sense that earlier flight data were used. This is due to the lack of

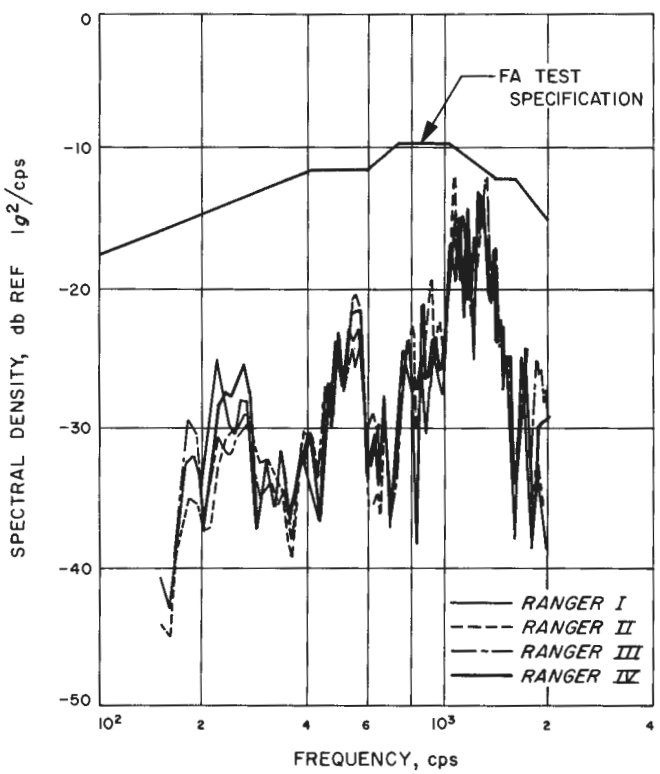

Fig. 63. Flight data vs vibration specification, lateral, *Ranger I, II, III, IV*

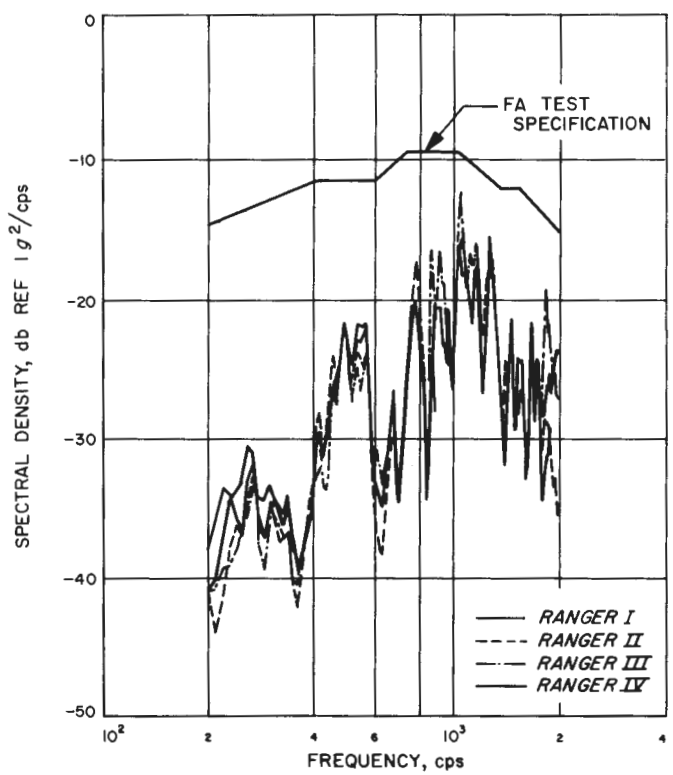

Fig. 64. Flight data vs vibration specification, axial, *Ranger I, II, III, IV*

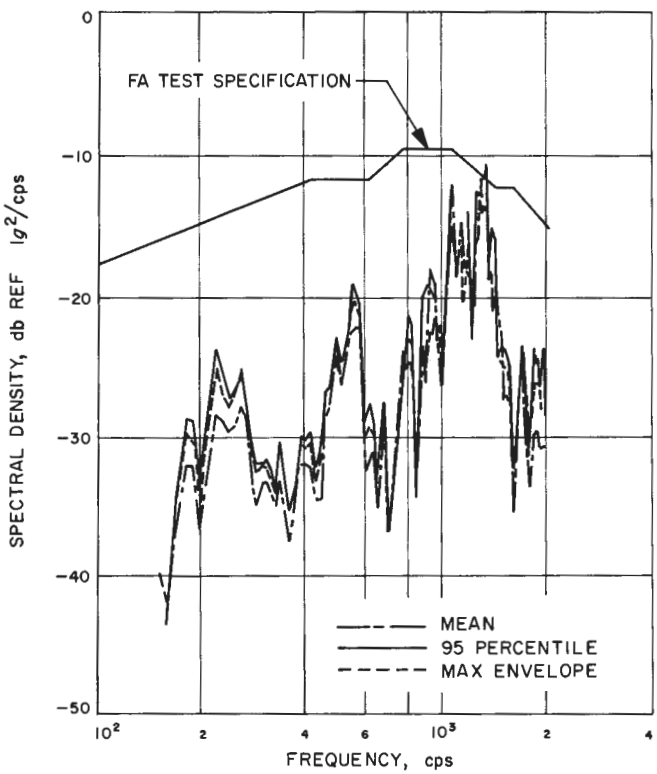

Fig. 65. Mean, 95 percentile, maximum envelope, lateral, *Ranger I, II, III, IV*

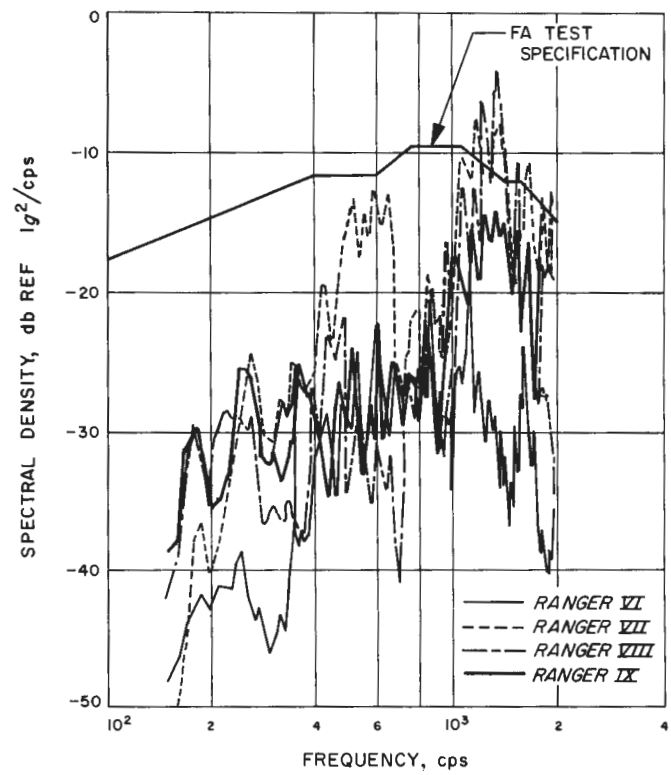

Fig. 66. Flight data vs vibration specification, lateral, *Ranger VI, VII, VIII, IX*

sufficient ground test data on each flight configuration to define properly a spectra ratio between flight location and S/C feet. Using the spectra-ratio approach, an attempt at correcting the flight measurements for the resonant mount condition of *Ranger VI, VII, VIII* was made, and then the flight measurements were "transferred" to the S/C feet. Figures 66 and 67 show the "best estimate" of the flight environment at the S/C feet for *Ranger VI, VII, VIII, IX*, with the final Block III FA test specification superimposed. It is noted in comparison with the earlier flights that the data from *Ranger VI* through *IX* show more spread. This is best explained by the variation in mounting configuration and weaknesses in the estimating procedure rather than by possible differences in the flight vibration levels. Another demonstration of the data spread is shown in Fig. 68 where the mean, the 95 percentile level, and the maximum envelope for *Ranger VI* through *IX* S/C-feet estimates are plotted. The high 95% level indicates weakness in the method of data interpretation, especially use of percentile level estimation with such a small sample of data.

As a rough comparison between the Block I and II environment and the Block III environment at the S/C feet, Fig. 69 is included. Due to structural changes incorporated in Block III, especially the removal of the sterilization diaphragm, some differences may be anticipated. Figure 69 shows the means of the "best estimates" of S/C-feet environments for each group.

B. Acoustic Data vs PTM Acoustic Test

An acoustic test was performed on the Block III PTM in the JPL reverberant chamber acoustic test facility. The specification* test level is shown in Fig. 70. Also shown on this Figure are the acoustic measurements made on the *Ranger VI* and *VII* flights during liftoff (see Fig. 41). The comparison between the PTM specification and the flight levels indicates an acceptable relationship; i.e., a 3 db increase in flight levels is still below the desired test level.

There were no flight acceptance (FA) acoustic tests performed on flight spacecraft.

*JPL Spec. RCO-50277-ETS, "Environmental Test Specification, *Ranger* Block III Flight Equipment Proof Test Model, Requalification," November 15, 1964.

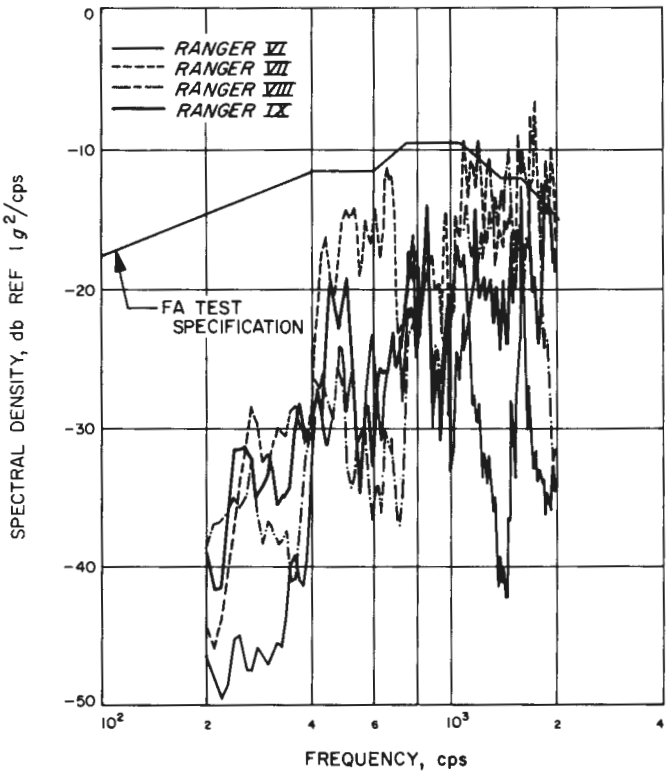

Fig. 67. Flight data vs vibration specification, axial, *Ranger VI, VII, VIII, IX*

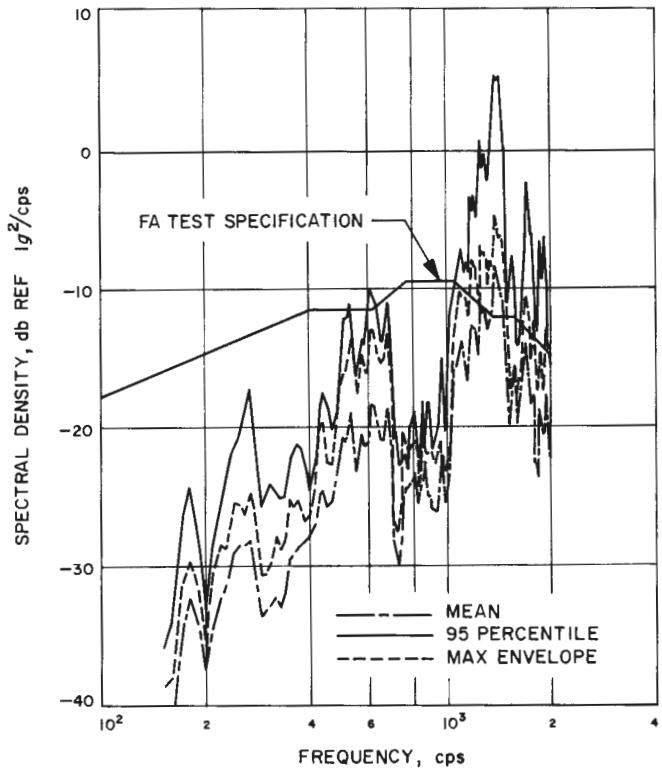

Fig 68. Mean, 95 percentile, maximum envelope, lateral, *Ranger VI, VII, VIII, IX*

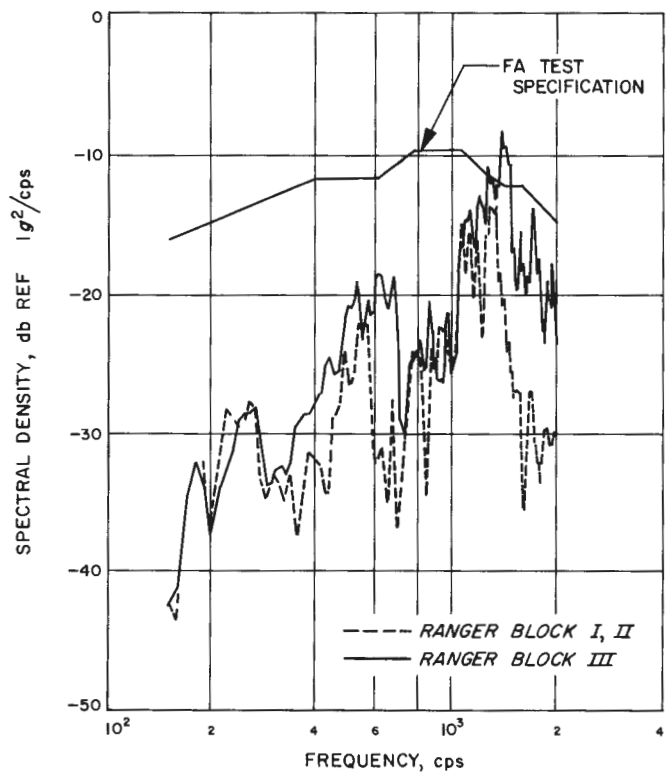

Fig. 69. Average spacecraft foot environments, Block I and II vs Block III

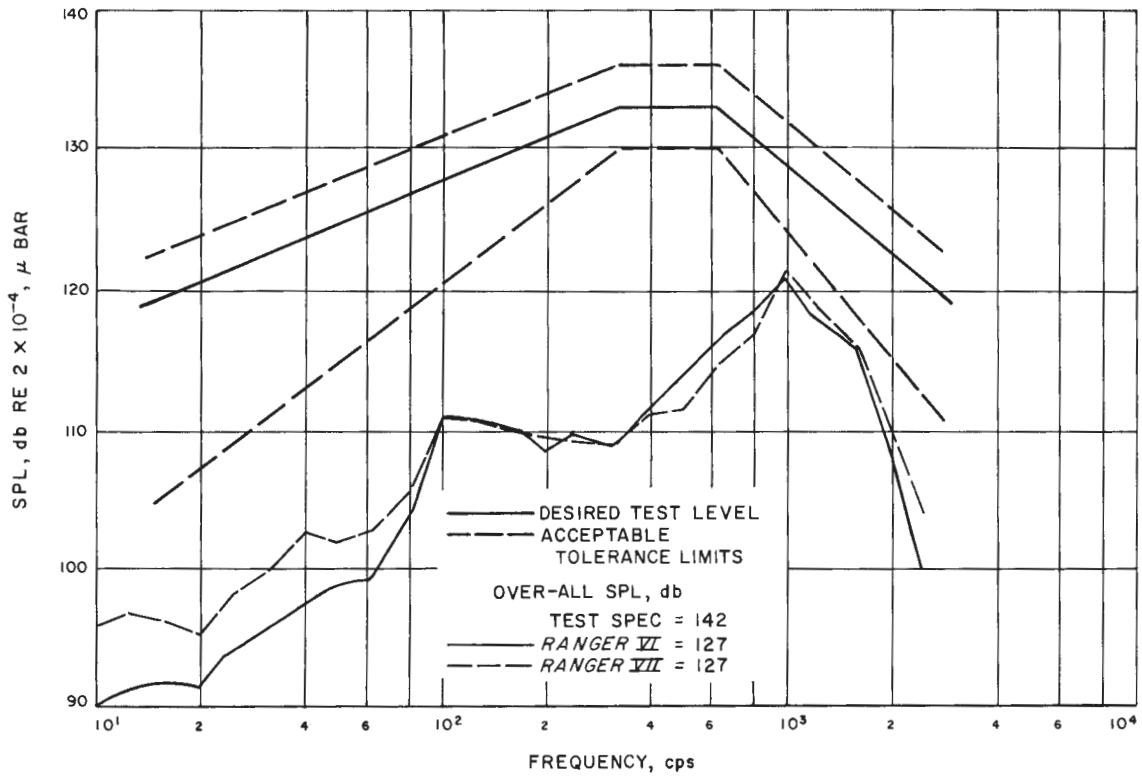

Fig. 70. Liftoff acoustics vs PTM (proof test model) acoustic specification

C. *Flight Data vs Spacecraft Test (Low-Frequency Sine)*

The low-frequency vibration environment is not as easily defined as is the high-frequency random environment. The low frequency data having significant acceleration levels occur in the form of transient vibrations or shocks. Boost-engine transients and staging events are the primary sources of excitation.

The data from this portion of the environment are shown in Section II in the form of shock spectra. The FA test specification* which will be compared to this transient flight data is that for a sine-sweep vibration test. No general S/C shock test was used in the *Ranger* program although assembly-level shock tests were performed. The method of comparison of flight transient data to the sine sweep test specification is the following.

The response of a single-degree-of-freedom system to each type of excitation (transient and sine-sweep) will be compared. This allows direct use of the flight shock-spectra information. The sweep rate used in specifying the sine-sweep test is based on exciting a single-degree system, having a $Q = 10$, to at least 95% of maximum resonant response (maximum resonant response is the response resulting from an infinitely slow sweep rate). The shock-spectra analysis shown in Section II assumes a $Q = 20$. The specified test sweep rate will allow approximately 90% response for a system having $Q = 20$ (see Ref. 4). Thus, the specified test-response used here for comparison to flight transients has been derived by multiplying the specification test level by (0.90) (20) = 18 as a minimum response.**

The selection of flight data shown in Fig. 71 is the maximum of each group of data presented in Section II; i.e., from the available data, a maximum envelope of spectra was established for each transient. These envelopes are then compared to the sine-sweep specification.

The validity of the above described comparison should be qualified. No attempt has been made to estimate the

*JPL Spec. RCO-50107-FAT-A, "Environmental Test Spec., *Ranger* Block III Flight Equipment, Spacecraft Flight Acceptance, *Ranger VIII* and *IX*," November 13, 1964.

**The 95% and 90% of Q response is a minimum response and occurs only at start frequencies of the sine sweep (20 and 100 cps). The response approaches 100% of Q value as the sine sweep progresses above 20 and 100 cps.

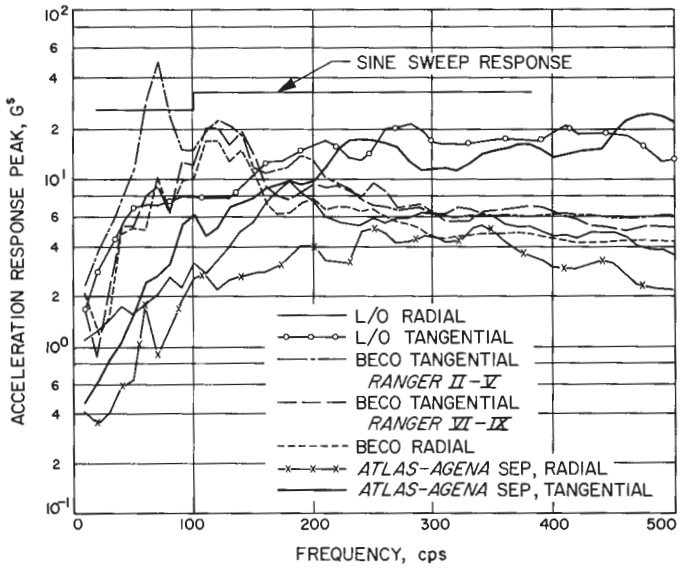

Fig. 71. Flight transients (low frequency) vs sine vibration specification

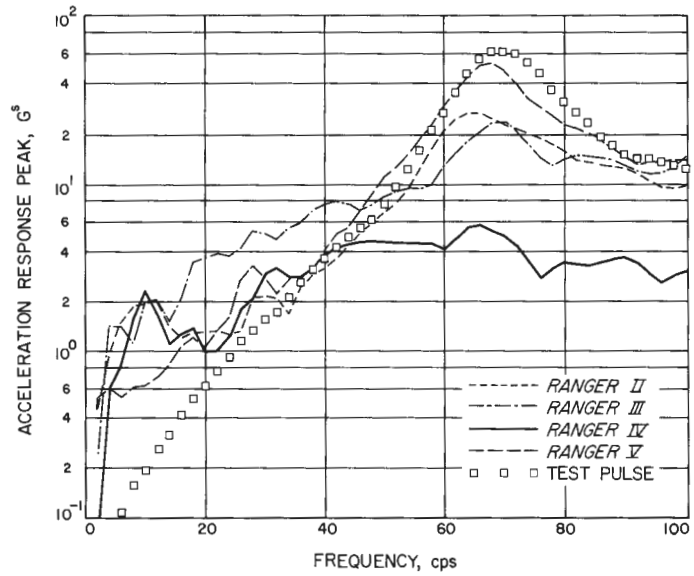

Fig. 72. Flight BECO transient (Block I and II) torsional pulse specification

transient motion at the S/C foot. All transient data were measured at some location (as described in Section II) in the adapter. In addition, all flight measurements were lateral (i.e., radial or tangential). No attempt was made to separate directional differences. These qualifications are required because of the lack of good transfer function information and because of the low quantity of flight data. Consequently, the comparison made on Fig. 71 gives at best a general relation between test and environment.

The peak occurring at 70 cps in Fig. 71 is from the *Ranger V* BECO event. The torsional pulse test discussed below considers this event in more detail.

D. Flight Data vs Spacecraft Test (Torsional Pulse)

The *Ranger I, II, III, IV* tangential measurements (Channel 12) consistently indicated a significant transient at booster engine cutoff (BECO). However, it was not until *Ranger V* that two tangential measurements were made, and it was determined that a significant portion of the transient was of a torsional nature. Of special concern was torsional excitation in the range of 60–70 cps because of a natural structural mode in this frequency range. A torsional test pulse was incorporated in spacecraft FA testing to cover this torsional environment.

The actual test pulse was shown in Fig. 62. Figures 72 and 73 show shock spectra for the measured tangential transients and the shock spectrum for the devised torsional test pulse. All spectra are again for $Q = 20$. The

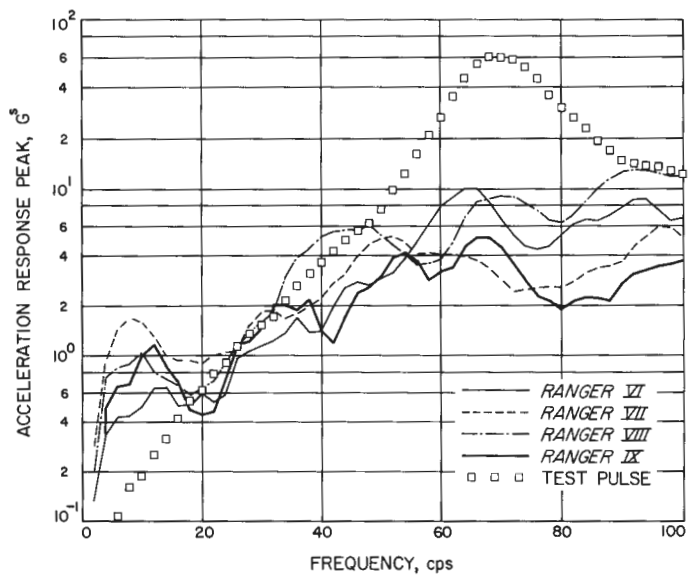

Fig. 73. Flight BECO transient (Block III) vs torsional pulse specification

specification test pulse spectrum was computed for a pulse having a peak amplitude of 6 g, the specification level. In the 65–70 cps region, the test spectrum is seen to envelope the flight data.

Below 50 cps, the flight data show a spectrum level comparable to or exceeding the test pulse; however, the sine-sweep test does cover flight data in this range (see Fig. 71). It should be mentioned that the torsional pulse

test was intended to qualify the spacecraft for the 65–70 cps transient environment which was verified to be primarily torsional motion.

E. Estimated Flight Environment vs Assembly Level Test

Component or assembly testing is performed prior to spacecraft assembly and system level tests. These assembly level tests are performed at a relatively high vibration level when compared to measured and estimated flight vibration. The comparison between estimated flight environment and assembly-level test specification made in this Report uses the *Ranger I* through *IV* flight data and the previously discussed spectra-ratio approach to estimate spacecraft environment in the areas of the spacecraft bus and spacecraft television. The estimates, shown in Fig. 74 and 75, were derived by applying appropriate spectra ratios, as measured in ground acoustic tests, to the spacecraft foot estimates of Section IV-A-1. The resulting estimates are omnidirectional and apply to zones of the spacecraft (Ref. 2).

One check on the validity of these estimates is made from the accelerometer on the *Ranger VIII* and *IX* spacecraft. This accelerometer, Channel 18, is the only flight measurement on any *Ranger* spacecraft and is in the spacecraft bus region. Comparison of these flight measurements, Fig. 38, to the estimate of Fig. 74 indicates reasonably good agreement.

No attempt has been made to extrapolate the *Ranger VI* through *IX* flight measurements and estimate spacecraft assembly vibration. This is due to the poor repeatability

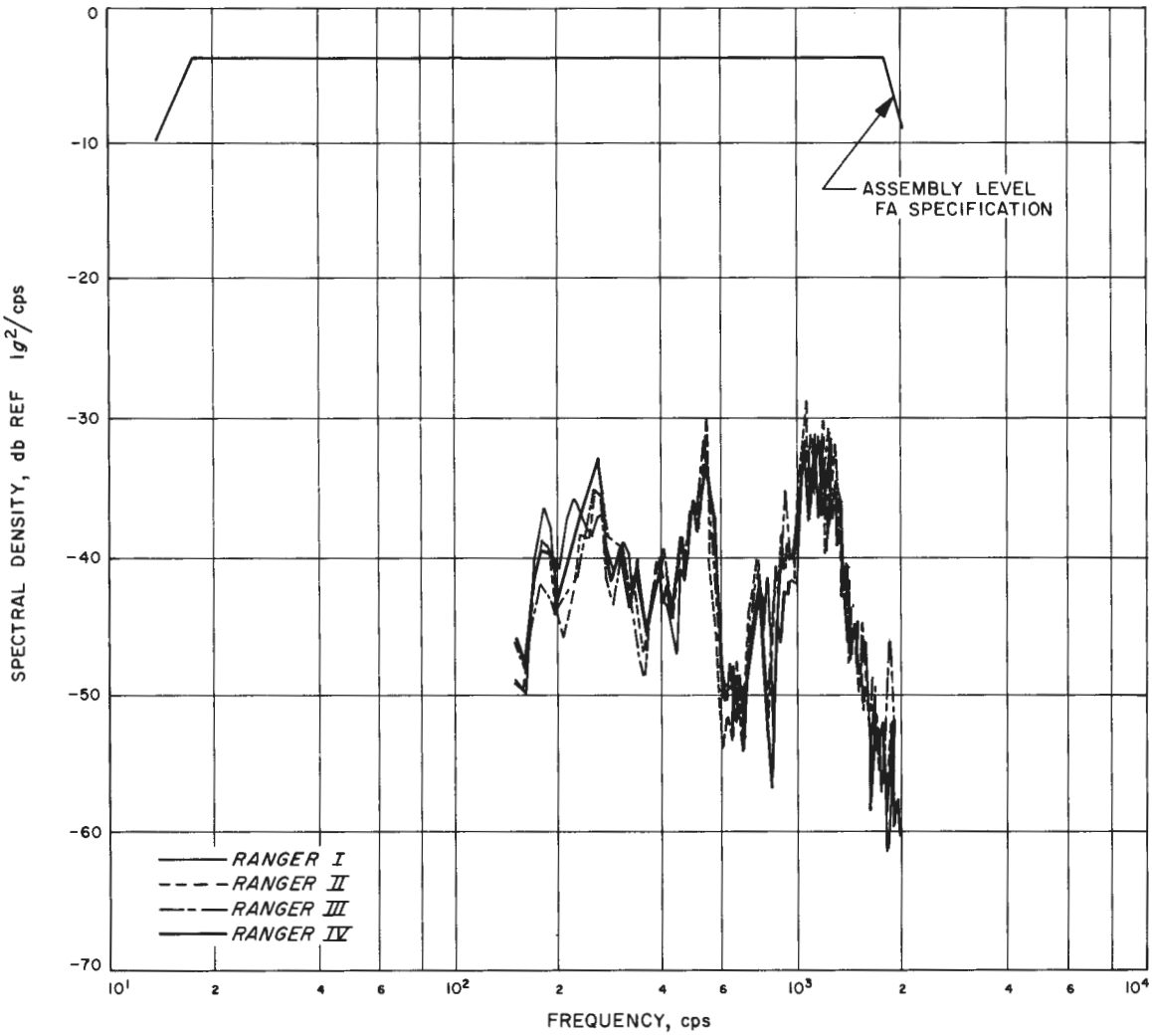

Fig. 74. Estimated flight environment, bus assemblies

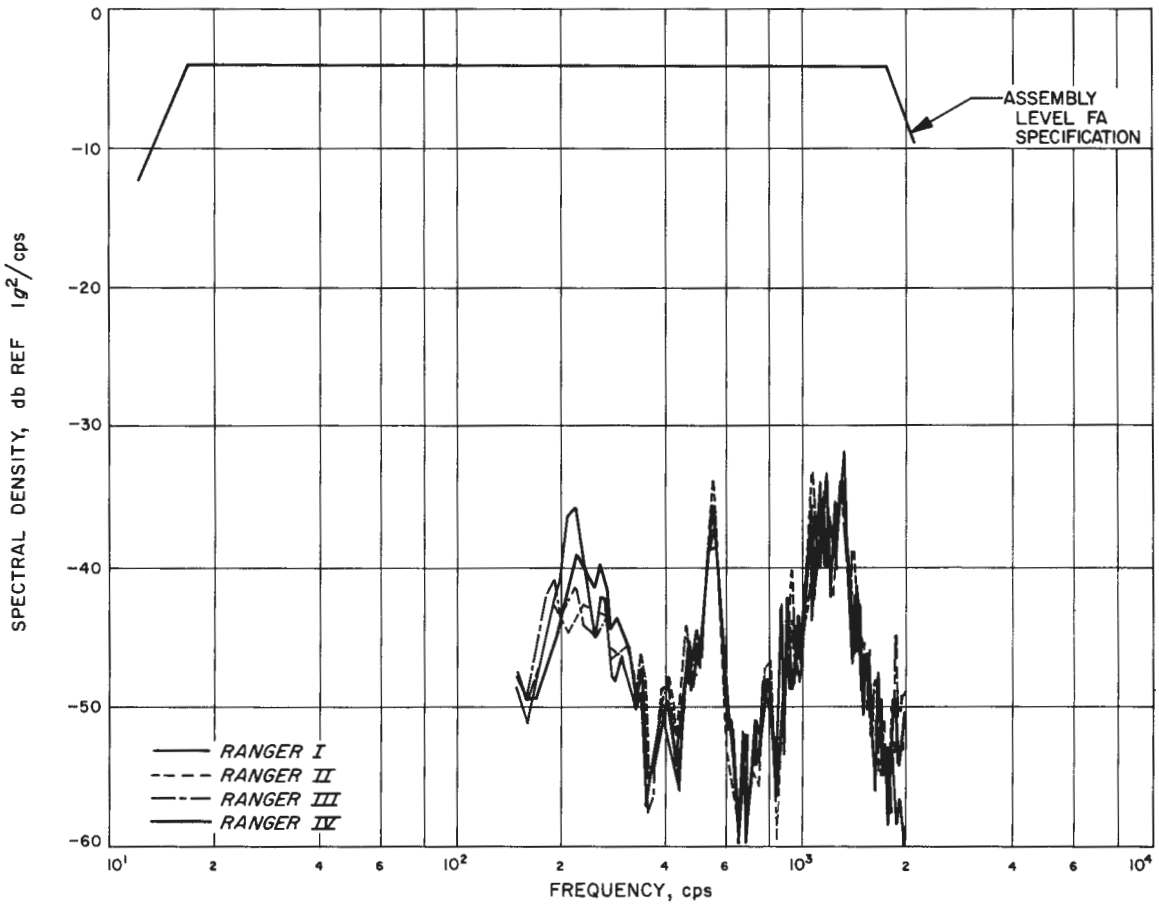

Fig. 75. Estimated flight environment, TV assemblies

and resulting lack of confidence in the spacecraft-foot estimates for these flights.

A considerable margin is seen to exist between spacecraft assembly test specification levels and estimated flight levels. An explanation for part of this difference is the following. The spectra ratios used to estimate assembly level vibration using spacecraft-foot vibration as a reference were measured in a spacecraft *acoustic* test. It has been observed that similar ratios measured during spacecraft *vibration* tests exhibit higher values (i.e., structural resonances are more pronounced in vibration tests than in acoustic tests) at some frequencies. A comparison of the spectra ratio used in the *Ranger I* through *IV* estimates (derived from acoustic test) and the spectra ratios measured on *Ranger VIII* and *IX* FA vibration tests is shown in Fig. 76. At discrete frequencies, differences of 15 db may be seen. The *vibration* spectra ratios shown here are for the flight accelerometer location only. Similar comparisons with other locations would show resonant peaks at other frequencies. Since assemblies must undergo system vibration tests and the associated resonances, a considerable pad over flight data has been provided in assembly level tests.

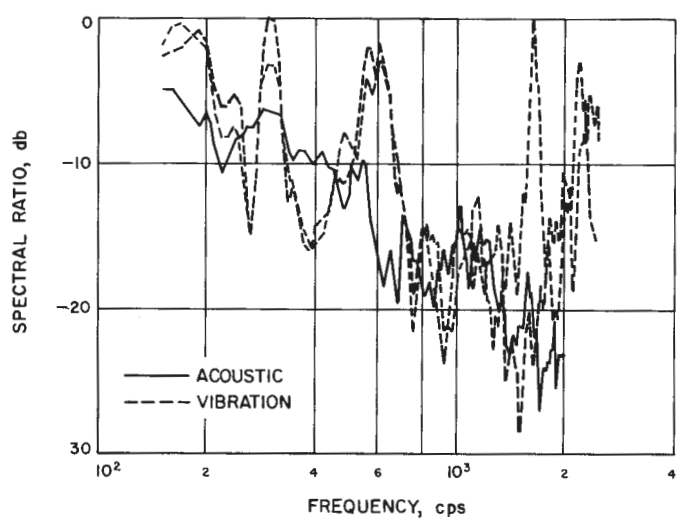

Fig. 76. Spectra ratios, acoustic test vs vibration test

V. CONCLUSIONS AND RECOMMENDATIONS

The areas of the dynamic environmental program for the *Ranger* spacecraft which have been covered in this Report are the data acquisition task and the post-program comparison of these data with test specification levels. To a lesser degree the areas of specification formulation and testing have been discussed. Using hindsight, one can conclude that the total engineering task relating S/C success and the dynamic environment was adequate because the *Ranger* program was successfully completed. However, weaknesses existed in various phases of the program and are briefly discussed below.

A. Data Acquisition

The best source of data for environmental definition is the actual measurement of the flight test environment. A bare minimum of such data was available in the *Ranger* program.

It is essential that the instrumentation system be thoroughly understood to interpret properly the resulting data. Some lack of confidence existed at JPL in the quality of data received from the flight test. This was a result of lack of knowledge about the instrumentation components and the lack of data properly defining the instrumentation parameters (i.e., calibration, frequency response, etc.). The most useful piece of information, for the environmental engineer in providing information about the instrumentation system, is an end-to-end calibration. Such a calibration was performed on *Ranger VIII* and *IX* with results which were a qualified success. *It is strongly recommended that end-to-end calibration of environmental instrumentation be designed into the system wherever possible.* Such a practice could be performed at a minimum of cost and trouble if incorporated in the instrumentation system design. The benefit to improved understanding and increase in data value would seem to be easily justified.

Data analysis techniques are available to extract almost any type of information from existing data. However, the type of analysis to be applied is dependent on the end use of the data. Also, when several similar flights occur in a program such as *Ranger*, it is always desirable to compare data from different flights. This requires a standard approach and data format for the data analysis. The conclusion or recommendation in this area is that preliminary planning of the data analysis scheme be made early in a program. *With ultimate use of the data always in mind, the analysis system should be defined and analysis parameters selected as early as possible.* Such early planning allows standardization of data presentation; this alone makes the data much more useful.

B. Environmental Prediction

The use of flight data depends critically on measurement location. In the *Ranger* program, all wideband vibration data used to estimate the S/C foot environment was sufficiently removed from the S/C foot to require the application of some experimental or analytical estimation technique or extrapolation of flight test data. Such extrapolation techniques require much detail study and ground test investigations, and the results are very dependent on specific hardware configurations. When such techniques are required, as in the *Ranger* program, it has been demonstrated that repeated measurements from flight to flight are much more useful than new individual measurements (e.g., changing measurement orientation or location). Of course, the most satisfactory approach is to *instrument the locations at which the environmental definition is desired. These same locations should then be instrumented and used as control points during ground test.*

The use of spectra ratios as described in Section IV for estimating vibration at noninstrumented locations was used in the *Ranger* program for lack of a better technique. Some valid estimates are probably derived with this method; however, theoretical basis for this technique is inadequate. The derivation from ground test of spectra ratios to be applied to flight data requires at least (1) similar excitation mechanisms in ground and flight, and (2) ground test levels roughly equivalent to flight levels to avoid possible nonlinearity problems.

Some verification of success with this technique was shown in Section IV where *Ranger VIII* and *IX* flight bus measurements compared reasonably well with previously estimated *Ranger I, II, III, IV* bus vibration.

A summary of above-mentioned recommendations which might be applicable to many dynamic environment programs is given below. Most items would only

be considered "good engineering," but the *Ranger* program results should serve to emphasize their importance.

1. More flight instrumentation
2. End-to-end calibration of flight instrumentation
3. Early planning of data-analysis scheme
4. Identical instrumentation for flight and ground test

If the fourth recommendation is not possible, repeated flight measurements are probably more useful than new, different measurements.

REFERENCES

1. Asquith, C. F., "Frequency Response, Noise, and Pulse Transmission in an FM/FM Telemetry System," U. S. Army Missile Command, Redstone Arsenal, Alabama, Report No. RG-TR-65-3, February 1, 1965.
2. Trummel, M. C., "Ground Test Simulation of Liftoff and Transonic Vibration Excitation Mechanisms on the *Ranger* Spacecraft," Shock and Vibration Bulletin No. 35; also JPL Technical Memorandum No. 33-256, November 1, 1965.
3. "Noise and Noise-Induced Structural Vibration of the *Ranger* Spacecraft," Report No. 1038A of Bolt, Beranek, and Newman, Inc., May 20, 1965.
4. Harris, C. M., and Crede, C. E., "Shock and Vibration Handbook," Vol. 2, McGraw-Hill, 1961.